FLOW FIELD AROUND SINGLE AND MULTIPLE HOLLOW HEMISPHERICAL ARTIFICIAL REEFS USED FOR FISH HABITAT

HARYO DWITO ARMONO

FLOW FIELD AROUND SINGLE AND MULTIPLE HOLLOW HEMISPHERICAL ARTIFICIAL REEFS USED FOR FISH HABITAT

By

©Haryo Dwito Armono

A thesis submitted to the School of Graduate Studies
in partial fulfillment of the requirements for the degree of
Master of Engineering

Faculty of Engineering and Applied Science
Memorial University of Newfoundland
August, 1999

St. John's Newfoundland Canada

Abstract

The term "artificial reefs" is being used by many researchers to refer to a variety of submerged structures. These structures are widely used to reduce the wave energy as well as to provide a safe and productive environment for fish. Hydraulic properties of artificial reefs made with hollow hemispherical shaped balls are presented in this study. The hydraulic parameters such as wave heights, particle velocities, fluid flows, wave breaking and dissipation of wave energy in the vicinity of reefs are investigated using Finite Volume methods. The study considers two-dimensional and three-dimensional fluid motion over an artificial reef constructed with one or more reef units.

As water moves through the reefs, the incoming wave energy is dissipated by turbulence; furthermore, pressure waves, which can be detected by fish, are produced as water exits through the holes on the top and sides of the hemispherical balls. Turbulent water, which exits/enters through the holes on the top and sides, moves upward/ downward and modifies the incoming/outgoing wave field. This movement of water is found to be effective in attracting fish swimming near the sea surface. It was also confirmed that the water velocities decrease considerably within the reef facilitating the attachment of marine organisms and their subsequent growth.

In the two-dimensional model, use of reefs with less than six units does not seem to reduce the wave height, significantly. However, use of a 12 unit reef seems to reduce the wave climate inside the basin, considerably. Provision of proper reefs placement provides a conducive environment and suitable locations wherein the fish can congregate and spawn;

in addition it also provides areas wherein the benthic diatoms and seaweed spores can develop and grow.

It was observed in three dimensional model that the energy dissipation was not due to the breaking of waves as observed in the two dimensional model, but due to the flow separation occuring at the crest and around the reefs. Therefore, the wider the crest of the reef within one or two wave lengths will result in more wave energy dissipated. Numerical studies by Tsujimoto, et. al (1999) as well as field observations by Ohnaka and Yoshizawa (1994) have confirmed the results of three-dimensional model presented here.

Acknowledgement

I would like to thank the Government of Indonesia for supporting my graduate study at Memorial University of Newfoundland. The financial support from May 1997 to November 1999 is gratefully acknowledged.

My deep gratitude goes to my supervisor Dr. A.S.J. Swamidas for suggesting the research topic. His guidance and assistance have helped me over the last two years. His helpful hand has been completely invaluable and unforgettable.

Acknowledgements are due to Dr. R. Shesadri, Dean of Engineering and Dr. M.R. Haddara, Associate Dean of Engineering, for the excellent computational facilities provided by the Faculty of Engineering and Applied Science, Memorial University, St. John's, Newfoundland.

I am also indebted to my wife Wienta and my son Nugroho for their continuous support, encouragement, and understanding.

Table of Contents

Abstract ii

Acknowledgments iv

Table of Contents v

List of Tables vii

List of Figures viii

List of Symbols xii

Chapter 1. Introduction 1

1.1. Aims and Motivation of the Thesis 1

1.2. Outline of the Thesis 5

Chapter 2 A Review of Artificial Reefs 7

2.1. Introduction 7

2.2. Artificial Reefs Deployment in the World 8

2.3. Purpose, Types, and Materials of Artificial Reefs 15

2.4. Design and Engineering of Artificial Reefs 21

2.4.1. Environmental Characteristics 21

2.4.2. Ecological View and Fish Behavior 23

2.4.3. Geographic Location and Reefs Placement 30

2.4.4. Physical Criteria 35

2.4.5. Stability Consideration 40

2.4.6. Artificial Reefs as Wave Dissipating Structures 41

2.5. Summary 46

Chapter 3 The Volume of Fluid (VOF) Method 47

3.1. Introduction 47

3.2. Volume of Fluid Method (Nichols and Hirt, 1981) 48

3.3. Approximation of VOF by FLOW3D..... 52
3.3.1. Notation..... 53
3.3.2. Momentum Equations in Variable Mesh..... 54
3.3.3. Continuity Equation..... 57
3.3.4. Volume of Fluid (VOF) Function..... 60
3.3.5. Boundary Conditions..... 62
3.4. Summary..... 64

Chapter 4 Two Dimensional Modelling of Artificial Reefs with Hollow Hemispherical Blocks..... 65
4.1. Introduction..... 65
4.2. Numerical Model..... 66
4.3. Results and Discussion..... 71
4.4 Summary..... 96

Chapter 5 Three Dimensional Modelling of Artificial Reefs with Hollow Hemispherical Blocks..... 97
5.1. Introduction..... 97
5.2. Numerical Model..... 98
5.3. Results and Discussion..... 102
5.4. Summary..... 122

Chapter 6 Conclusions and Recommendations for Future Study..... 123
6.1. Conclusions..... 123
6.1. Recommendations..... 125

References..... 127
Appendix A..... 135
Appendix B..... 142
Appendix C..... 146

List of Tables

Table	Title	Page
2.1	Types of artificial reefs according to their purpose (Harris, 1995)....	16
2.2	Types of material used for artificial reefs (Groove et al, 1991).....	20
2.3	Various parameters affecting selection of reef sites.....	30
2.4	K_D values for breakwater blocks (CERC, 1984)	41
4.1	Number of Cells Used in Varying Grid Sizes.....	70
4.2	Breaking wave characteristics and the surf similarity parameter (Battjes, 1974)	72
5.1	Number of cell used in computational domain.....	99
A.1	Namelist in 'prepin dat'.....	138

List of Figures

Figure	Title	Page
1.1	Manufactured concrete breakwater blocks (Mottet, 1985)	2
1.2	SAB chamber structures (Mottet, 1985)	3
1.3	Smooth-shaped reefs (Mottet, 1985, RBDG, 1997)	4
2.1	Various types of artificial reefs	17
2.2	Type of fishes according to their response to the reefs ('Reefiness') (Nakamura, 1985)	25
2.3	Wake behind the artificial reefs (Takeuchi, 1991)	27
2.4	Current shadow behind a two dimensional obstacle (Takeuchi, 1991)	28
2.5	Lee wave due to artificial reefs (Nakamura, 1985)	29
2.6	Turbulent wake due to wave action (Takeuchi, 1991)	30
2.7	Preferred reef location (Grove and Sonu, 1985)	31
2.8	Fish path due to internal waves (Grove and Sonu, 1985)	32
2.9	Fish position during the passage of an internal wave (Grove and Sonu, 1985)	32
2.10	Currents patterns around artificial reefs (Yoshioka et al, 1993)	33
2.11	Typical size scales of artificial reefs (Kakimoto, 1991)	37
2.12	Typical horizontal configuration of a reef group (Grove et al, 1991)	38
2.13	Geometry of artificial reefs	41
2.14	Typical incipient wave breaking (Smith and Krauss, 1990)	43
2.15	Breaker Height as a function of deepwater steepness	43
2.16	Typical wave frequency distribution (Yoshioka et al, 1993)	44
2.17	Wave breaking effect of artificial reefs (Toshioka et al, 1993)	45
2.18	Longitudinal artificial reefs	46

3.1 Computational mesh..... 48

3.2 Location of variables..... 49

3.3 Typical free surface cells..... 51

3.4 Control volume in x-y plane used in finite-difference approximation for u momentum (Hirt and Nichols, 1981) 56

3.5 Definition of variables η in free surface pressure boundary condition... 59

3.6 Examples of free surface shapes used in the advection of F. The cross-hatched region in b-d are the actual amounts of F fluxed (Hirt and Nichols, 1981). 61

4.1 Typical reef and applied grids..... 66

4.2 Typical three-dimensional reefs arrangement..... 67

4.3 Placement of reefs and salient points of interest within a reef..... 68

4.4 Velocity magnitudes and water surface profile histories for varying grid sizes near reefs..... 70

4.5 Types of breaking waves on the shore (Wiegel, 1964) 72

4.6 Water surface profile without reefs..... 74

4.7 Water surface profile with one reef..... 74

4.8 Water surface profile with two reefs..... 75

4.9 Water surface profile with three reefs..... 75

4.10 Water surface profile with six reefs..... 76

4.11 Water surface profile with twelve reefs..... 76

4.12 Water surface profile and surface velocity magnitudes time series for one reef at x:+15..... 77

4.13 Water surface profile and surface velocity magnitudes time series for two reef at x:+15..... 78

4.14 Water surface profile and surface velocity magnitudes time series for three reefs at x:+15..... 79

4.15 Water surface profile and surface velocity magnitudes time series for six reefs at x:+15.0m..... 80

4.16 Water surface profile and surface velocity magnitudes time series for twelve reefs at x:+15.0m..... 81

4.17 Velocity magnitudes for a beach without reefs at various times..... 84

4.18 Velocity magnitudes for a beach with one reef at various times..... 85

4.19 Velocity magnitudes for a beach with two reefs at various times..... 86

4.20 Velocity magnitudes for a beach with three reefs at various times..... 87

4.21 Velocity magnitudes for a beach with six reefs at various times..... 88

4.22 Velocity magnitudes for a beach with twelve reefs at various times... 89

4.23 Velocity magnitude time series for one reef at points A, B, and C..... 91

4.24 Velocity magnitude time series for two reefs at points A, B, and C.... 92

4.25 Velocity magnitude time series for three reef at points A, B, and C.... 93

4.26 Velocity magnitude time series for six reefs at points A, B, and C..... 94

4.27 Velocity magnitude time series for twelve reef at points A, B, and C. 95

5.1 Typical three dimensional reef arrangement 98

5.2 Computational grid used for three-dimensional model with twenty-four reef units..... 100

5.3 Points of interest within the reef units..... 101

5.4 Wave profile without reefs, T: 5.0 sec..... 103

5.5 Wave profile with twelve reefs, T: 5.0 sec..... 103

5.6 Wave profile with fifteen reefs, T: 5.0 sec..... 104

5.7 Wave profile with twenty-four reefs, T: 5.0 sec..... 104

5.8 Wave profile without reefs, T: 4.0 sec..... 105

5.9 Wave profile with twenty-four reefs, T: 4.0 sec..... 105

5.10 Wave profile without reefs, T: 3.5 sec..... 106

5.11 Wave profile with twenty-four reefs, T: 3.5 sec..... 106

5.12 Surface wave history for three different reefs at x: +18.0 Ho: 1.0m, L: 27.94m, T: 5 sec..... 108

5.13 Surface wave history for three different periods at x: +18.0 m..... 109

5.14 Time series of velocity magnitude for a beach without reefs at y=+2.0m..... 111

5.15 Time series of velocity magnitudes for a beach with twelve reef at y=+2.0m..... 112

5.16 Time series of velocity magnitudes for a beach with fifteen reefs at y=+2.0m..... 113

5.17 Time series of velocity magnitudes for a beach with twenty-four reefs at y=+2.0m..... 114

5.18 Time series of velocity magnitudes for the beach without reefs shown three dimensionally..... 115

5.19 Time series of velocity magnitudes for the beach with twelve reefs shown three dimensionally..... 116

5.20 Time series of velocity magnitudes for the beach with fifteen reefs shown three dimensionally..... 117

5.21 Time series of velocity magnitudes for the beach with twenty-four reefs shown three dimensionally..... 118

5.22 Velocity magnitudes time series for twelve reefs at points A, B, and C. 119

5.23 Velocity magnitudes time series for fifteen reefs at points A, B, and C. 120

5.24 Velocity magnitudes time series for twenty-four reefs at points A, B, and C..... 121

A.1 FLOW3D Modules.. 135

A.2 File structure for regular run (non restart; t=0) 136

A.3 File structure for non regular run (restart; t>0) 137

A.4 Flow chart for SOLA-VOF..... 139

List of Symbols

A	projection area of reef
A_x	fractional areas open to flow in the x axis
A_y	fractional areas open to flow in the y axis
A_z	fractional areas open to flow in the z axis
AFR	fractional area A_x for flow along x axis at right cell
AFB	fractional area A_x for flow along y axis at back cell
AFT	fractional area A_x for flow along z axis at top cell
B	the width or thickness of reefs structural member, the width of reefs
c	adiabatic speed of sound in the fluid
C_D	drag coefficient
d	water depth
D	reef height
f_x	viscous accelerations at x direction (VISX)
f_y	viscous accelerations at y direction (VISY)
f_z	viscous accelerations at z direction (VISZ)
FUX	advective flux of u in the x axis
FUY	advective flux of u in the y axis
FUZ	advective flux of u in the z axis
FVX	advective flux of v in the x axis
FVY	advective flux of v in the y axis
FVZ	advective flux of v in the z axis
FWX	advective flux of w in the x axis
FWY	advective flux of w in the y axis

FWZ	advective flux of w in the z axis
F	fractional volume of fluid
F'	freeboard of the reef
Fr	Froude number
g	gravitational acceleration
g_x	accelerations due to gravity in the x axes
g_y	accelerations due to gravity in the y axes
g_z	accelerations due to gravity in the z axes
h	height of the reef
H	wave height
Hb	breaker wave height
Ho	deep water wave height
Ht	transferred wave height
i	spatial step at x direction
j	spatial step at y direction
k	spatial step at z direction
k	wave number
K_D	stability coefficient
Kt	coefficient of transmission
Lr	reef length
Lo	deep water wave length
n	computational time step
N	number of reef units
N_s	reefs stability number
p	pressure

S' deployment area of reef units

S projection area of the maximum envelope of reef.

t time

T wave period

u fluid velocity in the x direction

u' velocity of shadow currents (wake)

v fluid velocity in the y direction

V_F fractional volume open to flow.

w fluid velocity in the z direction

W_a weight of reefs

Wr reef width

x horizontal axis

X shadow area of an average reef units

y lateral axis

Y offshore reefs distance from shoreline

z vertical axis

α slope of beach

β slope of triangular reefs

γ specific weight

θ slope angle of the reef toe

ρ density

σ wave angular frequency

Ω_b breaker height

ξ surf similarity

Chapter 1
Introduction

1.1. Aims and Motivation of the Thesis

Breakwaters, as an example of coastal structures, are usually adopted to protect and stabilize the coastal areas from the effect of waves and other hydrodynamic forces. They are generally built parallel to the shore with their crests above high water. Some structures are designed to reflect wave energy, while other structures attempt to decrease most of the wave energy through wave breaking and dissipation upon and within a permeable structure. Other types of breakwaters, which have their crests below the water surface have been considered by many researchers due to their economic advantage (Ahrens, 1987). These breakwaters are called as low-crested breakwaters, submerged breakwaters, reef breakwaters, or artificial reefs (Ahrens 1987, Harris, 1995). In this thesis, since every immersed object can potentially be considered as a reef, these submerged man-made structures are called artificial reefs.

Artificial reefs, commonly referred as submerged structures, are used either as energy dissipating structures or fish aggregating devices (FADs) in the coastal

environment. However, since both of them have similar purposes, the term "FADs" is being used to refer to suspended structures in water column, as "artificial reefs' refer to structures placed on the seabed. Artificial reefs were widely and traditionally used since early times to attract fish and increase their productivity beside FAD's (Bohnsack et. al. 1991, Bombace 1989, Ino 1974, Seaman & Sprague 1991,)

The popularity and the beneficial uses of artificial reefs are growing rapidly. Many countries, such as Japan, USA, Italy, Spain, and Australia, have been very active in the design, development, deployment and utilization of artificial reefs. More over, Japan is the only country where reef design processes have been codified into official manuals.

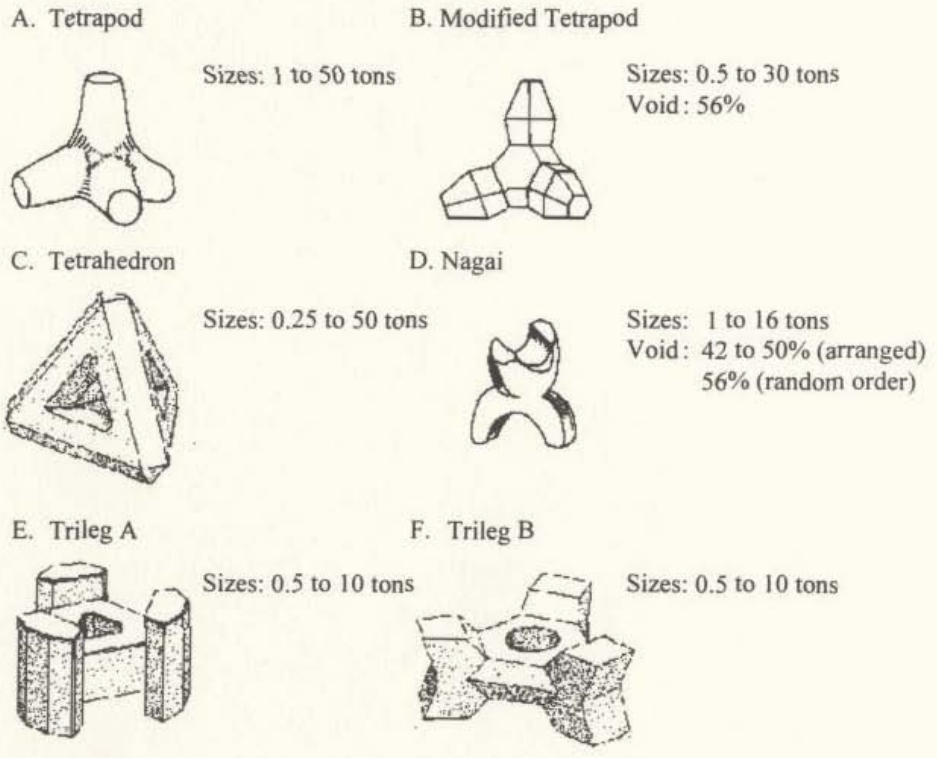

Figure 1.1. Manufactured Concrete Breakwater Blocks (Mottet, 1985)

The engineering properties of artificial reefs are similar to the submerged breakwaters. Concrete breakwater blocks such as tetrapod, tetrahedron, or trileg (Figure 1.1), are commonly used as artificial reefs because they have large surface areas. Some breakwater blocks such as tetrapod may be more effective in growing seaweed than many substrate blocks (Mottet, 1985).

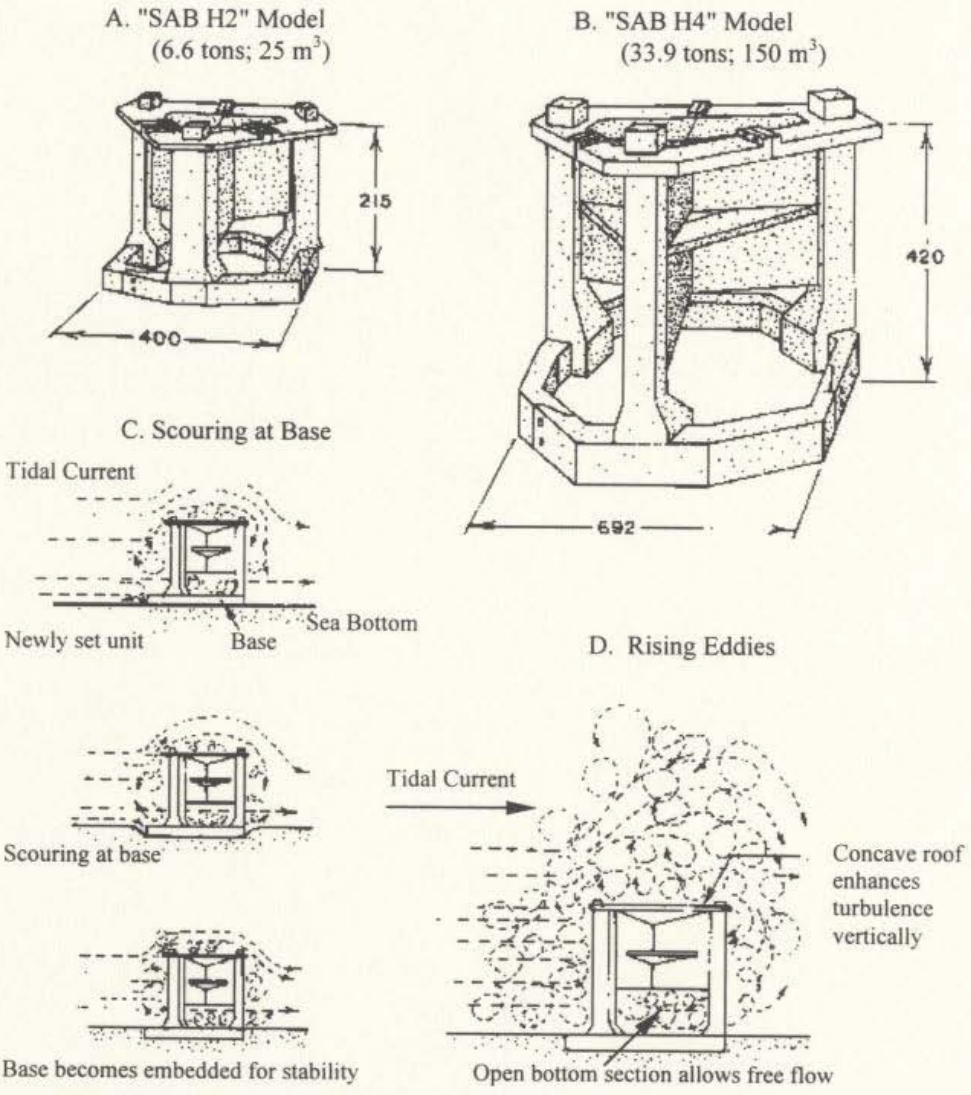

Figure 1.2 SAB Chamber Structures (Mottet, 1985)

Various artificial reefs have been used to attract fish by producing coherent eddies with upward flow as well as by providing hiding places for fish such as the "SAB Chamber Structure" model (Figure 1.2) (Mottet, 1985). Most of these reefs have rectangular shapes and cause tearing of fishing nets. In order to reduce entanglement of fishing nets, bottom-seated smooth-shaped reefs were proposed as alternatives, such as cylindrical shapes, turtle blocks, and reef balls as given in Figure 1.3 (Mottet 1985, Reefball Development Group 1997).

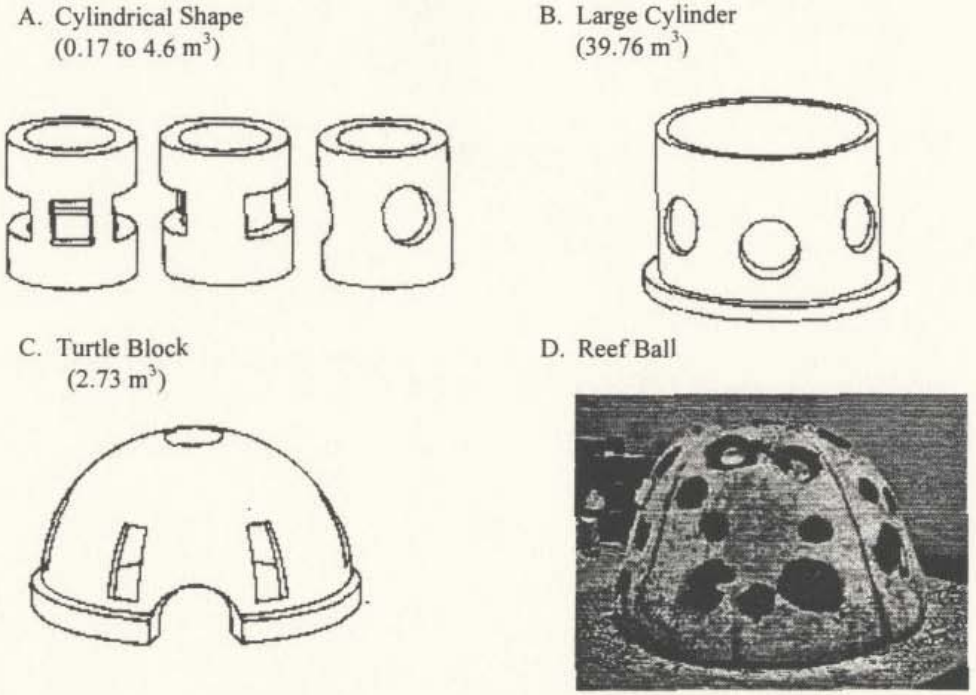

Figure 1.3. Smooth-shaped Reefs
(Mottet 1985, Reefball Development Group 1997)

The reefs should generate enough vortices and turbulence for fish, since their abundance was influenced by current vortices (Lindquist and Pietrafiesa, 1989), and the fish tended to face into the current to maintain its position while capturing food (Bohnsack et. al., 1994).

Flow field in the vicinity of artificial reefs, as shown in Figure 1.2 D, can be determined from either field observation, experimental investigation or numerical calculation. Very few studies have been carried out on predicting numerically the fluid flow characteristics around a submerged artificial reef. Field observation carried out by Ohnaka & Yoshizawa (1994) and experimental studies by Smith & Kraus (1990) detail the influence of reef geometry on wave breaking and wave characteristics. Even though they discuss about the wave dissipation characteristics, no conclusive evidence has been presented on the scheme. This thesis focuses on the numerical analysis of the flow field around an artificial reef with a view to facilitate aquaculture developments. The intent of this thesis is to implement a numerical model for fluid flow around artificial reefs made of single and multiple hollow hemispherical blocks, and to compute the optimum form for the reef that will minimize the fluid velocities and wave amplitudes inside the basin as well as within the individual reef blocks.

1.2. Outline of the Thesis

The thesis consists of six chapters. This chapter briefly describes the salient features of artificial reefs besides outlining the aim and the motivation for the thesis. The remaining chapters of the thesis describe the use of artificial reefs in coastal areas and their characteristic features. In addition, the development of finite volume methods for numerical analysis of fluid flow and its use in the modelling of artificial reefs are given along with a comprehensive set of numerical results obtained from this study.

Chapter 2 presents a detailed review of the work carried out on artificial reefs. The history and utilization of reefs in coastal environment, function, type and design are given

in detail. Submerged artificial reef characteristics, the numerical method used in analysis, and their implementation are presented in Chapter 3. In Chapter 4, two-dimensional analyses of single and multiple hollow artificial reefs are discussed and the results presented. Furthermore, analyses of three-dimensional models are discussed in Chapter 5 along with the presentation of results. Finally, in Chapter 6, the contributions of this thesis are summarized and suggestions for further study are presented.

Chapter 2
A Review of Artificial Reefs

2.1. Introduction

Most of the earlier studies on artificial reefs have been carried out by biologists and marine scientists rather than coastal engineers. Their investigations were merely on the biological-environmental aspects such as assemblage of fish in the vicinity of reefs, reef productivity, or comparative studies between artificial and natural reefs. Only a few of them investigated the hydraulic or engineering aspects of artificial reefs. Meanwhile, other studies, mostly carried out by coastal engineers emphasized the utilization of reefs as breakwaters only.

This chapter presents a synopsis on artificial reefs especially those for fish enhancement habitats. A brief history of artificial reef utilization and its deployment are given in Section 2.2. The materials used in reef construction along with the purpose and reef type are presented in Section 2.3. Section 2.4 covers the environmental factors considered and the design and engineering aspects of artificial reefs.

2.2. Artificial Reefs Deployment in the World

Artificial reefs may refer to man-made structures that serve as shelter and habitat, source of food, and breeding area (White et al., 1990) for marine animals; they are also used for shoreline protection (Creter, 1994) or as surf-waves generating devices (Craig, 1992). Recently, the term has been used to refer to a variety of submerged structures sunk in the nearshore area (Harris, 1995). They are normally placed in designated areas to improve or recover their environmental resources, viz., in an area with (i) low productivity or where habitat and environment has been degraded such as an eroded shoreline (Creter, 1994); (ii) natural reef flat degradation (Clark and Edwards, 1994) or (iii) in an area where waves need to be generated for surfers (Craig, 1992). However, most of the artificial reefs have been used successfully as fish production enhancement structures for a long time, especially in Japan and United States of America (Grove et al., 1989 and 1994; McGurrin and Reeff 1986; Mc Gurrin et al, 1989; Stone 1985; and Stone et al., 1991).

According to Stone et al (1991) Japan's artificial reef history can be divided into three phases of development. First phase was started in the Kansai Era (1789 - 1801), probably earlier (Ino, 1974). At that time, submerged object such as fallen trees and cut brush, as well as sunken ship and intentionally placed rocks, were used to aggregate fish. The first phase was characterized by small-scale and traditionally constructed reefs installation. The second phase was marked by actively promoted construction of artificial reefs, backed up by numerous financial grants from the government in power, lasting from 1954 to 1974. The traditional name for artificial reefs *Tsukiiso* (man-made shore

rock) was replaced by official name Gyosho (fishing reef). In this phase, the large-scale (Oh-gata) as well as the ordinary scale (Nami-gata) reefs were deployed in several areas, and cost approximately US $ 93 millions (Ino, 1974). In 1974, the final stage of Japan's program was begun when the Coastal Fishing Ground Development Act was ratified. Then in 1975 the Artificial Reef Fishing Ground Construction Program was initiated to use artificial reef technology to create new fishing grounds. Serious efforts by Japanese fisheries technology firms, using the Ensei Financial Program have published two guidelines for reef design and constructed the first marine ranch in Saiki Bay on Kyushu Island in 1984. Japanese government founded a semi governmental organization "Marine Forum 21" in 1985 to consolidate the nation's fishery resources; through the Ensei Program, Japan is trying to change the conventional "catch fishery" approach to "culture fishery" approach (Grove et al., 1989 and 1994).

Similar to Japanese efforts, artificial reefs have been used to improve fisheries history for over 100 years in United States. However, their utilization as a resource enhancement technique have been known and developed only recently (McGurrin et al., 1989). Initially, the efforts were carried out by local communities or local associations separately. Only after the National Fishing Enhancement Act was passed in 1984 resulting in the mandated development of the National Artificial Reef Plan in 1985, the fisheries resource enchancement, using artificial reefs, become a synergized effort by a wide society including fishermen, divers, researchers, conservation group, companies, and government agencies (McGurrin and Reeff, 1986). Recently, artificial reef development has been carried out not only in the coastal or estuarine areas, but also in the freshwater areas present in various temperature zones.

First artificial reef was built in South Carolina in 1860s (Stone, 1985) using logs, while large scale ocean artificial reef constructions were made in 1935 using boat and other material in New Jersey (McGurrin and Reeff, 1986). After World War II, the first reef built was the"Beer-Case Reef" off the New York coast in 1950s which was made from 14.000 wooden beer cases filled with concrete.

Private sector, especially oil companies in Gulf of Mexico, has been involved intensively in "Rigs to Reefs" program. Their efforts together with the state agencies in submerging obsolete oil and gas offshore platforms as artificial reefs can lead to increasing sophistication of artificial reef technology and more innovative artificial reef application. In the future, since the problems encountered in artificial reefs have become site specific, US government expects private sector such as utility (coal ash reefs) and LNG industries (rigs-to-reefs) to work closely with state agencies to become active sponsoring and supporting agencies for artificial reef research (McGurrin et al, 1989).

Meanwhile in the Mediterranean Seas, artificial reefs, consisting of car wrecks, have been deployed in a limited zone to counter illegal trawling since the early 1970's. The use of artificial reefs in the Mediterranean (Italy, France, Spain) is still in an experimental stage and is limited to a few coastal areas, mainly to protect the marine meadows (*posidonia oceanica*) and to enhance the traditional fisheries (Bombace, 1989). As already known, the marine meadows are widely distributed in the Mediterranean Sea and has ecological importance in producing oxygen, providing nursery areas for young ones, and stabilizing the sea-bed (Guillen et al, 1994). In the southeastern area with the lowest fisheries productivity in the Mediterranean Sea, an experimental tire reef

construction was planned and the model tested in Haifa (Spanier et al. 1985): the installation was intended to increase the fishery production.

In Spain, on the Southwest and Western Mediterranean, the construction of artificial reefs was proposed as a possible solution for over-exploitation of near-shore fishery resources. There are three period of reefs construction in Spain, 1979-1986, 1987-1991, and 1992-1996 (Gomez-Buckley and Haroun, 1994). During the first stage and before, the construction techniques and design of artificial reefs were poorly developed, and the materials used were mainly materials of opportunity (car bodies, concrete blocks, ceramic pieces, etc). The second and third stages were the systematized stages, when a Multi-annual Guidance Program (MAGP) was released in 1987 by the Spanish Government. Under the supervision of the European Economic Community (EEC), the reefs construction, as well as its assessment, was organized. The MAGP integrated artificial reefs construction criteria (i.e: materials, design, place, selection, etc) also ensured the proper scientific assesment for all future artificial reefs to be established in the Spanish coastal zone. The second MAGP, which was approved by EEC in 1991, enabled Spain to continue its efforts in ecological enhancement using artificial reefs for the next 5 years (Gomez-Buckley and Haroun, 1994).

Several installations of artificial reefs were reported from Spain. Off the shores of Barcelona, in 1979, the first big scale artificial reef was constructed covering 1000m^2 area which consisted of several materials (concrete blocks, ceramic pieces, fiber-cement and car bodies) [Gomez-Buckley and Haroun, 1994]. In the Balearic water (1989 - 1990), numerous 'boulders' made from concrete were deployed to prevent further damage to the seabed as well as to enhance its natural regeneration (Moreno et al, 1994). In Canary

Islands (1990-1991), concrete blocks were immersed (Haroun et al. 1994), and in the marine reserves of Tabarca, Alicante, they were used to protect the degradation of marine meadow due to illegal bottom trawling fishing and to provide alternative fishing sites (Bayle-Sempere et al. 1994).

France started artificial reefs in 1982 to prevent illegal trawling and has also made several experimental efforts to build artificial reefs in five protected marine parks (Bombace, 1989). Most of the materials consisted of old tires, car wrecks, concrete cylinders blocks and other building materials, deployed at several sites such as Palavas-les-Flots (1968), Concarneau (1970-1973), Gulf of Juan and Villefranche-sur-mer (1980's), and Port La Nouvelle (1980).

Among the Mediaterranean countries, Italy is very active in deploying reefs and developing scientific studies in habitat enhancement especially for shellfish. Two different periods were noted in Italy: initially, small sporadic experiments were carried out before the 1970s, and then a better scientifically coordinated effort. Since commercial fishermen receive the benefits from the artificial reef projects, they actively supported and promoted the projects, from the beginning.

The first artificial reef in Italian waters was submerged in December 1970 near Varazze in the Ligurrian Sea (Gulf of Marconi) by a group of fishermen without any scientific support. The reef consisted of 1300 car bodies and 16 wooden barges (immersed later, during 1979) to prevent illegal trawling and to improve sports fishing in the area (Relini and Relini, 1989a).

In 1974, the first systematic plan in the Mediterranean Sea was started in Ancona, Italy, through the Marine Fisheries Research Institute (IRPeM) by deploying concrete

blocks and some old boats in Adriatic Sea. Financial supports were obtained from the Italian state and European Economic Community (Bombace, 1989). In the Ligurian Sea (Marconi Gulf), an artificial reef was completed between 1980 - 1985 consisting of concrete blocks, barges, dock-gates, and other materials such as gravel, sand and coarse pebbles. The reef was intended to offer a hard substrata to spores, seedlings and larvae of sessile organisms, as well as to offer shelter and protection to eggs, juveniles and molting animals; they protect small-scale fishing resources (Relini and Relini, 1989a). Furthermore, from 1987-1988, five artificial reefs using cubic concrete block (2 x 2 x 2 m), in the pyramidal arrangement, were constructed along Italian Adriatic coast resulting in a gradual increase of fish abundance, species richness and diversity (Bombace et al 1994). Currently, coal ash is being used for reefs under construction in Italy (Sampaolo and Relini, 1994)

Artificial reefs utilization in Australia were mainly promoted by recreational fishermen and divers (Branden et all 1994) and recently, by surfers (Anderson, 1997). Australia's experiences with artificial reefs began in 1965 when the Victorian Departement of Fisheries and Wildlife deployed 300 waste concrete pipes in Port Philip Bay near Melbourne. However, derelict vessels were scuttled in Queensland in the late 1960's by private divers groups. Since the Australian government restricted the materials for reefs to be at little or no cost and durable for at least 20 years, ballasted tires and derelict vessels have become the widely accepted materials for reefs; no large-scale concrete blocks have been deployed so far (Pollard and Matthews, 1985)

In the Arabian Gulf reports of artificial reef activities have come from Kuwait and Qatar. Three experimental tire modules were deployed in the waters off Ras Al-Zoor.

Kuwait, in 1981 as the first artificial reef in the Arabian Gulf (Downing et al. 1985). The purpose of these structures was to concentrate fish in the area. In Qatar, reefballs were deployed by Qatar Science Club in Arabian Gulf, sponsored by an oil company in 1997 (Reefball Development Group, 1997).

Studies in Taiwan, confirmed the effectiveness of artificial reefs for natural resource preservation, habitat reconstruction, and nursery ground. Concrete blocks ($1m^3$ and 12 m^3), scrapped boats, junk cars, used tires, and bamboo were used as reefs. However, the most effective and most often used materials were concrete blocks and scrapped boats (Chang, 1985).

As noted by White et al (1990), widespread interest of Southeast Asian countries in artificial reef construction, as a part of coastal zone management for resource enhancement, developed in the late seventies. Thailand initiated an artificial reef construction program in 1978, covering seven coastal provinces along the Gulf of Thailand and the Andaman Sea (Sinanuwong, 1991). In Malaysia, artificial reefs were established in the early 1970s where they started as initiatives of the small-scale fishermen in the east coast of Peninsular Malaysia, particularly in the states of Kelantan and Trengganu, by sinking derelict wooden boats, branches of trees and rocks (Delmendo, 1991). The Philippines started a national program in 1981 and has established 70 small-scale artificial reefs in different parts of the country. In Singapore, the National University of Singapore initiated an artificial reef project on an experimental basis in 1989 under ASEAN/US Coastal Resources Management Project (CRMP). In Darussalam, Brunei, artificial reef construction began in 1984 for fish aggregation and habitat enhancement (White et al, 1990). Indonesia has experimented in Jakarta Bay

where *becak* (tri-cycles/pedicabs) which are banned by the city of Jakarta, and used busses have been dumped into the bay to attract fish since 1985 (Hardjono, 1990).

From the various national plans and programs above, Stone (1991) classified them into three categories;

- Governments that may have a plan and hence fund deployment such as Japan (Grove et al, 1989, 1994; Stone, 1991)
- Goverments that may have a plan but have spent nil or only minimal funding such as USA (Stone, 1991), Australia (Branden et al, 1994), France (Bombace, 1989),and Italy (Bombace, 1989); and
- Governments without a plan yet, but were committing modest funding to experimental or full-scale deployment of reef. This commonly occurred in developing countries such as India (Stone, 1991), Kuwait (Downing, et al. 1985), and Southeast Asian countries such as Malaysia, Thailand, Philipines, and Indonesia (White, et.al, 1990),

2.3. Purpose, Types, and Materials of Artificial Reefs

As noted above, artificial reefs were widely and traditionally used since early times to attract fish and increase the productivity of fishing, besides being fish aggregating devices (FADs). According to Chou (1997), the major functions of artificial reefs are to:

- aggregate organisms to enable more efficient fishing,
- increase natural productivity by providing new habitats for encrusting organisms which contribute to food chain,
- create habitats for desired target species, and

- protect small/juvenile organisms and nursery areas from destructive fishing gears.

Furthermore, the reasons for the uses of artificial reefs are summarized as follows (Harris, 1997):

- Environmental enhancement [to increase the amount of hardbottom (perplexing rocky outcrops) and the associated community]
- Fish aggregating devices (FADs) and aquaculture
- Mitigation of damages (replace the damaged hardbottoms)
- Attraction for eco-tourism (diving)
- Shoreline erosion control and harbor protection (breakwaters and wave absorbers)
- Surfing enhancement

The first two of the above represent the traditional uses of artificial reefs, while the latter four are more newly developed uses. According to the purposes listed above, Harris (1995) classified the artificial reefs into five types as given in the Table 2.1 below:

Table 2.1. Types of Artificial Reefs According to Their Purpose (Harris, 1995)

	Reef Type	Purpose	Water Depth[1]	Structure Type[2]
1.	Environmental Enhancement	Increase hardbottom, mitigation	0 – 100m +	B or F
2.	Fishing Reefs	FADs, upwelling, aquaculture	0 – 100m +	B or F
3.	Diving Reefs	Snorkeling and diving, eco-tourism	0 – 40m	B
4.	Breakwaters	Wave height reduction	0 – 10m +	B or F
5.	Surfing Enhancement	Breaking wave form enhancement	1 – 5 m	B

Notes:

1. Typical water depths, + signs indicate some deeper applications possible
2. B = Bottom mounted reef structure, F = floating reef structure
3. FAD = fish attracting device

Artificial reefs also can be classified according to their structural design. Depending on the purpose of the reefs and the design depth, artificial reefs can be either bottom mounted or floating. The reef may be made up of a number of reef units or the reefs may consist of one large individual unit, such as a ship. Various types of artificial reefs are given in Figure 2.1

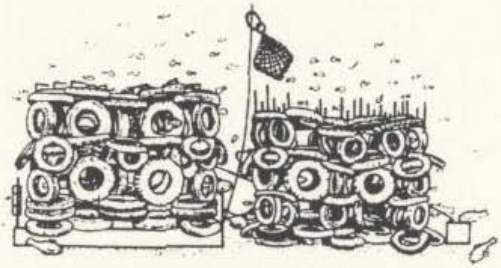

A. Fish habitat enhancement; Used Tire (Spanier et al 1985)

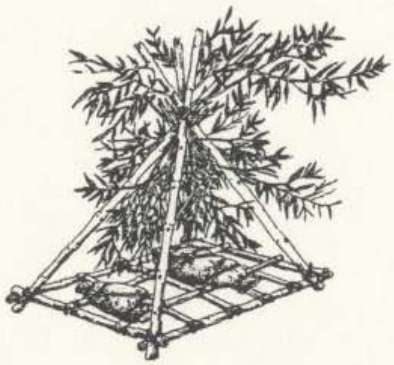

B. Fish habitat enhancement; Bamboo. (White et al 1990)

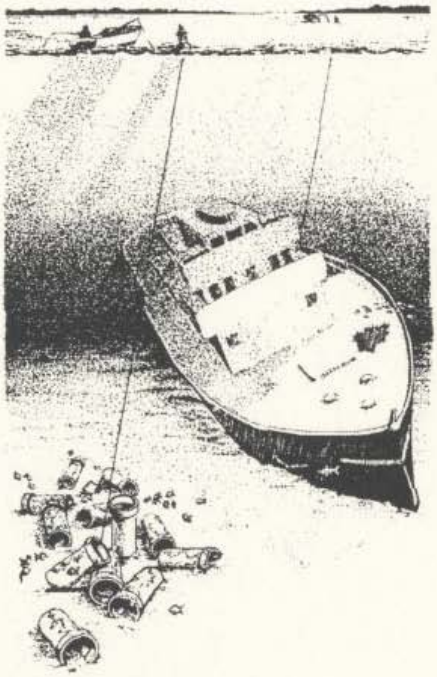

C. Fish habitat enhancement; Materials of opportunity (Seaman and Sprague 1991)

Figure 2.1 Various Types of Artificial Reefs

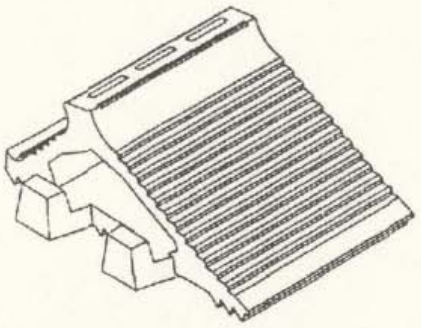

D. Shoreline protection, Concrete (Creter 1994)

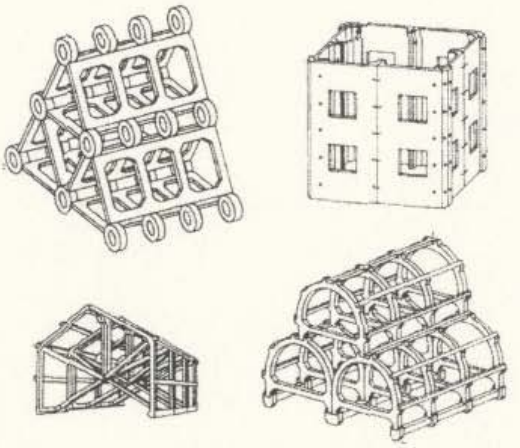

E. Fish habitat, Prefabricated Ferroconcrete (Mottet. 1985)

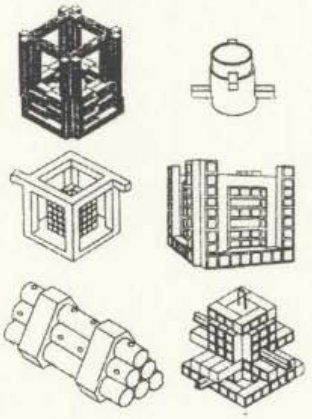

F. Anti-trawling structures and restoration/ production modules: Fabricated concrete blocks (Gomez-Buckley & Haroun 1994, and Moreno et al, 1994)

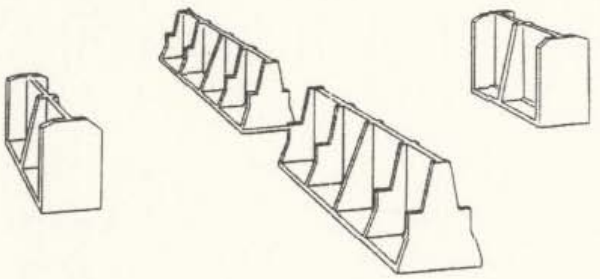

G. Upwelling System, Concrete (Otake et al 1991)

Figure 2.1 Various Types of Artificial Reefs (continued)

Essentially, various materials used for artificial reefs can be divided into two types: natural and man-made. The natural materials include rocks, and vegetations such as bamboo, log cribs, and brush piles which can be placed either individually, or as a pile. The man-made materials include new materials such as fabricated reinforced concrete,

steel, FRP (fiberglass reinforced plastics) or used materials such as worn-out tires, vessels, and coal ash.

The abundance of used and waste materials has reduced the costs involved in artificial reef construction, usually an important consideration for developing countries (Chou, 1997). Therefore a waste materials or material of opportunity reef (Harris, 1990, Harris et al 1996) consisted materials such as used tires, old vehicles, ships, boats, etc., are not recommended by environmentalists for use in as artificial reefs. Furthermore, Harris (1995) classified materials of artificial reefs as:

- Waste disposal (or "material of opportunity")
- Custom designed materials, or
- Combinations of the above

Special materials can also be used for the custom designed reef units. Concrete units, for example, can be fabricated from concrete containing fly ash, micro silica, and other additives used to increase the strength, durability, and compatibility of the material with the marine environment (Reefball Development Group, 1997). The surface of the concrete can be roughened, native rocks can be cemented in, and different size voids and surface areas can be created to provide the habitat required by various marine organisms: and to minimize settlement and reduce scour, geotextile can be used underneath reef units (Harris, 1995). Another reef was constructed from waste products of coal combustion (Collins et al, 1994a, 1994b) and mineral accretion where calcium carbonate and magnesium hydroxide were precipitated from seawater onto conductive materials using direct electrical currents (Hilbertz and Goreau, 1996).

Grove et al (1991) classified materials for reefs. in the aquatic environment. as given in the Table 2.2 below.

Table 2.2. Types of Material Used for Artificial Reefs (Grove et al. 1991)

Material and Structure	Environment and application		
	Ocean	Estuary	Freshwater
Natural Material			
▪ Bamboo	C	-	-
▪ Brush	A	-	
▪ Coconut	A	-	-
▪ Oyster Shell	-	H	-
▪ Quarry Rock	R,H,M,E	R	-
▪ Rope	A	-	R
▪ Stone (piled or in gabions)	H	H	-
▪ Trees, Logs	H	-	R
▪ Wooden Frames	R	R	R
			-
Manufactured or Scrap Products			
▪ Concrete			
▪ Poured structures	R,C,H,E	R,H,E	E
▪ Rubble	R,H	R	R
▪ Fiberglass/plastic			
▪ Benthic reef Modules	R,C,	-	-
▪ Midway buoys, streamers	R,C,A,E	R,H	-
▪ Seaweed	H	-	R
▪ Incineration ash	E	-	E
▪ Rubber			
▪ Automobile tires	R,C,A,H,E	R,H	R
▪ Steel			
▪ Automobile bodies	R,C,H	R,H	-
▪ Benthic reefs modules	C	-	-
▪ Fuel Storage tanks	R	-	-
▪ Petroleum Production Platforms	R	-	-
▪ Street Cars (trolleys)	R	-	-
▪ Vessels	R,H	R	-
▪ Wood			
▪ Vessels	C	-	-

Note: A: Artisanal (small-scale) fishing; C: Commercial Fishing; E: Experimental; H: Habitat enhancement; M: Mitigation; R: Recreational Fishing

In Southeast Asia (Chou, 1997) and other developing countries, natural materials for reefs such as bamboo and wood are commonly used. In Japan, materials approved for use in reef project were required to provide durability for 30 years or more of useful life: therefore, concrete, steel, FRP and stone were used widely. However, in some countries, such as Italy (Relini and Relini, 1989b), scrap materials such as car bodies, old ships or similar waste materials were not suggested due to the possibility of damaging the environment due to the hazardous nature of the byproducts of corrosion.

2.4. Design and Engineering of Artificial Reefs.

Suitable structures used to enhance aquaculture habitats, must have such functions as providing shelters to eggs, larval and juvenile fish as well as providing prey organism. These structures must also be based on the clear understanding of the ecology of the target species (Kakimoto, 1991). From this point of view, the engineering and design of artificial reefs will be discussed based on the environmental, ecological, biological, hydrodynamical and topographical aspects.

2.4.1. Environmental Characteristics

Once the reefs were deployed, environmental condition in the reefs vicinity would be changed. Sessile plankton was able to aggregate in the shaded area of reefs. Subsequantly, new fish species that depended on these organisms were established. Physical characteristics such as currents, bed load deposition, or bottom materials would also be changed once the reefs were installed. Phenomena such as vortex shedding and wake formation in the lee of the reefs, zones of acceleration, stagnation and turning of

currents on the upcurrent side of the reef, geometrical shade and shadow in the surrounding space and within the reef, and generation of topographic wave and perturbations associated with internal waves would occur in the vicinity of the reefs. Furthermore, these phenomena would encourage the attachment of sessile organisms, growth of seaweed and algae, and local settlement of drifting algae, and finally provide diversity in substrate types. Artificial reefs also provide shelter, feeding, spawning, playing grounds, rest area, and temporary stop-over for fish and create their local ecological system (Takeuchi, 1991). Therefore, the reefs must be properly designed so as to avoid the generation of a hazardous and unstable wave environment in the area.

Currents are important in carrying nutrients and organic matter across artificial reefs from inlets along the coast as well as bringing planktonic larvae to the reefs for settlement. Baynes and Szmant (1989) noted that the higher coverage and species diversity corresponded to areas of high velocity flow and low sedimentation, while areas of decelerated flow and increased sedimentation resulted in regions of less cover and lower species diversity. Furthermore, to increase the sessile benthic growth on artificial reefs, they suggested to maximize the amount of exposed surface area to current flow and the amount of vertical substrate.

Lindquist and Pietrafesa (1989) showed that fish species abundance was influenced by current vortices and tended to face into the current to maintain its position while food such as planktivores tended to concentrate along the upcurrent side, above the reefs (Bohnsack et al, 1994). Pressure waves and current shadows (wake) also affect ocean fishes. As described by Nakamura (1985), pressure waves created by currents impinging on solid reef structures are recognized by fishes and provide them orientation to the reefs.

Chang (1985) concluded that sites shielded from strong currents are preferred by fish. Lin and Su (1994) also observed that the assemblages of fishes were affected by current speed in the vicinity of reefs which distribute water temperature and salinities. However, study by Bortone et al (1994) on artificial cone reefs made from plastics noted that current shadow seems to have little impact on the substrate in the system which is dominated by strong ebb tidal surges such as in the estuaries of Gulf of Mexico.

Water quality parameter such as turbidity, temperature and salinity may affect assemblages depending on the tolerance of individual species (Lin and Su, 1994, Bortone et al, 1994, Bohnsack et al, 1991, 1994). In the Liguarian Sea, Relini and Relini (1989a) observed the unsuccessful effort of deploying an artificial reef in the turbid (muddy bottom with high sedimentation rate) and polluted areas. Study in Philippines resulted in the highest initial recruitment and percent coverage of benthic organism in turbid/silty water area rather than in the clear water when the artificial reefs were deployed. As mentioned earlier, the availability of benthic organisms influenced considerably the assemblage of fish. However, clear site patterns follow the same development as with the silty site (Pamintuan et al, 1994). Other studies noted that turbidity and pollution did not affect fish assemblages. Similar results were obtained when reefs were placed in clear water and in turbid water for accumulating large fish communities in the coastal waters off Taiwan (Chang, 1985).

2.4.2. Ecological View and Fish Behavior

Theoretically, the ecology of artificial reefs would be similar to the natural reefs except the differences due to design and positioning of structures. The ecological factors

such as physical disturbance, recruitment, competition, and predation also occur in the artificial reefs. Since artificial reefs have been constructed under various water conditions ranging from shallow to deep, tropical to temperate, clear to turbid, weak or strong currents with zero to high turbulence, better understanding will allow better design and more effective use of these structures which also may answer questions about the worth of building reefs under different circumstances (Bohnsack, et al, 1991).

Many species in the aquatic habitats have different ecological roles depending on their size and the stage of their life cycle. As noted by Anderson et al (1989), juveniles and small-bodied fishes tend to stay near artificial reefs for protection, but larger or older fishes, which are less vulnerable to predation, spend more time away from the artificial reefs.

Fish pattern studies by Ogawa (1968) cited in Grove and Sonu (1985) indicated five different fish patterns associated with the availability of reefs:

Pattern I : Species which prefer strong physical contact with their bodies against hard objects.

Pattern II : Species which like to remain in physical touch with an object with their pectoral fin or belly.

Pattern III : Species which like to remain in close proximity to a hard object, without really touching it.

Pattern IV: Species which do not always require the presence of a hard object, but when one is offered, occupy a certain typical position relative to it.

Pattern V : Species which are indifferent to the presence of a hard object. They rather tend to respond to fluid excitations.

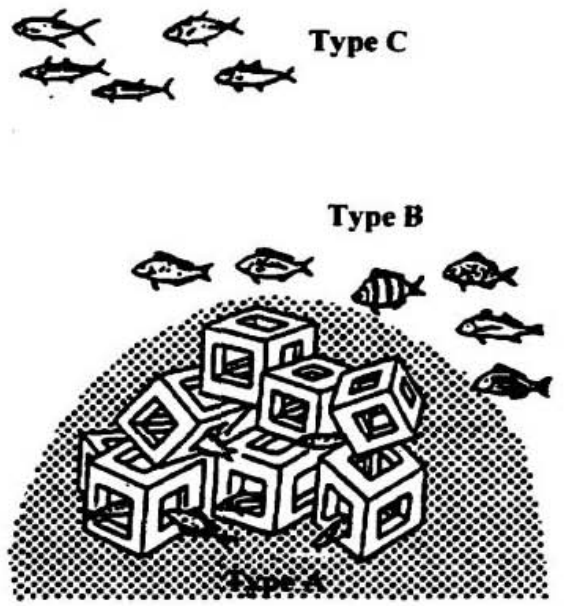

Figure 2.2. Type of Fishes According to Their Response to The Reefs ('Reefiness') (Nakamura, 1985)

Moreover, Nakamura (1985) classified fishes into three types according to their respective position to the reefs. Type A fishes prefer physical contact with the reef, and occupy holes, crevasses and narrow openings. They are dominantly benthic dwellers, such as rock cod and rockfish. Type B fishes are linked to the reef through vision and sound. These fishes are mostly reef dwellers (coral fish), and like to swim around the reef while remaining near the bottom and spend most of their life cycle in the vicinity of reefs. Type C fishes tend to hover above the reef while remaining in the middle and upper parts of the water column. Anchovy, Mackerel and Sardine belong to this category. Their responses (called "reefiness") vary by species and their stage of maturation as given in the Figure 2.2.

Various fish instinct or response to their environment are described using the following terms: *rheotaxis* (fish tends to place itself parallel to currents), *geotaxis* (fish tends to balance its abdomen downside, *thigmotaxis* (fish navigates through physical contact), *phototaxis* (fish responds to light), *and chemotaxis* (fish responds to smell) (Nakamura, 1985).

Fish species can also be classified as residents, visitors, or transients (Bohnsack and Talbot 1980, Bohnsack et al 1994). Residents tend to stay at a structure for long periods once they colonize or settle. Visitors use artificial habitats for brief periods, from a few minutes, to hours, days or seasons. Transients are species observed at artificial habitats but they do not respond to it differentially than the surrounding structures. Behavior of the species may differ between reefs. A species may be a resident on a large reef but only a visitor to a small reef because there is insufficient food (in the large reef) to support a permanent population (Bohnsack et al. 1991).

From an ecological view, the structure of the reefs will depend on the target species planned to populate the reef. For example, for type A fishes, the reef should have holes or gaps equivalent to the size of the fish which occupy the reefs. The reef must also be permeable to the passage of the currents.

For type B fishes, space between the structural members of the reefs should be less than 2 m from each other (Nakamura, 1985), since the fishes perceive structural members, 2m apart, as an individual object but clearly notice any object at a distance less than 1m (Ogawa (1968), in Grove and Sonu, 1985). The reefs should also generate enough vortices and turbulence for fish to identify sessile organisms attached to the reefs. According to Nakamura (1985), vortex shedding in a current with a velocity of u

(cm/sec) occurs at the reefs with the thickness or width of structural member B (cm) when the following condition is satisfied:

$$Bu > 100 \text{ (cm}^2\text{/sec)} \tag{2.1}$$

For practical purposes, Takeuchi (1991) suggested $Bu \geq 10^5$ (cm^2/sec). However, when the current increases, fishes tend to take refuge in the lee of the reefs as shown in Figure 2.3. The current in this area may be approximated by (Nakamura, 1985):

$$u' = u(1 - \frac{C_D A}{2S}) \tag{2.2}$$

in which C_D is a drag coefficient for the reef, A is the projection area of the physical portion of the reef, and S is the projection area of the maximum envelope of the reef.

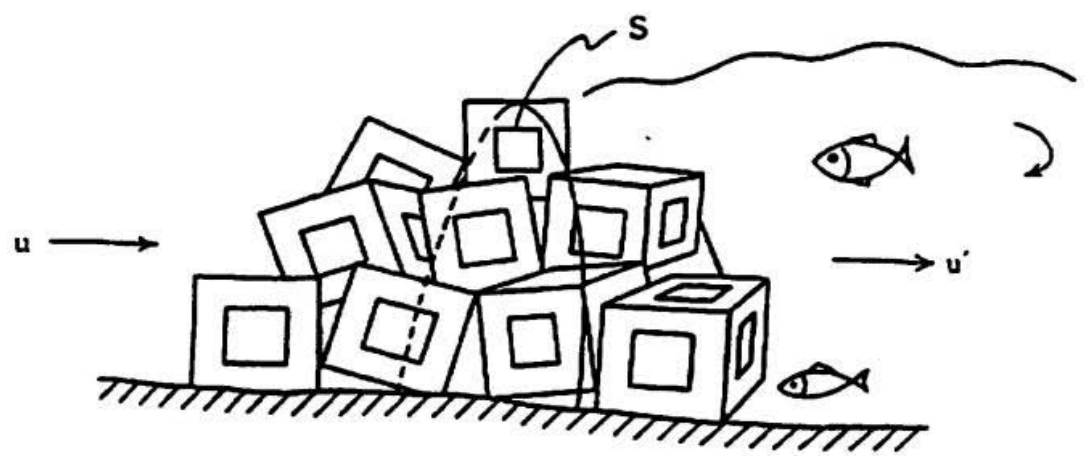

Figure 2.3. Wake behind The Artificial Reefs (Takeuchi, 1991)

The wake captures drifting objects and suspended mud which contributes to the improvement of environment for fish. The length of the wake, as shown in the Figure 2.4, is typically about 4 times the height of permeable reef, and about 14 times for an impermeable reef.

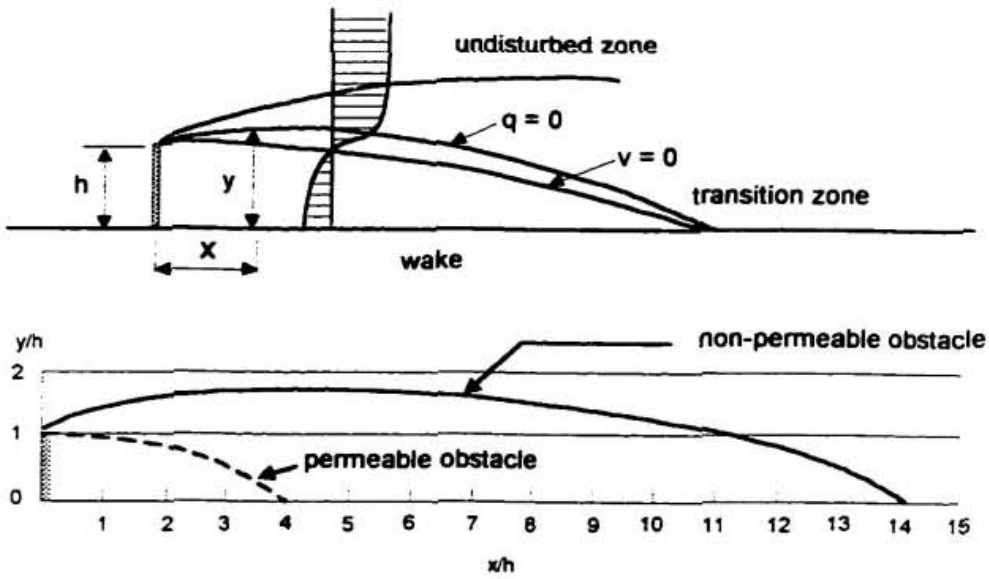

Figure 2.4. Current Shadow behind A Two-dimensional Obstacle (Takeuchi, 1991)

Furthermore, for type C fishes, the reefs should provide a high shadow and be able to block the currents and shed vortices (Takeuchi, 1991). The linkage between the fish and the reefs may result from flow-field instability, pressure fluctuations, and sound emitted by the reef which are detected by fish instinct (Nakamura, 1985). In a continuously stratified slow-moving current, the reef triggers a lee wave which helps the fishes to find an optimum hovering position relative to the reef. The optimum height of a reef structure to generate the lee wave, is approximately 10% of the water depth in which the internal wave may rise as high as 80% of the water column at this condition (Kakimoto, 1991). A lee wave is best developed under the condition where the densimetric Froude number is 0.09 (Nakamura, 1985):

$$Fr = \frac{u}{\sqrt{gd(\frac{\rho_1 - \rho_2}{\rho_2})}} = 0.09 \qquad (2.3)$$

in which u is the current speed, d is water depth, ρ_1 and ρ_2 are water density in the upper and lower layer. When the current speed exceeds $1/\pi$ (=0.32), the lee wave will generate a plain wake as described above. Figures 2.5 shows the typical formation of a lee wave due to artificial reefs.

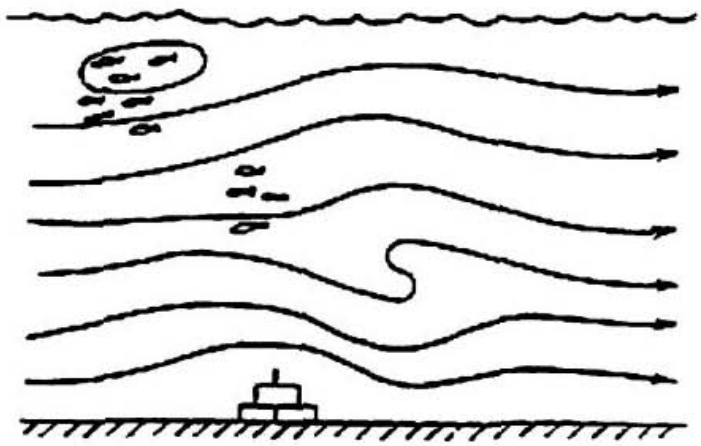

Figure 2.5. Lee Wave due to Artificial Reefs (Nakamura, 1985)

For the turbulent wake, generated by wave action, the velocity u is substituted by horizontal velocity component of the orbital wave motion at the crest of the reefs (Grove and Sonu 1985, Sorensen 1993):

$$u = \frac{\pi H}{T}\frac{\cosh(kD)}{\sinh(kd)}\cos(kx - \sigma t) \qquad (2.4)$$

where H is the wave height, T is wave period, t is time, σ is the wave angular frequency $(2\pi/T)$, L is wavelength, d is water depth, k is wave number $(2\pi/L)$, and D is the reef height. Figure 2.6 typically shows the turbulent wake generated by wave action.

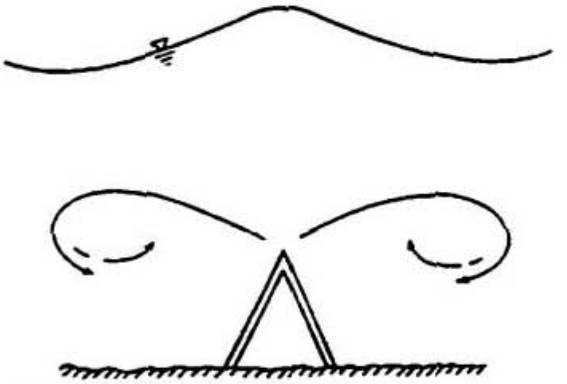

Figure 2.6. Turbulent Wake due to Wave Action (Takeuchi, 1991)

2.4.3. Geographic Location and Reefs Placement

Based on Japanese experience, geographic location has also been recognized as an essential parameter for artificial reefs. Site selection was regarded to be more important than reef design itself (Bohnsack and Sutherland, 1985). A new reef location should be complementary or remedial to the existing condition (Nakamura, 1985). Artificial Reefs placement at an adequate distance from the existing natural reef is recommended to avoid competition for the same species in the neighborhood (Grove and Sonu, 1985). Nakamura (1985) presented various parameters affecting decision of reef site selection, as described in Table 2.3.

Table 2.3 Various Parameters Affecting Selection of Reef Sites

Site Selection		
Topography	Oceanography	Hydrodynamics
Discontinuities ▪ Peninsula, Headland, Canyon, Ridge, Island Substrata Diversity	Upwelling Downwelling ▪ Gyre ▪ Drift Internal wave	Turbulence Ascent of Nutrient Salts Plankton Entrainment Eddy-shedding

Based on the above table, topographic discontinuities as shown in Figure 2.7 are conducive to the desirable location. Since the currents generally follow the bottom contours, and parallel to the coastline in the nearshore region, the longitudinal axis of artificial reefs of the deployment pattern should be perpendicular to the contour line. This orientation would allow the reefs to intercept the fish path as they move along the current (Grove and Sonu, 1985).

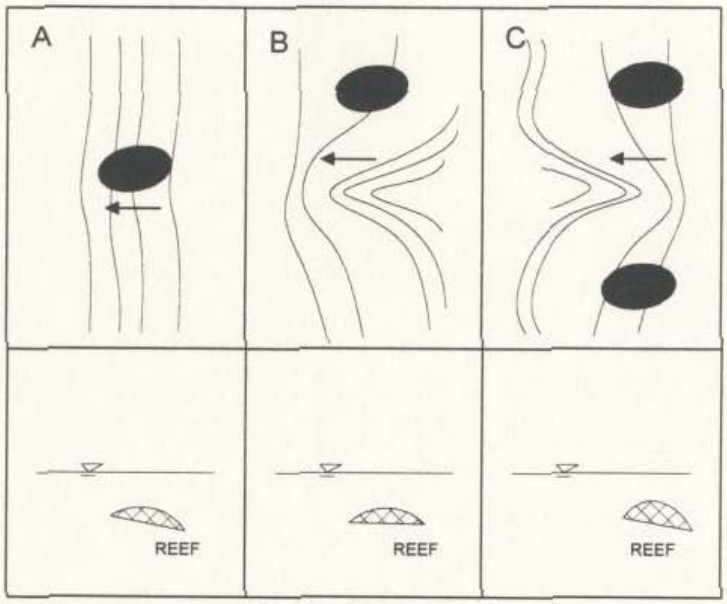

Figure 2.7. Preferred Reef Locations (Grove and Sonu, 1985)

As currents flow perpendicular to the contour of seabed, location A in Figure 2.7 above is expected to catch the fish school in its path following the currents. As shown in Figure 2.8, when the internal wave is moving upward and downward to the shore, the fish school maintains its position in front of the internal wave. Location B and C would also be expected to allow the fish to remain in the reefs as the internal wave would impinge on the obstacle (underwater wall). The front of the internal wave which is preferred by fish

school is then deflected upward at the point of contact with the obstacle as illustrated in the Figure 2.9.

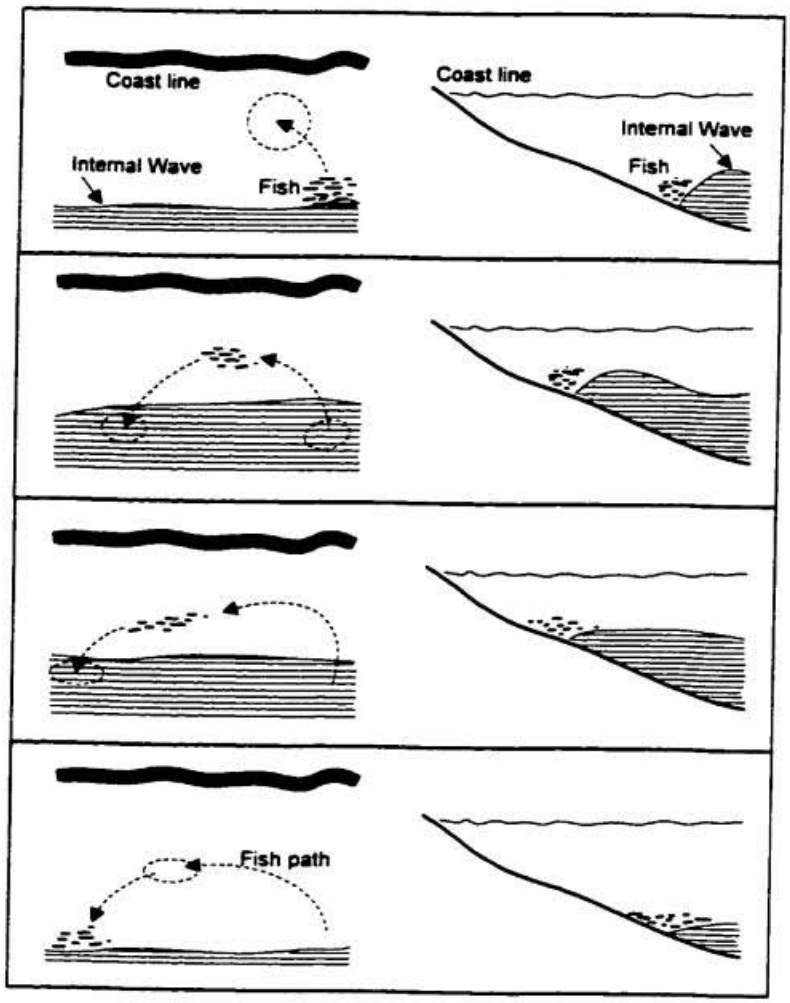

Figure 2.8. Fish Path due to Internal Waves (Grove and Sonu, 1985)

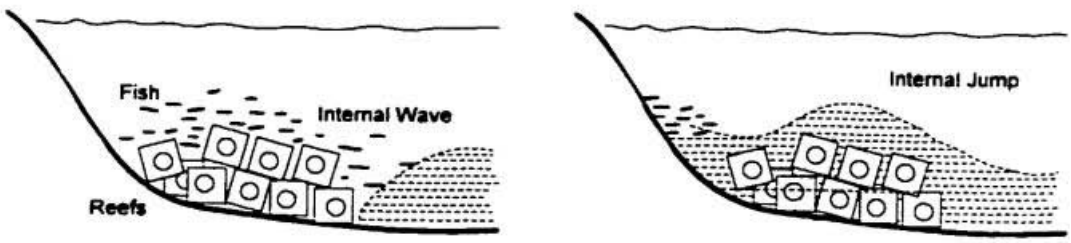

Figure 2.9. Fish Position during the Passage of Internal Wave (Grove and Sonu, 1985)

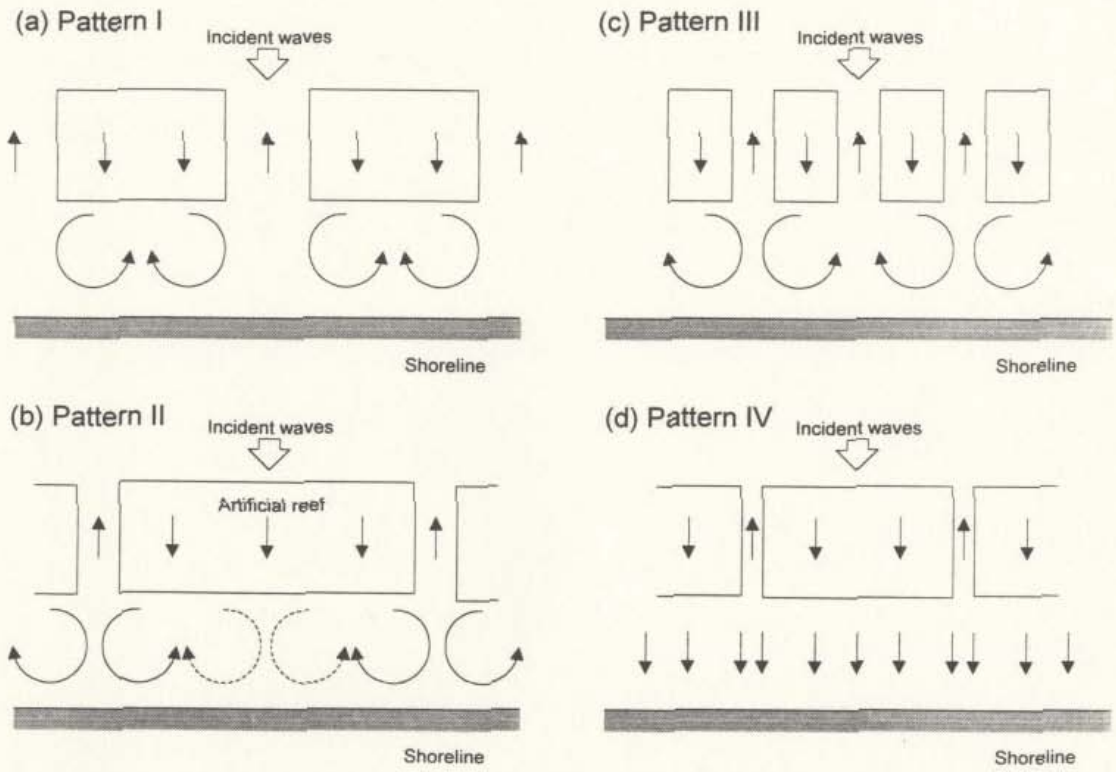

Figure 2.10 Current Patterns around Artificial Reefs (Yoshioka et al, 1993)

According to Yoshioka et al, (1993), current flow patterns on the on-shore end of artificial reefs can be classified into four types as shown in Figure 2.10. Pattern I shows that couple circulation currents develop behind the reefs. As the length of reef (Lr) increases, the effect of opening section does not reach the central part of the reefs (Pattern II). When the distance between reefs are so narrow, a couple of circulation currents develop behind the two adjacent reefs (Pattern III). Furthermore, pattern IV is developed when no circulation currents are developed; i.e., when the reef width (Wr) is small compared to reef length (Lr).

Behind artificial reefs, a developed couple of circulation currents as well as longshore currents would reduce the rate of littoral drift and accumulate sediments which

cause the growth of a cuspate spit from the shoreline. For the offshore breakwater with the crest above the water level, if the structure's length (Lr) is great enough in relation to its distance offshore (Y); i.e: Lr < 2Y, the cuspate spit may connect to the structure, forming tombolo (CERC, 1984). However, as observed by Newman (1989), the artificial reef does not induce the circulation current that leads to the tombolo effect.

For the purpose of controlling sand accumulation and littoral drift a placement, which will produce flow Pattern I, is recommended by Yoshioka et al, (1993). This is approached by setting the broad opening at Wr > 0.25 Lr and Y<Lr<4Y. Similar to Pattern I, a relatively good coastal littoral drift control effect can be obtained by flow Pattern II, although circulation currents only develop at the tips of reefs. Furthermore, when a permeable reef structure is used and the distance between the reefs and the shoreline is short; i.e: Lr <Y (CERC, 1984), onshore current flowing over the reef almost reaches the beach line and some times sand accretion does not develop behind the reefs.

Field observations (Newman, 1989) as well as laboratory studies (Bruno, 1993) confirmed that the artificial reef is effective in limiting the offshore transport of sediments. Moreover, Newman (1989) noted that the reef converts a significant amount of wave energy into current energy and produces a strong current along the crest of the reef. Therefore, more wave energy is converted to current energy along a coastline protected by the reef than an unprotected coastline that undergoes continuous wave breaking. Another fact found by Newman (1989) was that the reef also does not reduce the longshore current; therefore the longshore littoral drift can bypass the reef shadow zone without sediment deposition.

2.4.4. Physical Criteria

Physical reef characteristics such as materials, texture, size and geometry, have been known to affect fish assemblages. Material for artificial reefs must be selected appropriately and should provide suitable substrates for the benthic assemblages which constitute the source of food for fish. In Japan, the government stipulated that the artificial reefs should fulfill the required standard of durability, safety, functionality, and economy. For instance, the material must have a minimum of 30-year expectation life, demonstrate fish-aggregation capability, must be cost-effective and be free from toxic or hazardous materials such as PCB (polychlorinated biphenyl), mercury, cyanide, cadmium, lead, chrome, and arsenic. Bell et al (1989) also suggested that the selection and design of a manufactured reef must be based on their durability, stability and biological effectiveness as well as the cost of construction.

Irregularity and rough surface texture of reef substrate as well as vertical reef profile (reef relief) affect coral settlements (Carleton and Sammarco, 1987), epibenthic reef settlement (Hixon and Bronstoff, 1985) and influence fish composition (Chandler et al, 1985). Substrate texture is mainly affected by the characteristics of reef material. Studies in Hawaiian waters have shown that coral attaches itself more to metal surfaces than to rubbers. Concrete is recommended for structures since it provides fouling assemblages most similar to natural coral substrate (Fitzhardinge and Bailey-Brock, 1989). It was also observed that a nontoxic artificial plastic substrate such as PVC (polyvinyl-chloride) supported the same epibenthic assemblages as flatly-cut natural dead coral rock substrate for invertebrate abundance and algal biomass, coverage, and species composition (Hixon and Brostoff, 1985). Also in Hawaiian waters, Brock and Norris

(1989) observed that reefs composed from randomly dumped scrap materials (automobiles and concrete pipes) showed low life expectancies and were found highly unstable. Moderate enhancement was found at reefs composed of automobile tires set in concrete bases and was found relatively stable. Significantly greater enhancement effects were attained on a reef constructed from concrete cube modules.

Studies in Taiwan also found that concrete blocks and scrapped boats proved to be the most effective. However, the concrete blocks were observed to be much more durable, effective and economical in long term than of scrapped boat (Chang, 1985). Furthermore, observations off Southeast Florida showed the effectiveness of wood as fish concentrating material than steel despite its low service life (Shin and Wicklund, 1989).

Some studies have significantly identified the influences of reef size to the total number of species and biomass (Bohnsack et al 1994). Other studies have mentioned the reefs appeal to fish (Ambrose and Swarbrick, 1989), fish assemblages and catches (Bombace et al, 1994). Size is also to be considered according to its association to total volume, bottom coverage and surface area of reefs. Greater fish density was found in smaller reefs rather than on large reefs, but there were fewer species. This was due to the fact that they attracted fishes from a proportionally larger area due to a higher perimeter-to area ratio (Ambrose and Swarbrick, 1989). However, more individuals and species were found on multiple small reefs than on a single large reef made of similar material (Bohnsack et al, 1994). Practical experience in Japan indicated that the minimum effective size of a reef unit or a large single reef was about $400m^3$ (Grove and Sonu, 1985, Bohnsack et al, 1991).

The Japanese Artificial Reef Planning Guide has classified reefs into three categories in ascending order depending on the fishing ground to be created: single reef, unit reef, and compound reef (Kakimoto, 1991). The proposed classifications were merely typical cases; in the real site, this composition may deviate to suit the specific objective of each project, environmental condition, target species and their life cycle. Figure 2.11 shows the size scales of artificial reefs.

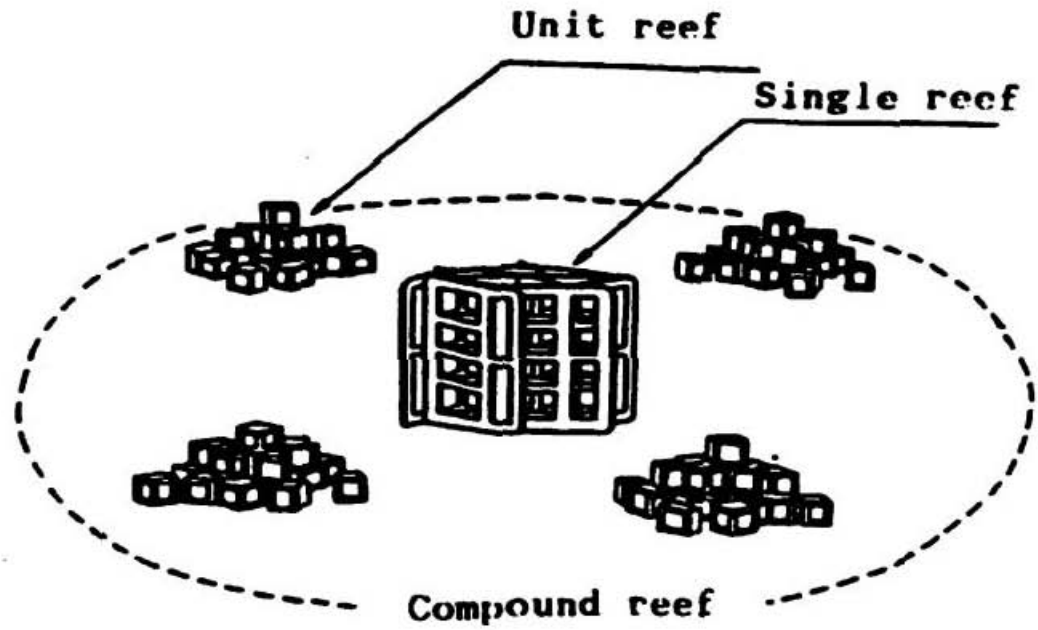

Figure 2.11. Typical Size Scales of Artificial Reefs (Kakimoto, 1991)

Single reef is a unitized structure which functions as a reef by itself. Single reef may have a small size such as concrete blocks (Figure 1.1) or large size (Figure 2.1E). Several small single reefs may form a unit reef. However, a single extra large reef may also be referred to as unit reef. Reef group or a compound reef (Kakimoto, 1991) or a Reef Complex (Grove and Sonu, 1985, Grove et al, 1991) is a fishing ground which

contains several unit reefs at a specified interval which allow movements of organisms from reef to reef. As noted previously, the distance between unit reefs in a reef group should not exceed 2m due to the lack of fish perception or sight (Nakamura, 1985).

Beside size, the spatial and temporal scales used in artificial reef studies are an important and essential consideration. Japanese Artificial Reefs guideline recommended that the deployment area of a reef should be less than 20 times the aggregate shadow areas of all single reefs, or expressed as:

$$S' < 20NX \qquad (2.5)$$

where S' is the deployment area of reef blocks, N is the number of reef blocks, and X is the shadow area of an average reef block (Grove et al, 1991). Figure 2.12 illustrates the typical horizontal configuration of a reef group in Japan.

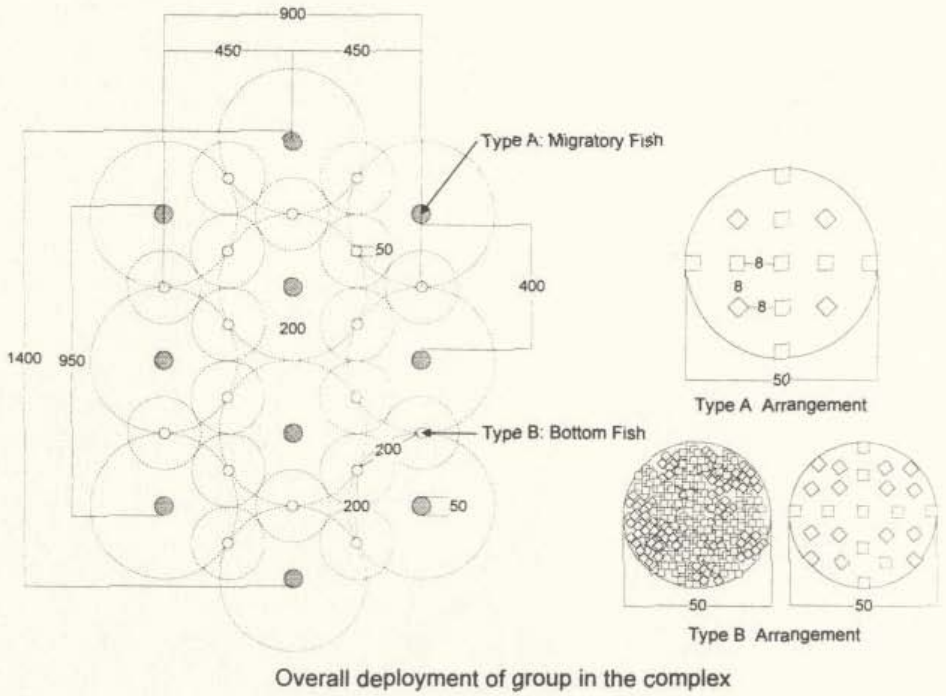

Figure 2.12. Typical Horizontal Configuration of a Reef Group (Grove et al, 1991)
(All dimension in meters)

Ecologically, the arrangement and spacing of reef materials within or between reefs can be important. Since many fishes feed away from a reef or on passing plankton. reef material that are too concentrated may limit plankton availability or may lead to overgrazing for surrounding bottom (Bohnsack et al. 1991). To avoid overlapping the enhanced fishing zones around individual reefs, the Japanese also attempted to place reef in a particular arrangement such as parallel strips or concentric circles (Mottet. 1985).

Taller reef structures may be effective in deeper water and appear to be more effective in attracting some fishes especially type B and C fishes. For type A fishes. the height does not appear to be as important. Extensive underwater observation in Japan on fish aggregation suggested that the height of structures should be about 10 percent of water depth (Mottet. 1985, Grove et al. 1991) and not to be higher than 5m (Grove at al. 1989. 1991) in order to attract type C fishes. It was also reported that most benthic fishes remain within 3m of the sea floor and higher reef might not be effective for these species (Grove and Sonu. 1985). Therefore. horizontal extensions seem to be more important than vertical dimension in attracting benthic fishes. However. total height did not appear as important as the total area and the number of protuberances; hence horizontal spread of the reefs is an essential factor in reef design.

Some experimental studies show that hole size and number influence fish assemblages. Walsh (1985) found that hole composition had little effect on fish assemblages during the day. but it was important at night for sheltering fishes. Bortone et al (1994), also concluded that reefs specific advantage and preference were orientation and height; hole size had no relationship to the fish assemblage. Anderson et al (1989) noted that juveniles and small-bodied fishes needed more shelter than large-bodied fishes

or older life stages. Shulman (1984) found that holes provided shelter from predation and increased juvenile recruitment, numbers of species, and total fish density on small reefs in the Virgin Islands. Ogawa (1982) noted that fishes did not inhabit chambers with opening 2m or larger, and recommended that 0.15m to 1.5m openings were best for fishery purposes.

2.4.5. Stability Consideration

Stability of reef due to wave and current also should be considered in the design. The reef must not overturn or slide. Therefore the friction between the reef and the sea floor must be greater than the horizontal component of the hydrodynamic forces (Takeuchi, 1991).

The stability of artificial reef blocks can be examined using Stability Number (N_s) (Hudson et al, 1979), as given below:

$$N_s = \frac{\gamma_a^{1/3} H}{(R-1) W_a^{1/3}} \qquad (2.6)$$

where H is waveheight, W_a is weight of reefs, γ_a is specific weight of reefs, R is the ratio between water and reef specific weight=γ_a / γ_w. In practice (CERC, 1984), the stability coefficient (K_D) is commonly used. To determine stability coefficient K_D, the stability numbers N_s obtained from laboratory test were plotted on a log-log paper resulting a straight line with the following realtionship, typically:

$$N_s = (K_D \cot\theta)^{1/3} \qquad (2.7)$$

where θ is the slope angle of the reef toe. Higher K_D values give more stability. As noted by Nakayama et al, (1993), the stability number can be considered to depend on the ratio

between reef depth and the incoming wave height (d/H) and wave period (T). As an illustration, K_D values for some breakwater block are given in Table 2.4 shown below. (CERC, 1984):

Table 2.4 K_D Values for Breakwater Blocks (CERC, 1984)

Armor Unit	Structure Trunk		Structure Head		
	Breaking	Non Breaking	Cot θ	Breaking	Non Breaking
Tetrapod and Quadripod	7.0	8.0	1.5 2.0 3.0	5.0 4.5 3.5	6.0 5.5 4.0
Tribar	9.0	10.0	1.5 2.0 3.0	8.3 7.8 6.0	9.0 8.5 6.5
Dolos	15.8	31.8	2.0 3.0	8.0 7.0	16.0 14.0
Hexapod	8.0	9.5	5	5.0	7.0

2.4.6. Artificial Reefs as Wave Dissipating Structures

Artificial reefs dissipate incoming wave energy by forcing them to break on top of the crest as the freeboard of the reefs decrease. Freeboard (F') is the difference between the height of the reef and the water depth as shown in Figure 2.13

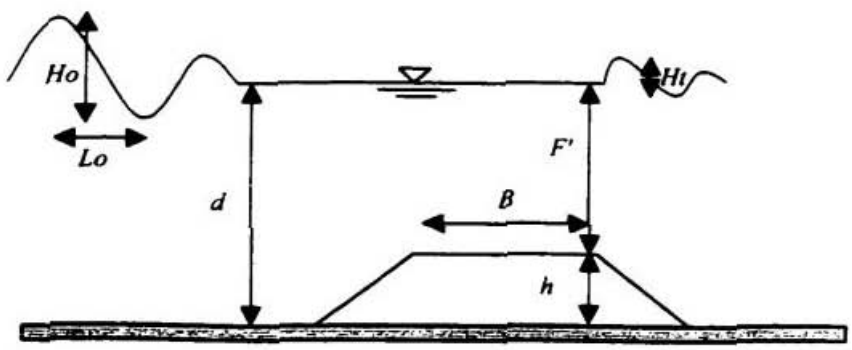

Figure 2.13 Geometry of Artificial Reefs

The wave transmission coefficients for artificial reefs are also much higher than those structures with crest above the water level. However, as the incident wave amplitude increases, the wave transmission coefficient generally decreases. This indicates that the structure is more effective in affecting larger waves; therefore an artificial reef can be used to trigger breaking of high waves (CERC, 1984). Field observation during construction of artificial reefs at Yugawara Coast in Japan (Ohnaka and Yoshizawa, 1994) showed that the reef with a large crown width had a considerable wave dissipation compared to that with a small crown width. It was also clearly observed that the transmitted waves were obstructed by the induced breaking wave due to the reef as modeled by laboratory experiments. Another observation by Aono and Cruz (1996) also confirmed the damping effect of the reefs on breaking and non-breaking waves.

A detailed breaking wave study over artificial reefs (represented by triangular submerged obstacles) outlined by Smith and Kraus (1990) reported that for regular waves, plunging and collapsing breakers were predominant, whereas spilling breakers occurred with a slope of 1/30. The breaking waveform was affected by the return flow. A secondary wave shoreward of the main wave crest was generated which caused the wave to break before the incident wave had reached the depth-limited breaking condition as shown in Figure 2.14. The breaker height ($\Omega_b = H_b/H_o$) as a function of deepwater steepness was increased in the presence of a strong return flow. The strongest return flow was obtained if the seaward slope β_1 was steep and the deep-water wave steepness H_o/L_o was small as shown in Figure 2.15.

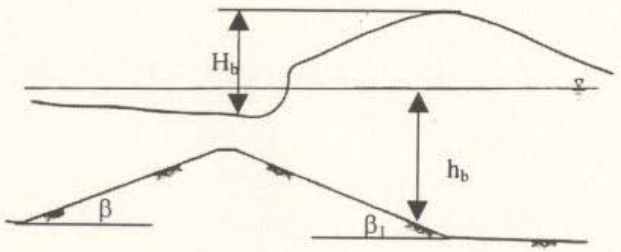

Figure 2.14 Typical Incipient Wave Breaking
(Smith and Kraus, 1990)

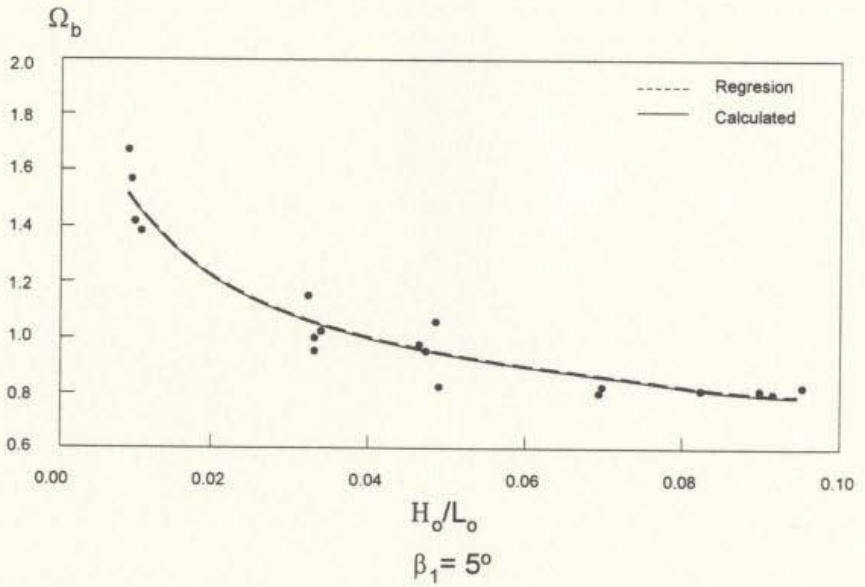

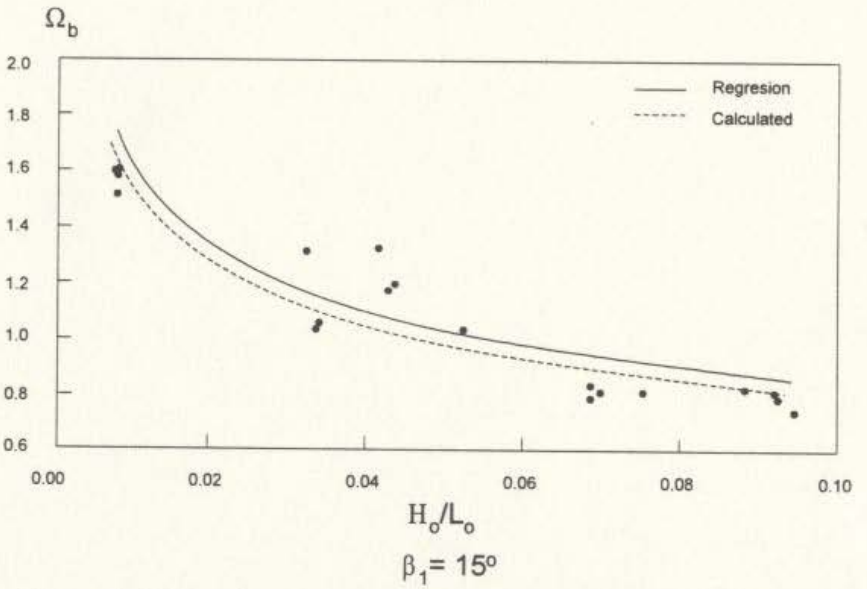

Figure 2.15 Breaker Height as A Function of Deepwater Steepness
(Smith and Kraus, 1990)

The attacking frequency distribution (number of waves in a given time) graph of incoming waves was essential in the design of an artificial reef as a wave dissipating structure. As shown in Figure 2.16 below, waveheight was the main consideration when the artificial reefs were intended as non-overtopping structure to dissipate wave energy (Yoshioka et al, 1993). As shown in Figure 2.16b, the attacking frequencies of 2m wave height were reduced after the installation of a high crown reef.

However, if the reefs were used to stabilize the beach line, the wave frequency occurence was the main consideration as shown in Figure 2.16c. For the same wave height, for example 2m, the lower attacking frequencies were obtained after the reefs with shallow crown depth were installed.

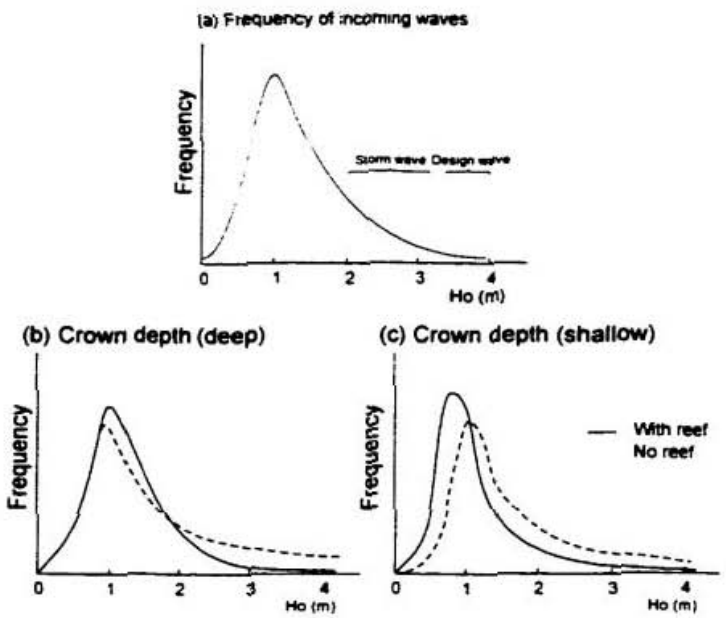

Figure 2.16. Typical Wave Frequency Distribution (Yoshioka et al, 1993)

The wave breaking effect increases with the decrease of crown depth as noted by Yoshioka et al (1993) and Ohnaka &Yoshizawa (1994). Also the longer the travelling distance of broken waves, i.e., the wider the crown of the reefs, the higher the wave-dissipating effect as shown in the Figure 2.17. The ratio of the crown width (B) and deep water wavelength (L_o) as a function of the transmission coefficient of wave height K_t is shown in Figure 2.16 above. By definition, K_t is the ratio between the transmitted wave height (H_t) and the incident wave height (Ho): $K_t = H_t/H_o$. Figure 2.13 shows the geometry of artificial reef and its parameters.

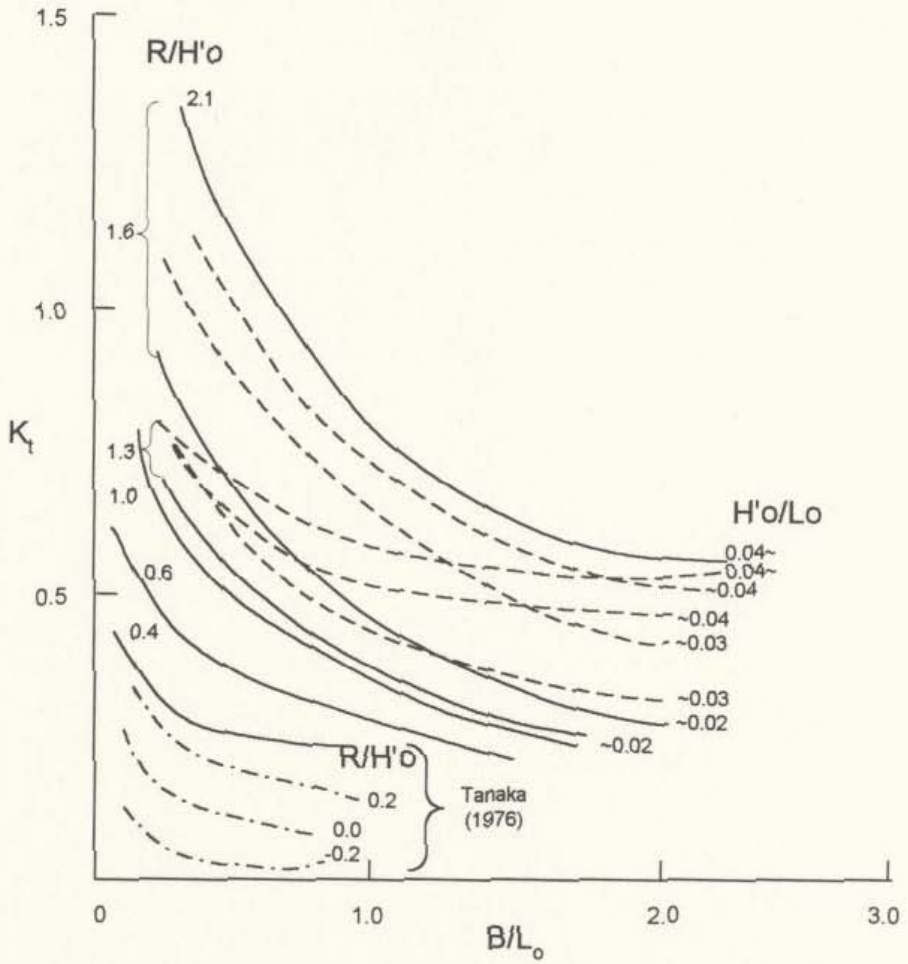

Figure 2.17. Wave Breaking Effect of Artificial Reefs (Yoshioka et al, 1993)

Moreover, numerical and experimental studies for different placement of artificial reefs were carried out by Goda and Takagi (1998). As reported, energy dissipation could be enhanced if the wave refraction effect were mobilized to increase the wave height before breaking. By arranging longitudinally as shown in the Figure 2.18, the artificial reefs were shown to be more efficient in dissipating wave energy than the conventional lateral artificial reefs system.

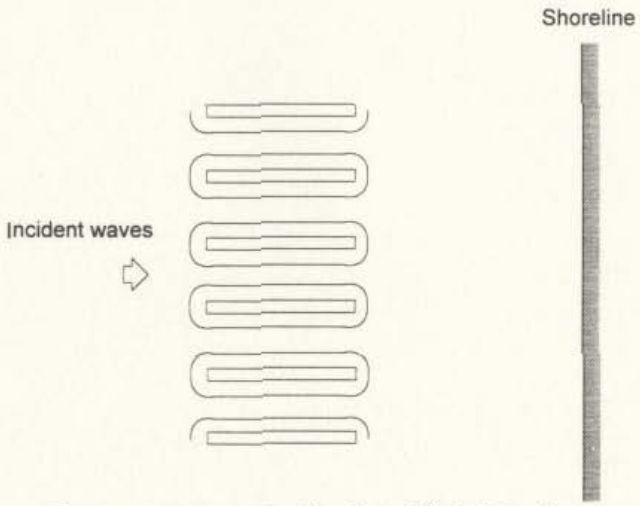

Figure 2.18 Longitudinal Artificial Reefs

2.5. Summary

This chapter has presented a brief overview of artificial reefs, their deployment around the globe, purpose, materials used, the design and the engineering aspects based on environment and ecology. Emphasis has been placed on highlighting the factors that influenced the engineering and design of artificial reefs. In the next chapter, the use of numerical methods to simulate the flow field in the vicinity of reefs as well as to characterize the wave breaking over the reefs will be presented.

Chapter 3
The Volume of Fluid (VOF) Method

3.1. Introduction

The Finite Volume Method is a special formulation of the Finite Difference Method (Versteeg and Malalasekera, 1995) which is also known as the Control Volume Finite Difference Method (Patankar, 1980). The Finite Volume Method has been widely used in the free surface flow studies. Some studies of wave breaking over the artificial reef were also examined using Finite Volume Method (Hayakawa et al., 1998, Kawasaki and Iwata 1998). The most widely known algorithm technique developed for the Finite Volume Method is the Volume of Fluid (VOF) method which was originally developed by Nichols et al (1980). VOF method has been proved to be useful to model even free surface flows due to its capability to define not only single free surface value as a function of space, but also multiply-connected surfaces/areas as obtained for breaking waves (Figure 3.3) or bubble drops. Furthermore, VOF has also been considered as a prime candidate for simulating realistic flows at sea defences and walls (Sabeur et al. 1996).

Section 3.2 of this chapter presents a brief review of the three-dimensional formulation of the Volume of Fluid Method whereas its implementation in the Computational Fluid Dynamic (CFD) software FLOW 3D will be covered in Section 3.3

3.2. Volume of Fluid Method (Nichols and Hirt, 1981)

Nichols and Hirt were the first to report on the solution algorithm of the Volume of Fluid (SOLA-VOF) method in 1975 and further extended it in 1981. The method used the Eulerian mesh of prismoidal cells shown in the Cartesian coordinate system of Figure 3.1.

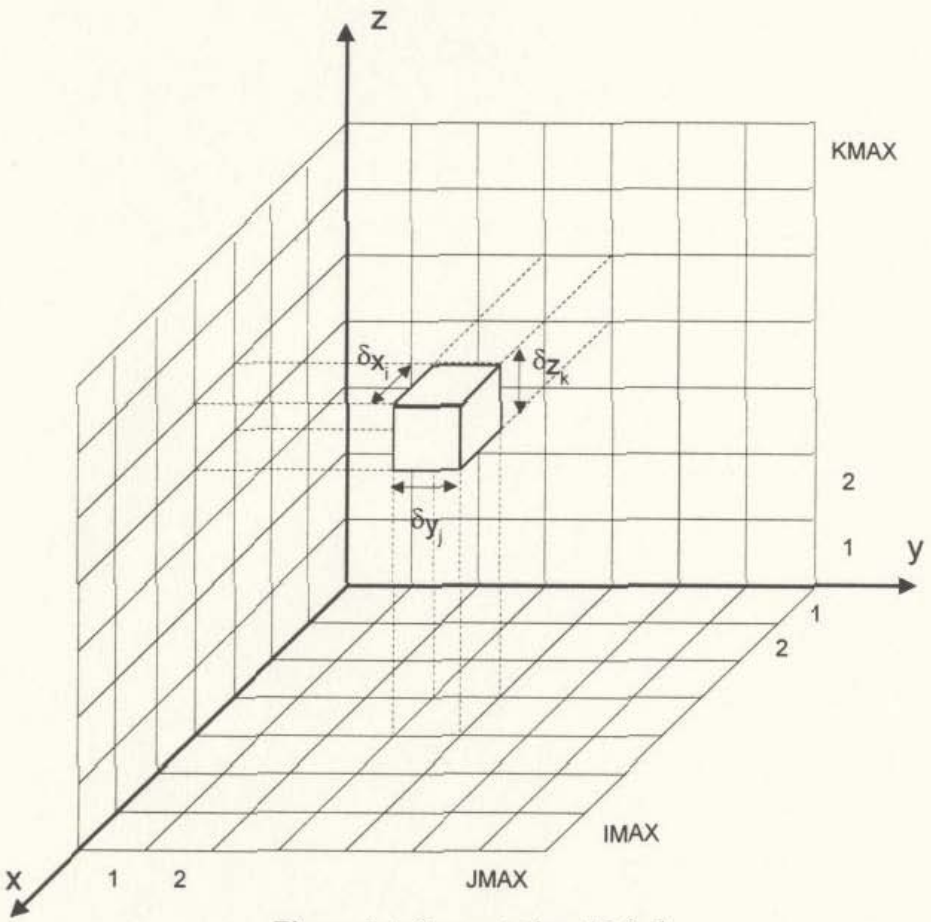

Figure 3.1 Computational Mesh

The three-dimensional fluid equations to be solved were the Navier-Stokes equations, viz.,

$$\frac{\partial u}{\partial t}+\frac{1}{V_F}\left[uA_x\frac{\partial u}{\partial x}+vA_y\frac{\partial u}{\partial y}+wA_z\frac{\partial u}{\partial z}\right]=-\frac{1}{\rho}\frac{\partial p}{\partial x}+g_x+f_x \tag{3.1}$$

$$\frac{\partial v}{\partial t}+\frac{1}{V_F}\left[uA_x\frac{\partial v}{\partial x}+vA_y\frac{\partial v}{\partial y}+wA_z\frac{\partial v}{\partial z}\right]=-\frac{1}{\rho}\frac{\partial p}{\partial y}+g_y+f_y \tag{3.2}$$

$$\frac{\partial w}{\partial t}+\frac{1}{V_F}\left[uA_x\frac{\partial w}{\partial x}+vA_y\frac{\partial w}{\partial y}+wA_z\frac{\partial w}{\partial z}\right]=-\frac{1}{\rho}\frac{\partial p}{\partial z}+g_z+f_z \tag{3.3}$$

where u, v, and w are fluid velocities in the Cartesian coordinate directions (x, y, z), A_x, A_y, and A_z are the fractional areas open to flow in the x, y, and z axis, V_F is the fractional volume open to flow, t is time, p is pressure, ρ is the density of ocean water, f_x, f_y, and f_z are viscous accelerations, g_x, g_y, and g_z are accelerations due to gravity in the x, y, and z axes. Furthermore, the second term in the left side of Equation 3.1, 3.2 and 3.3 are referred as the advection flux FUX, FUY and FUZ, respectively. Figure 3.2 shows the location of each variable in a typical cell used for calculation.

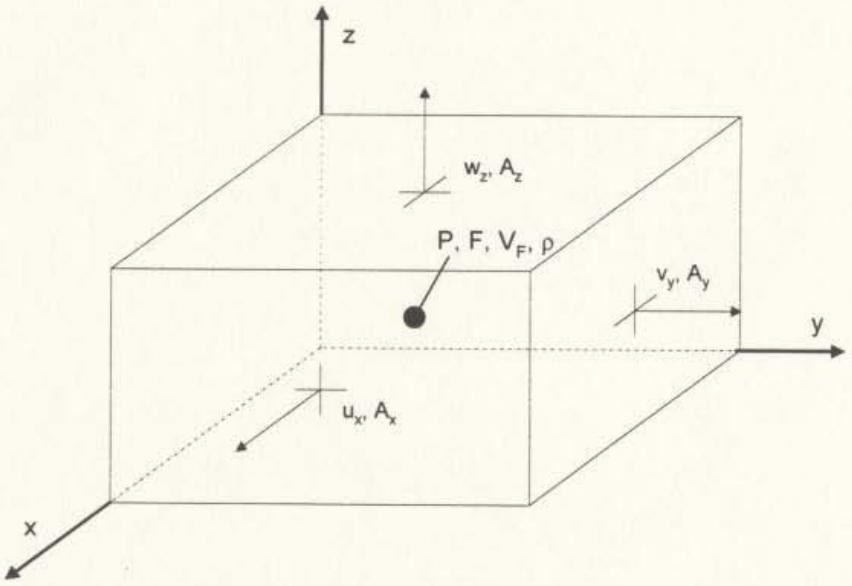

Figure 3.2 Location of Variables

Since the ocean water was assumed incompressible, the incompressibility condition below must be satisfied.

$$\frac{\partial u}{\partial x}+\frac{\partial v}{\partial y}+\frac{\partial w}{\partial z}=0 \tag{3.4}$$

However, to allow for limited compressibility effects, Equation 3.4 above was replaced by the general continuity equation (Hirt and Nichols 1981, Flow Science 1995).

$$\frac{V_F}{\rho c^2}\frac{\partial p}{\partial t}+\frac{\partial u A_x}{\partial x}+\frac{\partial v A_y}{\partial y}+\frac{\partial w A_z}{\partial z}=0 \tag{3.5}$$

where c is the adiabatic speed of sound in the fluid. All the dependent variables described in the equations above are arranged in a staggered grid as shown in Figure 3.2 above.

To define the fluid locally in space, a time dependent VOF (Volume of Fluid) function was given as follows:

$$\frac{\partial F}{\partial t}+\frac{1}{V_F}\left[A_x u\frac{\partial F}{\partial x}+A_y v\frac{\partial F}{\partial y}+A_z w\frac{\partial F}{\partial z}\right]=0 \tag{3.6}$$

with F as fractional volume of fluid. The F function is also used to identify the mesh cell that contains the fluid of density ρ_F. A cell will have a zero F value, unity, or in between them. For a case where only a single fluid is used, cells with zero F values are empty or contain no material; a full cell of fluid is a cell with non-zero values and no empty neighbours. An interface cell or free surface cell is defined as a cell containing a non zero value of F and having at least one neighboring cell that contains a zero value of F. The method also has capabilities to define an obstacle cell where fluid cannot flow. Figure 3.3 illustrates the two-dimensional idealization of the types of cells utilized by the VOF method.

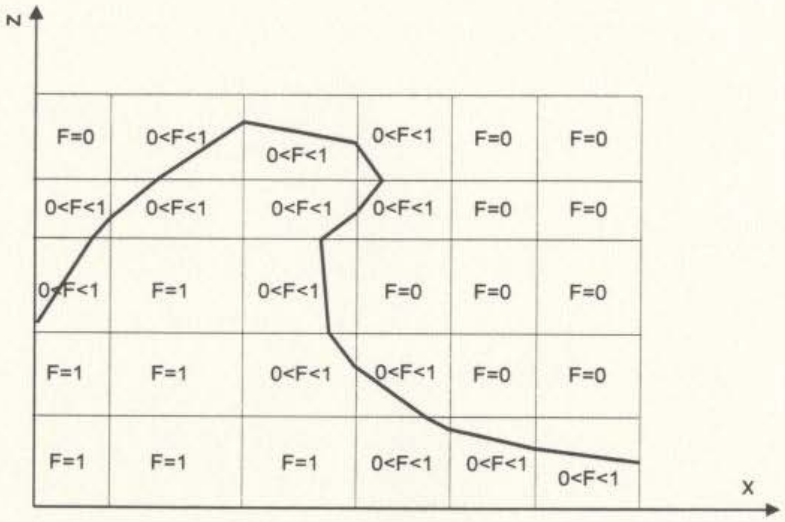

Figure 3.3 Typical Free Surface Cells

Nichols and Hirt (1981) briefly described the basic procedure to obtain a solution for one increment time δt as follows:

1 Explicit approximation of the Navier Stokes equations (Equation 3.1, 3.2 and 3.3) are used to compute the new time-level velocities using the initial condition or previous time-level values of advective, pressure, and viscous acceleration.

2 To satisfy the continuity equation (Equation 3.5) pressures are iteratively adjusted in each cell and the velocity changes induced by each pressure change are added to the velocities computed in step 1 above.

3 Finally the F function, defining fluid region, is updated using Equation 3.6 to give the new fluid configuration.

At each step, a suitable boundary conditions must be applied at all mesh boundaries, free-surface boundaries and internal-obstacle boundaries. These boundaries will be discussed in the subsection 3.3.5.

3.3. Approximation of VOF by FLOW3D

The Computational Fluid Dynamic (CFD) software package FLOW-3D® (Flow Science, 1997) was used to model the flow field in the vicinity of reefs. The software was based on the fundamental laws of mass, momentum and energy conservation, as described earlier in sub Section 3.2, to which finite difference method was applied to solve these equations.

The original development of the program was carried out in the Computational Fluid Dynamics Laboratory at the Los Alamos National Laboratory, New Mexico, USA, in the early 1960's. The numerical algorithm used was called "Solution Algorithm - Volume of Fluid (SOLA -VOF)", an extension of the SOLA method (Hirt et.al. 1975, and Hirt et.al. 1980). The obstacle geometries in the software were placed in the grids with Fractional Area Volume Obstacle Representation (FAVOR) methods. By implementing this method, the geometry and grids were made completely independent of each other. This technique generates smoothly embedded geometric features that were constructed from the program's pre-processor or imported from Computer Aided Design (CAD) programs.

FLOW3D employed the staggered grid arrangements. All variables were located at the center, except for velocities, which were located at the cell faces. The flow region was divided into a mesh of fixed rectangular cells. When free surfaces of fluid interfaces were present, it was necessary to identify whether those cells were empty, contained a partially filled volume, or were full of water. The software considered a cell with an F value less than unity, but with no empty neighbor, as a full cell.

At the mesh boundaries, a variety of conditions could be set using the layer of fictitious cells surrounding the mesh. Six types of boundary conditions were provided by FLOW3D; symmetry plane (default), rigid wall, specified velocity, specified pressure, continuative, and periodic boundary condition. However, in this study only the first three were used.

3.3.1. Notation

Since the fractional subscript index values cannot be used in the numerical code, therefore all fractional indicators were decreased to the nearest integer. For example, the u velocity at $i+\frac{1}{2}$ (for instance, $u_{i+\frac{1}{2},j,k}$) which was located on the cell face between cells (i,j,k) and $(i+1,j,k)$ was denoted by $u^n_{i,j,k}$, where subscript n refers to the n^{th} time step value. As shown in Figure 3.2, for the variables located in the center of cell, the following notation was used:

$p^n_{i,j,k}$ = pressure at center of cell (i,j,k) at time level n

Similarly for F, V_F, and ρ. For the variables located on the cell face, such as velocities and fractional areas, the following notation were used:

$u^n_{i,j,k}$ = velocity along the x axis at middle of $i+\frac{1}{2}$ cell face at time level n

$AFR_{i,j,k}$ = fractional area A_x for flow along x axis at right cell or face $(i+\frac{1}{2})$

$AFB_{i,j,k}$ = fractional area A_y for flow along y axis at back cell or face $(j+\frac{1}{2})$

$AFT_{i,j,k}$ = fractional area A_z for flow along z axis at top cell or face $(k+\frac{1}{2})$

$VF_{i,j,k}$ = fractional volume for flow at center of cell (i,j,k)

3.3.2. Momentum Equations in Variable Mesh

Flow Science (1995) used finite difference approximation for the Navier-Stokes equation (Equation 3.1, 3.2 and 3.3) as follows:

$$u_{i,j,k}^{n+1} = u_{i,j,k}^{n} + \delta t^{n+1}\left[-\frac{p_{i+1,j,k}^{n+1} - p_{i,j,k}^{n+1}}{(\rho\delta x)^{n}_{i+\frac{1}{2},j,k}} + g_x + VISX - FUX - FUY - FUZ \right] \quad (3.7)$$

$$v_{i,j,k}^{n+1} = v_{i,j,k}^{n} + \delta t^{n+1}\left[-\frac{p_{i,j+1,k}^{n+1} - p_{i,j,k}^{n+1}}{(\rho\delta y)^{n}_{i,j+\frac{1}{2},k}} + g_y + VISY - FVX - FVY - FVZ \right] \quad (3.8)$$

$$w_{i,j,k}^{n+1} = w_{i,j,k}^{n} + \delta t^{n+1}\left[-\frac{p_{i,j,k+1}^{n+1} - p_{i,j,k}^{n+1}}{(\rho\delta z)^{n}_{i,j,k+\frac{1}{2}}} + g_z + VISZ - FWX - FWY - FWZ \right] \quad (3.9)$$

where

$$\rho\delta x_{i+\frac{1}{2},j,k} = \frac{\left(\rho_{i,j,k}^{n}\delta x_i + \rho_{i+1,j,k}^{n}\delta x_{i+1}\right)}{2} \quad (3.10)$$

$$\rho\delta y_{i,j+\frac{1}{2},k} = \frac{\left(\rho_{i,j,k}^{n}\delta y_i + \rho_{i,j+1,k}^{n}\delta y_{i+1}\right)}{2} \quad (3.11)$$

$$\rho\delta z_{i,j,k+\frac{1}{2}} = \frac{\left(\rho_{i,j,k}^{n}\delta z_i + \rho_{i,j,k+1}^{n}\delta z_{i+1}\right)}{2} \quad (3.12)$$

VISX, VISY and VISZ are the x, y, and z components of viscous acceleration of f_x, fy, and fz, respectively, in Equations 3.1, 3.2 and 3.3. The advective acceleration terms are represented by FUX, FUY, FUZ for the advective flux of u in the x axis, FVX, FVY, FVZ for the advective flux of v in the y axis, and for the advective flux of w in the z axis the terms are FWX, FWY and FWZ, respectively. The advective flux accelerations are

the second term on the left side of Equations 3.1, 3.2, and 3.3. These terms are evaluated using the old time level (n) values for velocities.

In the beginning, the initial value of p^{n+1} is not known; therefore Equations 3.7, 3.8, and 3.9 cannot be used to evaluate u^{n+1}, v^{n+1} and w^{n+1} values. Therefore in the first step, p^{n+1} values are replaced by p^n to obtain the velocity values in the beginning.

Unfortunately, the use of variable meshes reduces the accuracy of the solution if the convective flux term was written in the divergence form $\nabla \bullet \mathbf{uu}$ instead of $\mathbf{u} \bullet \nabla \mathbf{u}$. The inaccuracies of using divergence term $\frac{\partial u^2}{\partial x}$ for FUX in the variable mesh has been described earlier by Hirt and Nichols (1981) as follows:

For simplicity, consider a two-dimensional control volume used for $u_{i,j}$ as indicated by dashed line in Figure 3.4, where all fractional areas and volumes are assumed equal to unity. Assuming the u velocity to be positive, the approximation of advective flux of u is:

$$FUX = \frac{\left[u_R \langle u_R \rangle - u_L \langle u_L \rangle\right]}{\delta x_{i+\frac{1}{2}}} \tag{3.13}$$

where $u_R = \dfrac{\left(u_{i+1,j,k} + u_{i,j,k}\right)}{2}$ and $\langle u_R \rangle = \begin{cases} u_{i,j,k} & \text{if } u_{i,j,k} \geq 0 \\ u_{i+1,j,k} & \text{if } u_{i,j,k} < 0 \end{cases}$

similar equation can be written for u_L.

Expanding the Equation 3.13 using Taylor series in x_{i+1}, yields:

$$FUX = \frac{1}{2}\left(\frac{3\delta x_i + \delta x_{i+1}}{\delta x_i + \delta x_{i+1}}\right)\frac{\partial u^2}{\partial x} + O(\partial x) \tag{3.14}$$

which is true only if the cell widths are equal; $\delta x_i = \delta x_{i+1}$.

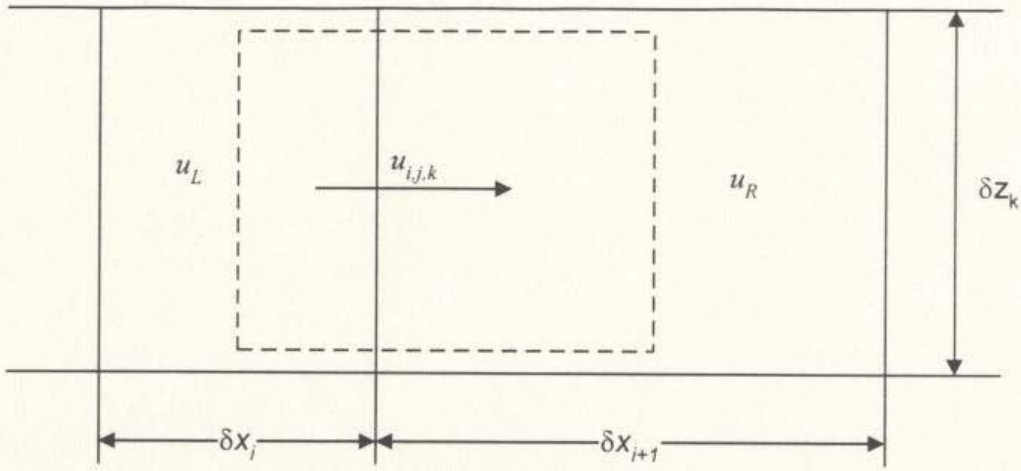

Figure 3.4 Control Volume in x-y Plane used in Finite-difference Approximation for *u* Momentum (Hirt and Nichols, 1981)

Therefore for the advection flux FUX, $u\frac{\partial u}{\partial x}$ form is used instead of $\frac{\partial u^2}{\partial x}$ for the variable mesh. Hirt and Nichols (1981), intoduced a parameter α to control the approximate methods, combining first order approximation and second order central-difference approximation to give the stability results. The general approximation form for $\text{FUX} = \frac{A_x}{V_F} u\frac{\partial u}{\partial x}$ is therefore:

$$FUX = \frac{0.5}{VFC}\left[\left(UAR - \alpha\,|UAR|\right)DUDR + \left(UAL + \alpha\,|UAL|\right)DUDL\right] \qquad (3.15)$$

where

$$DUDR = \frac{\left(u_{i+1,j,k} - u_{i,j,k}\right)}{\delta x_{i+1}}$$

$$DUDL = \frac{\left(u_{i,j,k} - u_{i-1,j,k}\right)}{\delta x_i}$$

$$UAR = 0.5\left(u_{i+1,j,k}AFR_{i+1,j,k} + u_{i,j,k}AFR_{i,j,k}\right)$$

$$UAL = 0.5\left(u_{i,j,k} AFR_{i,j,k} + u_{i-1,j,k} AFR_{i-1,j,k}\right) \quad \text{and}$$

$$VFC = \frac{\left(\delta x_i VF_{i,j,k} + \delta x_{i+1} VF_{i+1,j,k}\right)}{\left(\delta x_i + \delta x_{i+1}\right)}$$

VF is the fractional volume for flow at center of cell. VFC is the fractional volume open to flow. AFR is the fractional area along x axis at right face of cell as described in Subsection 3.3.1. When the mesh is uniform, or α=0. Equation 3.15 reduces to a second order central-difference approximation. and when the variable mesh is used (α=1). the first order donor-cell approximation is used.

By using this method. there is no loss of accuracy when a variable mesh is used. In Equations 3.7, 3.8, and 3.9. all convective flux terms were approximated with this method. whereas standard central-difference approximations were used to approximate viscous accelerations.

3.3.3. Continuity Equation

The continuity equation (Equation 3.5) must be satisfied by velocities computed from Equations 3.7, 3.8. and 3.9. By an iterative process. the pressure and velocitiy values in each computational cell were adjusted and therefore each cell full of fluid will change its pressure to either draw in or force out fluid to satisfy Equation 3.4. The finite-difference form used for Equation 3.5 is

$$\left(\frac{1}{\rho c^2}\right)_{i,j,k} \frac{V_{F\,i,j,k}\left(p_{i,j,k}^{n+1} - p_{i,j,k}^{n}\right)}{\delta t} + \frac{\left(u_{i,j,k}^{n+1} AFR_{i,j,k} - u_{i-1,j,k}^{n+1} AFR_{i-1,j,k}\right)}{\delta x_i} + \frac{\left(v_{i,j,k}^{n+1} AFB_{i,j,k} - v_{i,j-1,k}^{n+1} AFB_{i,j-1,k}\right)}{\delta y_j} + \frac{\left(w_{i,j,k}^{n+1} AFT_{i,j,k} - w_{i,j,k-1}^{n+1} AFT_{i,j,k-1}\right)}{\delta z_k} = 0 \qquad (3.16)$$

In each cell containing fluid, the pressure change needed to satisfy Equation 3.15 or 3.16 is

$$\delta p = \frac{-S}{(\partial S / \partial p)} \tag{3.17}$$

where S is the left side of equation 3.16. S is estimated with the latest velocity values in each cell (Flow Science, 1997). The computational mesh is swept cell by cell starting with the first non-boundary cell in the mesh. Sweeping is carried out on *i*, then *j*, and finally on *k* values. Calculations are only performed in cells that contain fluid and have no empty neighbours. The new estimate for the cell pressure is:

$$p_{i,j} + \delta p \tag{3.18}$$

and the new estimated velocities in *x*, *y*, *z* directions on the left and right of cell are:

$$u_{i,j,k} + \frac{\delta t\, \delta p}{\rho \delta x_{i-\frac{1}{2},j,k}} \tag{3.19a}$$

$$u_{i-1,j,k} - \frac{\delta t\, \delta p}{\rho \delta x_{i-\frac{1}{2},j,k}} \tag{3.19b}$$

$$v_{i,j,k} + \frac{\delta t\, \delta p}{\rho \delta y_{i,j+\frac{1}{2},k}} \tag{3.19c}$$

$$v_{i,j-1,k} - \frac{\delta t\, \delta p}{\rho \delta y_{i,j-\frac{1}{2},k}} \tag{3.19d}$$

$$w_{i,j,k-1} + \frac{\delta t\, \delta p}{\rho \delta z_{i,j,k-\frac{1}{2}}} \tag{3.19e}$$

$$w_{i,j,k-1} - \frac{\delta t \, \delta p}{\rho \delta y_{i,j,k-\frac{1}{2}}} \tag{3.19f}$$

In a free surface, since the pressure was assumed specified at the surface. Hirt and Nichols (1981) defined the S function as:

$$S = (1-\eta)p_N + \eta p_s - p_{i,j,k} \tag{3.20}$$

In this case, to satisfy the boundary condition, the surface cell pressure $p_{i,j,k}$ is set equal to the value obtained from a linear interpolation (or extrapolation) between the desired pressure at the surface p_s and a pressure inside the fluid (p_N). $\eta = d_c / d$ is the ratio between surface cell centers and interpolation cell center to the distance between the surface cell and the center of the interpolation cell as given in Figure 3.5

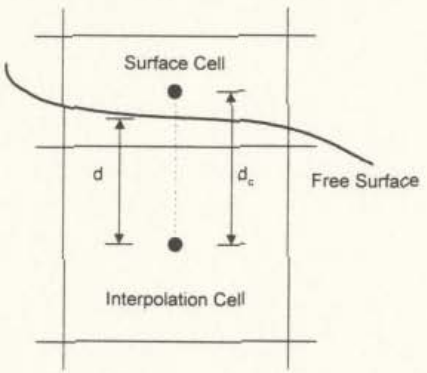

Figure 3.5 Definition of Variables η in Free Surface Pressure Boundary Condition

Finally, a complete iteration consists of adjusting pressures and velocities in all cells occupied by fluid according to Equations 3.17, 3.18, and 3.19, where S is given by Equation 3.17 for an interior cell and by Equation 3.20 for a surface cell. Convergence of the iteration is achieved when all the cells have S values with magnitudes below some small number, (EPSI.$V_{Fi,j,k}$), typically, of the order 10^{-3}.

3.3.4. Volume of Fluid (VOF) Function

By using information about F downstream as well as upstream of a flux boundary an approximate interface shape can be established. Furthermore, the established shape is used to compute the flux in the next time step. The VOF function is given by Equation 3.6. Since the fluid is assumed incompressible, Hirt and Nichols (1981) combined Equation 3.6 with Equation 3.4 to give

$$\frac{\partial F}{\partial t}+\frac{\partial Fu}{\partial x}+\frac{\partial Fv}{\partial y}+\frac{\partial Fw}{\partial z}=0 \tag{3.21}$$

As described before, in every time step δt the fluid F need to be fluxed to the right cell crossing cell face per unit cross section area with volume equal to $L = uA_x\delta t$, where u is the normal velocity at the face as shown in Figure 3.6a. As described by Hirt and Nichols (1981), the donor and acceptor cells were determined by the sign of u. If u positive, the left cell is the flux donor, and the right cell is the flux acceptor, and vice versa.

The amount of F fluxed across the cell face in one time step in x axis is δF times the face cross sectional area ($\delta y\delta z$), where, Flow Science (1995) outlined δF as

$$\delta F = MIN\begin{Bmatrix} F_{AD}|L|+CF \\ F_D V_D \delta x_D \end{Bmatrix} \tag{3.22}$$

and $$CF = MAX\begin{Bmatrix} (F_{DM}-F_{AD})|L|-(F_{DM}-F_D)V_{F.D}\delta x_D \\ 0.0 \end{Bmatrix}$$

Subscript A and D represent the acceptor (A) and donor (D) cells, while subscript AD represents either the acceptor or donor cells depending on the orientation of the interface to the direction of the flow. F_{DM} is the maximum of F_D and the F value in the next cell upstream of the donor cell.

In Figure 3.6(b), when AD = D, the F value in the donor cell is used to define the fractional area of the cell face fluxing F. Therefore $F = F_D \mid L \mid$. Figure 3.6(c) shows the example of the MIN feature in Equation 3.22 to prevent the fluxing of more F from the donor cell than it has to give. When AD = A, the value of F in the acceptor cell is used to define the fractional area of the cell face across which F is flowing. In this case all the F fluid in donor cell is fluxed because everything lying between the dashed line and the flux boundary moves into the acceptor cell. The MAX feature accounts for an additional flux CF if the amount of void (1-F) to be fluxed exceeds the amount available or more fluid than the amount $F_A \mid L \mid$ must be fluxed, as shown in Figure 3.6(d). The computed flux is then multiplied by the flux boundary area to get the amount of fluid to be subtracted from the donor cell and added to the acceptor cell.

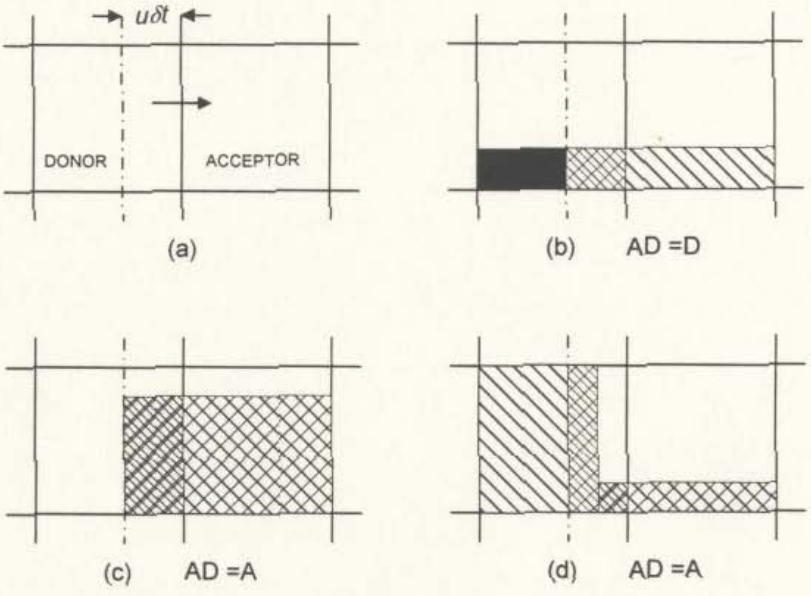

Figure 3.6 Examples of Free Surface Shapes used in The Advection of F. The Cross-hathced Region in b-d are The Actual Amounts of F Fluxed (Hirt and Nichols, 1981).

3.3.5. Boundary Conditions

Several conditions are defined for the mesh boundaries. Rigid free-slip wall, no-slip rigid wall, continuative or outflow boundary, and periodic boundary condition. For example in a two-dimensional rigid free-slip wall in the left boundary, the normal velocity must be zero and the tangential velocity should have no normal gradient.

$u_{1,j} = 0$

$v_{1,j} = v_{2,j}$

$p_{1,j} = p_{2,j}$

$F_{1,j} = F_{2,j}$

If the left boundary is a non-slip rigid wall, then the tangential velocity component at the wall should also be zero;

$u_{1,j} = 0$

$v_{1,j} = -v_{2,j}$

$p_{1,j} = p_{2,j}$

$F_{1,j} = F_{2,j}$

Generally, all rigid and free boundary surfaces are treated as free-slip boundaries (no tangential stresses on the surfaces) and referred to as symmetry plane boundary condition. For rigid wall boundary, the normal velocity is set to zero, and also the tangential velocities (free-slip wall). However, in the no-slip wall conditions, the tangential velocity can be set to any value by the wall shear stress model provided by the software. In the specified velocity condition, tangential velocities and normal velocities must be specified.

These boundary conditions are specified for the right, top and bottom boundaries of the mesh. The normal and tangential velocities at the top and bottom boundaries are v and u respectively. Similar conditions could be derived for a three-dimensional problem.

Internal obstacle boundaries within mesh were defined using a special technique called Fractional Area Volume Obstacle Representation (FAVOR) method (Flow Science, 1995). Solid geometry obstacles which were made using FLOW-3D geometry builder or CAD software such as I-DEAS or AutoCAD in stereolithography (STL) format data, were embedded into the prepared mesh in the input file.

The mesh cells occupied by obstacles will be flagged automatically by FLOW-3D. The portions of element surfaces and volumes blocked by obstacles were computed and stored before starting the hydrodynamics calculation. The quantity chosen as a flag was the volume fraction $VF_{i,j,k}$. When this quantity was zero, the cell was entirely within an obstacle and all fluid calculation in the cell were eliminated. No velocities or pressures were computed in full obstacle cells, and all velocity components on faces of obstacle cells were set to zero. Therefore in the cell blocked by obstacles, the following are applied:

$$u_{I,j,k} = 0$$

$$v_{I,j,k} = 0$$

$$p_{I,j,k} = 0$$

$$F_{I,j,k} = 0$$

3.4. Summary

A brief overview of Volume of Fluid Method and its numerical approximation by FLOW3D has been presented. More details of the VOF method can be obtained in Hirt and Nichols (1981) and its source code is given in Nichols et. al (1980). In the next two chapters, the results obtained from the use of computational fluid dynamic software package FLOW3D, to simulate the flow field in the vicinity of reefs as well as to characterize the wave breaking over the reefs, will be presented.

Chapter 4
Two Dimensional Modelling of Artificial Reefs with Hollow Hemispherical Blocks

4.1. Introduction

Studies on artificial reefs using Finite Volume Methods have been widely carried out (Tsujimoto et al, 1999; Hayakawa et al, 1998; Kawasaki and Iwata, 1998). However, most of these studies have investigated solid or rubble-mound reefs with trapezoidal or rectangular shapes. The sharp edges of these shapes would cause tearing of fishing nets. Therefore, in order to reduce the tearing of fishing nets, bottom-seated smooth-shaped hollow reefs were proposed as alternatives, such as Cylinders, Turtle Blocks, and Reef Balls™ (Mottet, M.G., 1981; Reefball Development Group, Ltd., 1997). The hemispherical shapes were also considered to be stable than the other shapes in resisting the wave forces (Roehl, 1996).

Based on the above requirement, the study on this thesis will focus on the implementation of numerical analysis in the vicinity of artificial reefs with hollow

hemispherical shapes. This chapter will cover the results of two-dimensional modelling of these reefs while those of three-dimensional modelling will be presented in the next chapter. The waveheight and wave velocity magnitudes at salient points are the parameters examined in this study. The first step was to simulate the wave profile without any reef, and then to compare the wave profile with that obtained due to the installation of one, two, three, six, or twelve reefs.

4.2. Numerical Model

The reef blocks were located on the ocean floor (see Figure 4.1) using a cartesian two-dimensional coordinate system (x,z) from the toe of the beach (0 m) to a distance of 13.0 m, from the toe, in the upward direction (depending on the configuration of reefs). The applied beach was straight with the toe located at 50.0 m from the open sea or at x=0 with 5% slope.

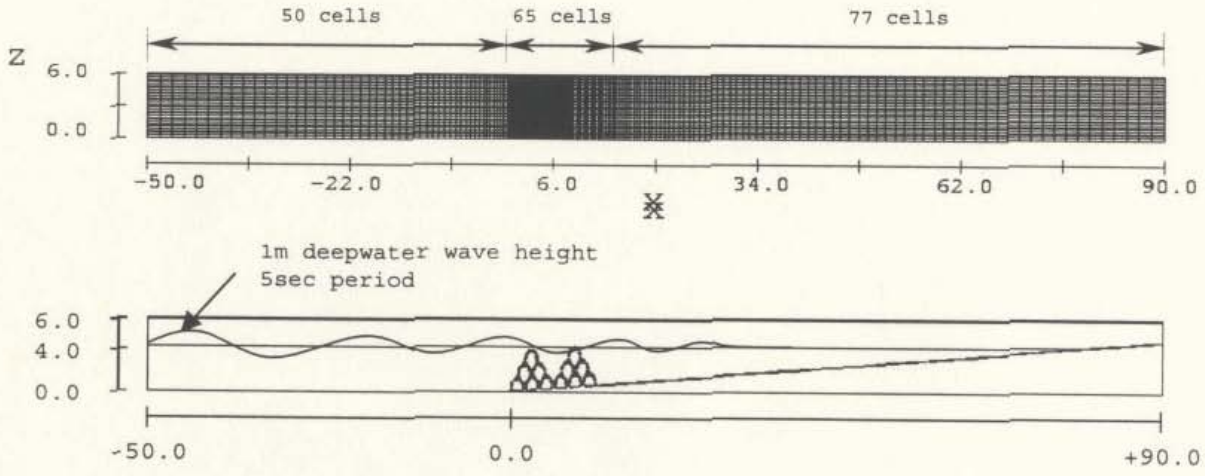

Figure 4.1. Typical Reef and Applied Grids

The computational grids used to cover the model consisted of 192 cells in the horizontal direction. Varying volume of fluid cells were used in the horizontal direction. Cells in the vicinity of reefs (between 0.0 to 13.0 m) were denser than in the other areas. In this area, 65 cells (each cell equal to 0.20 m wide, which gave nearly 10 cells within one hemispherical reef) were used to represent the reefs smoothly, while in the areas between -50.0 m to 0.0 and 13.0 m to 90.0 m, the width of each cell was equal to 1.0 m. The number of cells used in these areas were 50 and 77, respectively. In the vertical direction, total numbers of cells were 30, over a height of 6.0 m (each cell being 20 cm in height). Therefore, total cells used in both directions were 5760. These grids were used to cover the physical size of the computational domain which was 140.0 m in length and 6m in height, as shown in Figure 4.1 above.

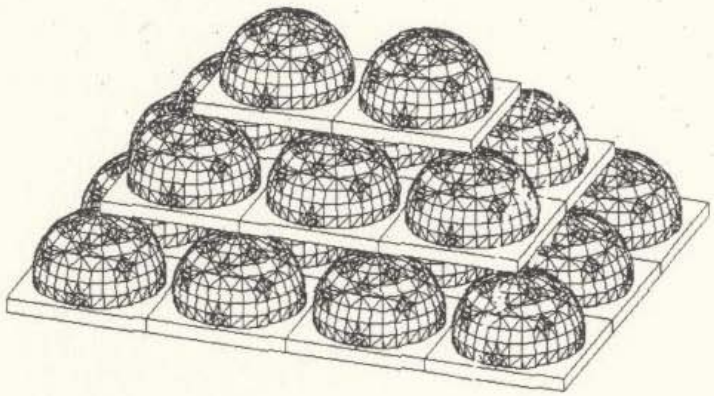

Figure 4.2 Typical Three-dimensional Reefs Arrangement

A typical three-dimensional reef configuration is shown in Figure 4.2. However, since the mathematical model was two-dimensional in nature, the reefs were inherently assumed to be hollow semi-cylindrical shapes in analysis. The reefs (2.0m diameter), each having four opening holes, were located between 0.0 to 13.0m from the toe, as

shown in Figure 4.3. For the purpose of analysis, one, two, three, six, and twelve reefs were installed at the specified location as shown in Figure 4.3. Three and six reefs were arranged in a triangular shape, while twelve reefs were constructed with two triangles of six reefs. The velocity magnitudes within the third reef in the bottom layer, at locations represented in the figure by A, B, and C, were also examined.

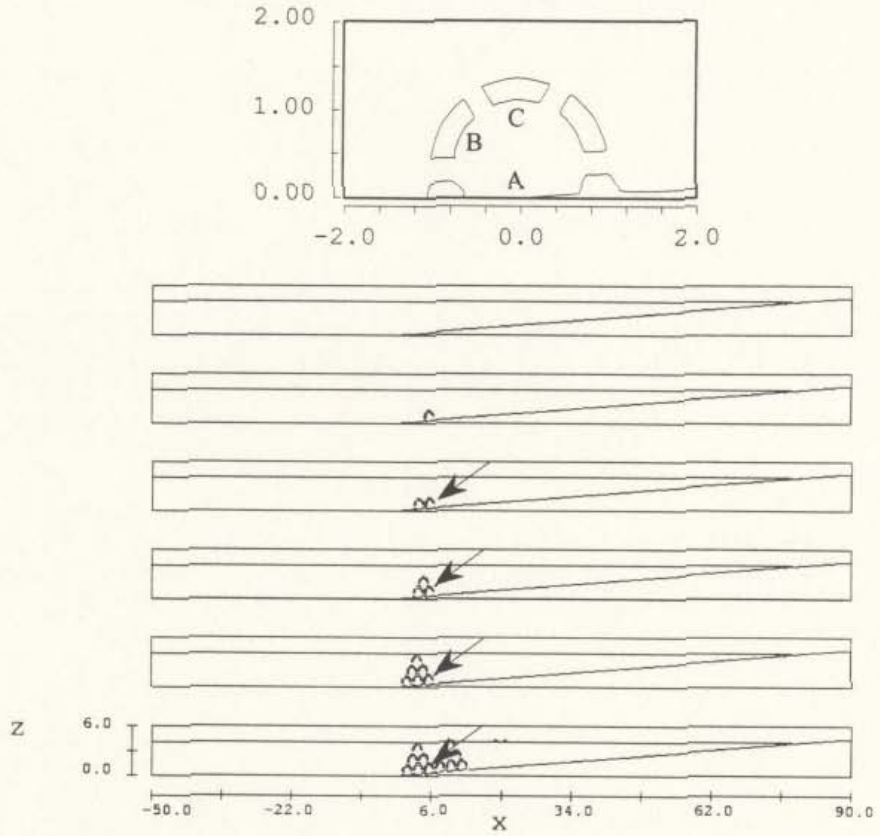

Figure 4.3 Placement of Reefs and Salient Points of Interest within A Reef

The water depth was set at 4.0 m, and the sea considered to be at rest. The velocities obtained from a sinusoidal wave, with 1.0m height and 5 seconds period (at deep-water location), were applied for all reef configurations, as the left boundary

conditions. Symmetry boundary conditions were used at the lateral boundaries and a rigid wall boundary condition was used at the right boundary.

The numerical calculations were carried out in a 500 MHz personal workstation DEC Alpha with 768 MB memory. The first step was to simulate the wave profile without any reef, and then to compare the wave profiles with those obtained from the installation of one, two, three, six, and twelve reefs. Since turbulence was present in the vicinity of reefs, a k-ε turbulence model was included by setting the input file to give a better representation of the turbulence around the reefs. The flow chart for the implementation of the numerical analysis, described in chapter 3 is given in Appendix A. A typical input file for FLOW-3D is given in Appendix B for two-dimensional flow.

To check the convergence of results obtained in this study with respect to mesh size, the total number of cells in the computational domain were varied in the vicinity of reefs. The comparison of time history results for water profile and velocity magnitudes in water surface near the reefs [at (-23.0m, 4.0m)] for the 12 reefs configuration are presented in Figure 4.4. For the coarse grids, the number of cells in the reefs vicinity were 13, and for the normal and fine grids were 39 and 65, respectively.

Total cells used in the horizontal direction for coarse grids were 140 cells, while for the normal and fine grids were 166 and 192 respectively. In the vertical direction the total cells for coarse grids were 6, for normal and fine grids were 18 and 30, respectively. Therefore, total number of cells used were 840, 2988 and 5760, respectively, for coarse, normal and fine grids as given in Table 4.1. Figure 4.4 below shows the velocity magnitudes and water surface profile histories for varying grid sizes near reefs.

Table 4.1. Number of Cells used in Varying Grid Sizes

Horizontal (x axis) : 140 m	**Coarse**	**Normal**	**Fine**
-50.0 m to +0.0 m	50	50	50
+0.0 m to +13.0 m	13	39	65
+13.0 m to +90.0 m	77	77	77
Vertical (z axis) : 6.0 m	**Coarse**	**Normal**	**Fine**
+0.0 m to +6.0 m	6	18	30
Total Cells	**840**	**3042**	**5760**

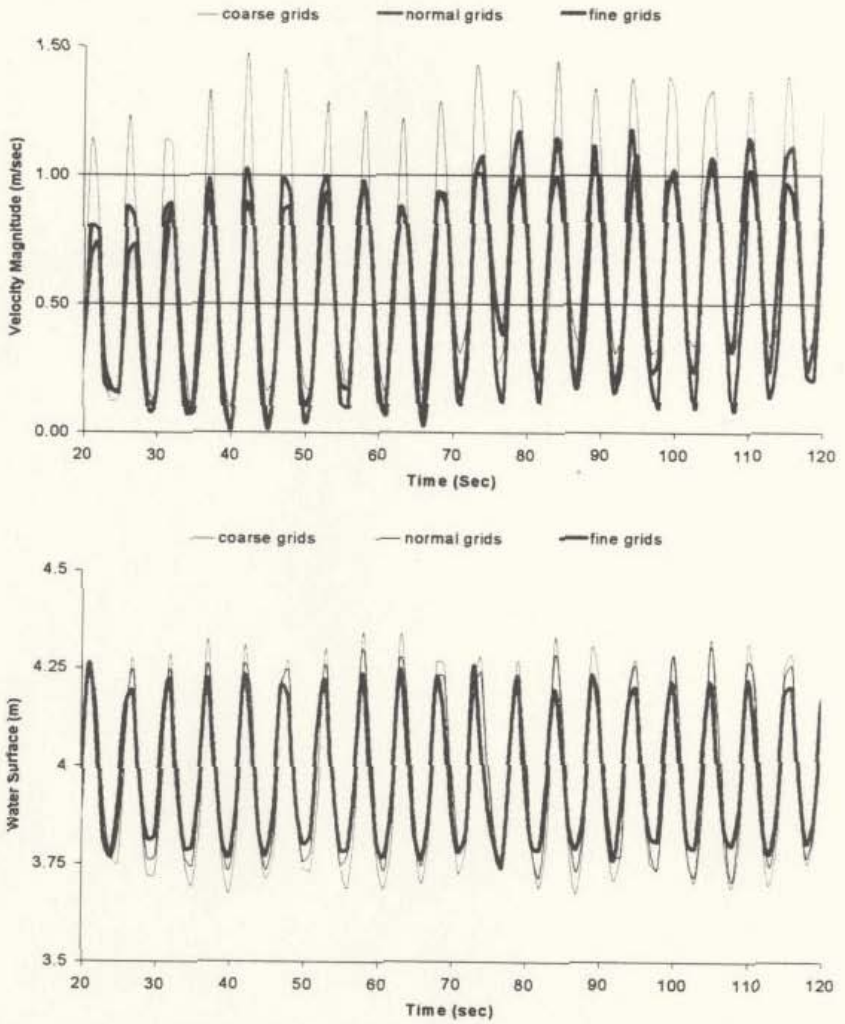

Figure 4.4 Velocity Magnitude and Water Surface Profile Histories for Varying Grid Sizes near Reefs

Figure 4.4. shows that there were no differences in phase due to those grids, but there were differences in wave profile and velocity magnitude time histories. The differences between the normal and fine grids were not significant in the water profile plots. However, for the velocity magnitude time history plots, generally, the coarse grids gave the highest values, while the fine grids gave the lowest. The differences in velocity magnitudes were around 10 to 40 percent between the normal and fine grids. Hence in this study, the fine grids were used to model the flow field in the reef's vicinity.

4.3. Results And Discussion

The model without reefs followed the surf similarity model that has been analyzed previously using FLOW3D (Richardson, 1996); that study was repeated to verify the results from the specified grid arrangements as described before. In this study, a 5% beach slope and 1.0 m deep-water wave height with 5 second period was used as input parameters, and the resulting breaking wave characteristics were examined and compared to the previous study.

Typical profiles of breaking waves and variation of breaking wave characteristics for three beach slopes were given by Wiegel (1964) and are shown by Figure 4.5. Each of the breaking wave type given in Figure 4.5, can be represented by Battjes' (1974), surf similarity parameter:

$$\xi = \frac{\tan \alpha}{(H / L_o)^{0.5}} \qquad (4.1)$$

where tan α is the beach slope, H is the incident wave height at the toe of the beach, and Lo is the deepwater wavelength. Table 4.2 shows the surf similarity parameter and breaking wave characteristic as defined by Battjes (1974).

Table 4.2 Breaking Wave Characteristics and The Surf Similarity Parameter (Battjes, 1974)

ξ	0.1	0.5	1.0	2.0	3.0	4.0	5.0
Type	spilling		plunging	collapsing/surging			no breaking

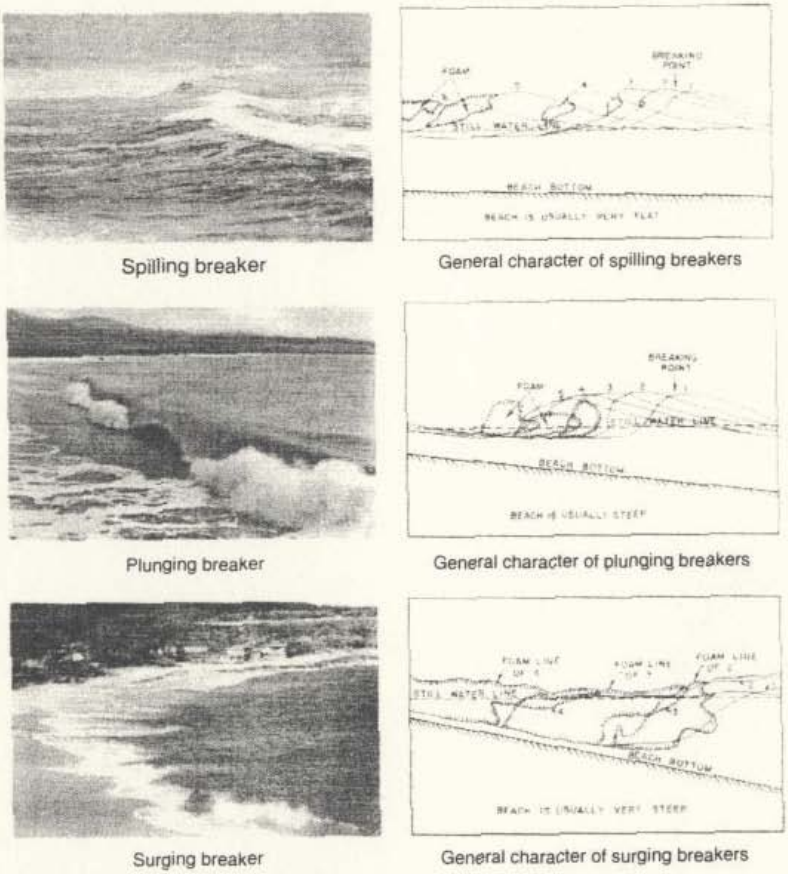

Figure 4.5 Types of breaking waves on the shore (Wiegel, 1964)

Since a 5% beach slope with 4m depth at the toe and 1.0 m deep water wave height with 5 second period (equal to 39.03 m deepwater wave length) were used in this study, the wave could be characterized as spilling, based on Equation 4.1 (with $\xi = 0.312$) and Table 4.1. The computed water surface profile agreed well with the results published in various literatures for spilling type of breaking waves as shown in Figure 4.5 (Wiegel, 1964, Gross, 1987 and Carter, 1988). The wave amplitude profiles for every 10 seconds are given in the Figure 4.6. The computed wave height in the left boundary in Figure 4.6 (x: -50.0m), where the depth was 4.0 m resulted in 0.8m wave height, while computation based on linear wave method (CERC, 1984) was 0.93m. The 14% difference might be due the nonlinear effects produced by the 5% slope (not considered in the linear formulation), influence of spilling of waves and residual error in numerical computations. As soon as the wave travels forward, the wave feels the effects of the sloping bottom and the waveheight is reduced, as seen in Figure 4.6 (without any reef) for $t \geq 20$ sec.

The energy dissipation in computation was achieved by using the "k-ε turbulence model" available in FLOW3D and setting the viscosity to 0.0012 kg/m sec. Even though other models are available in FLOW3D, this model only was used in this study since many other researchers have favoured this model.

Typical water surface plots for models without reefs, and with one, two, three, six, and twelve reefs installed around 6.0 m from the toe of beach are given in Figures 4.6 to 4.11. These figures show that the wave amplitudes, within the basin enclosed by the reefs and the shore, get reduced when the number of reefs installed are increased. Below six reefs, the waves do not break over the reefs as shown in Figures 4.6 to 4.9. Above six reefs the waves break around the region where the reefs are located as seen from Figure 4.10 and 4.11.

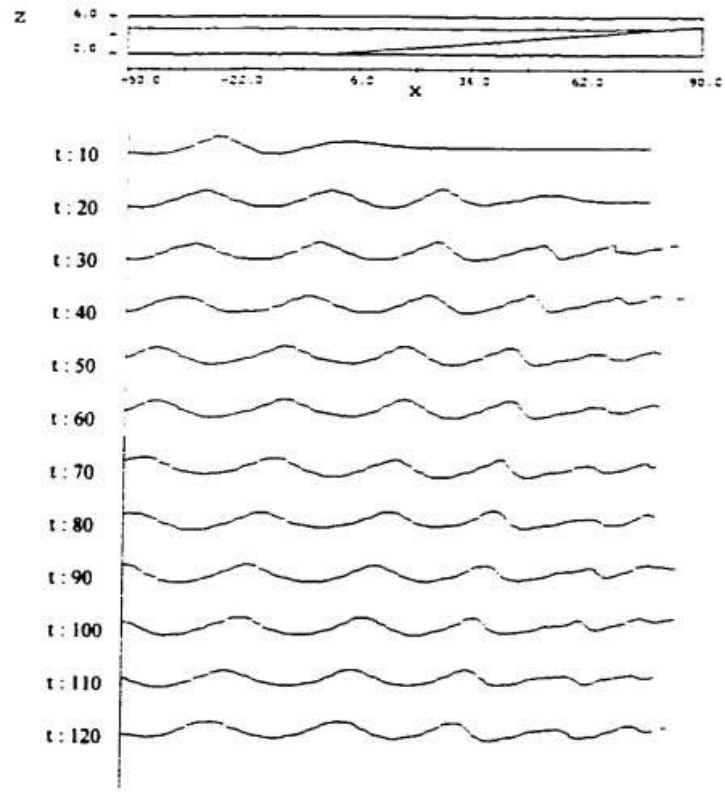

Figure 4.6. Water Surface Profile without Reefs

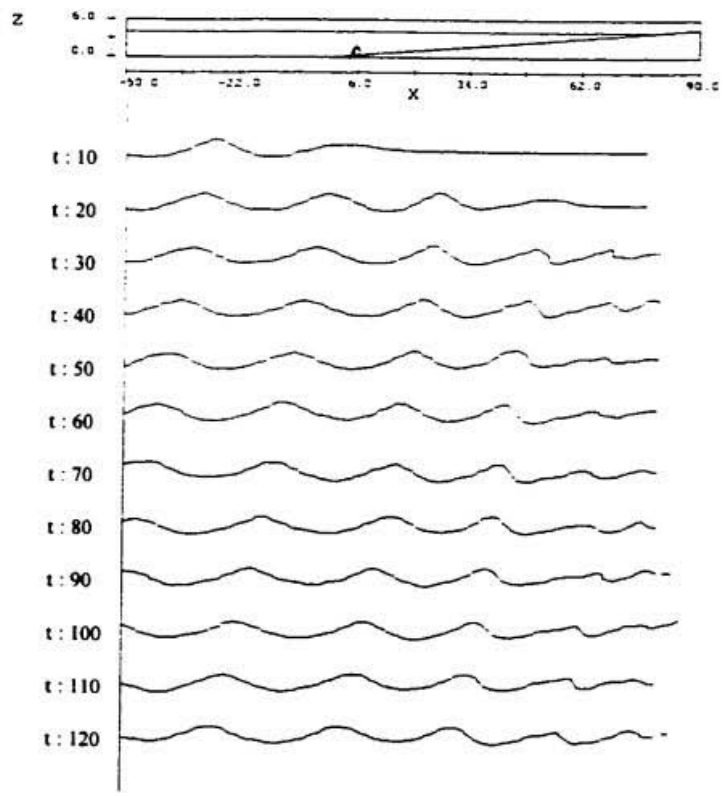

Figure 4.7. Water Surface Profile with One Reef

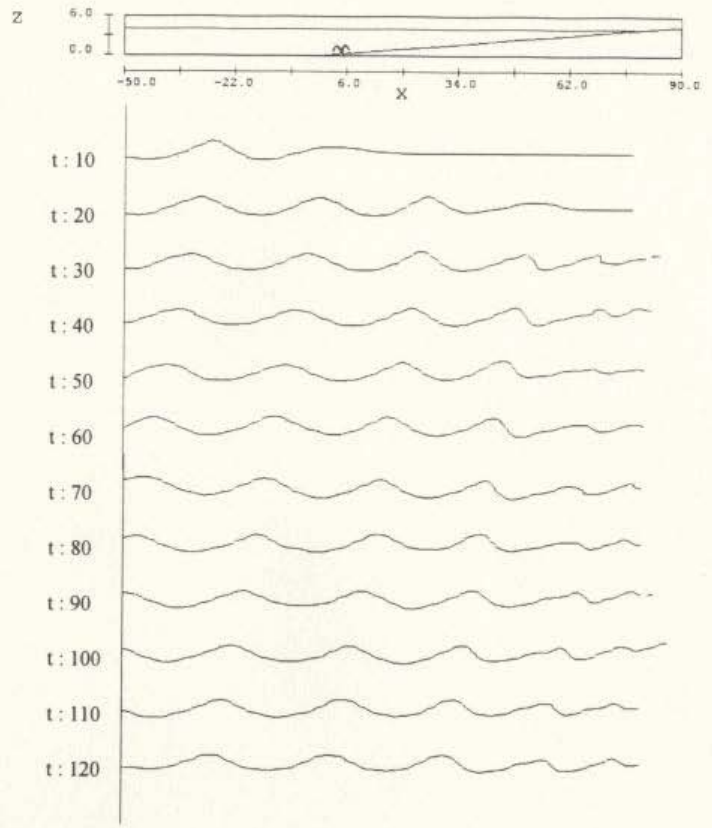

Figure 4.8. Water Surface Profile with Two Reefs

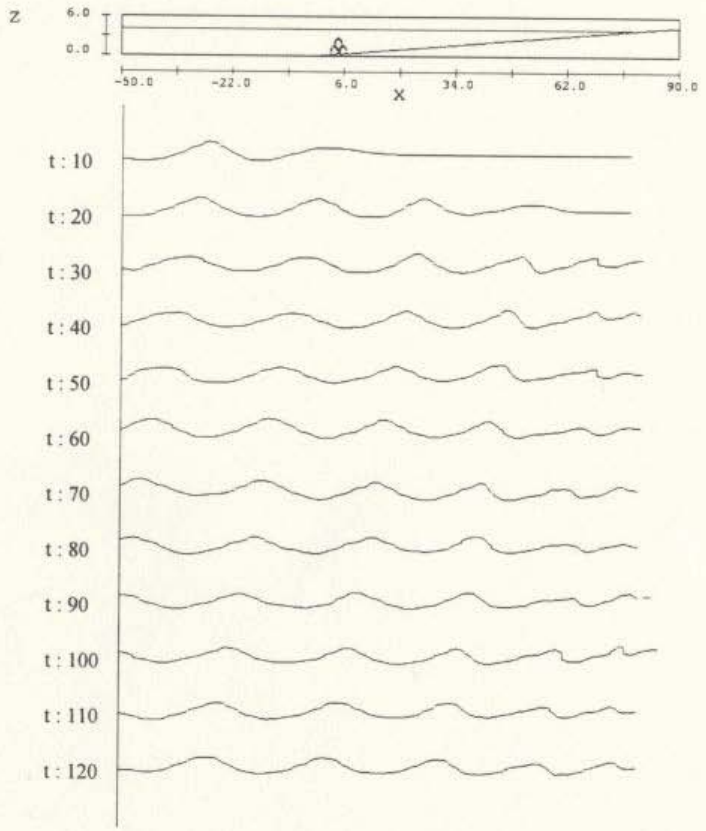

Figure 4.9 Water Surface Profile with Three Reefs

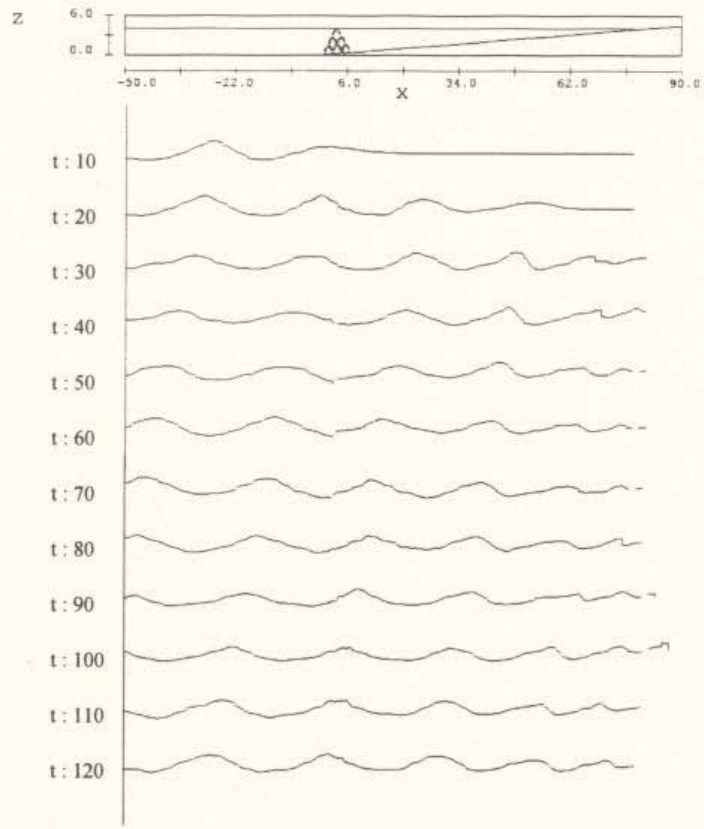

Figure 4.10. Water Surface Profile with Six Reefs

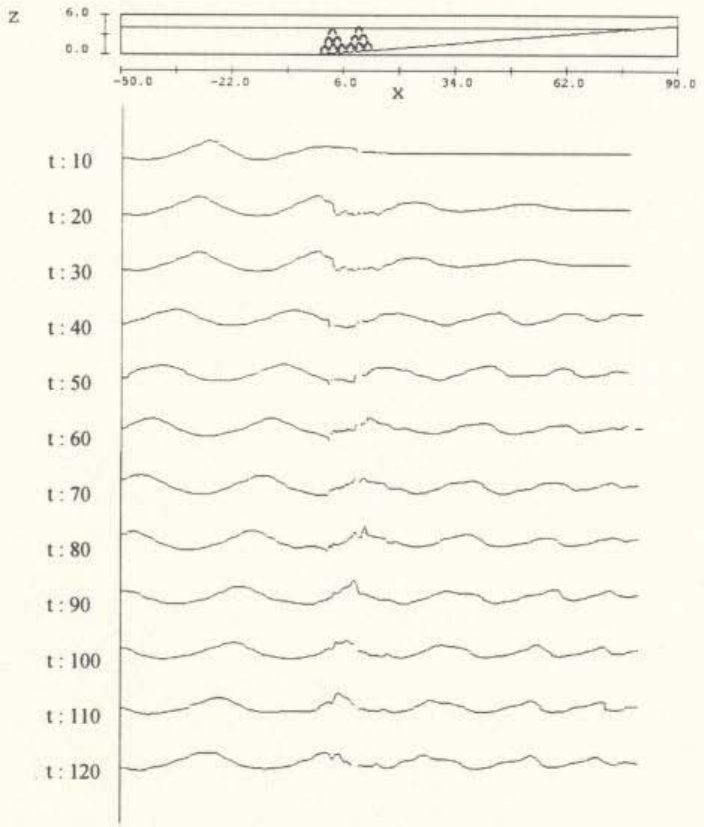

Figure 4.11 Water Surface Profile with Twelve Reefs

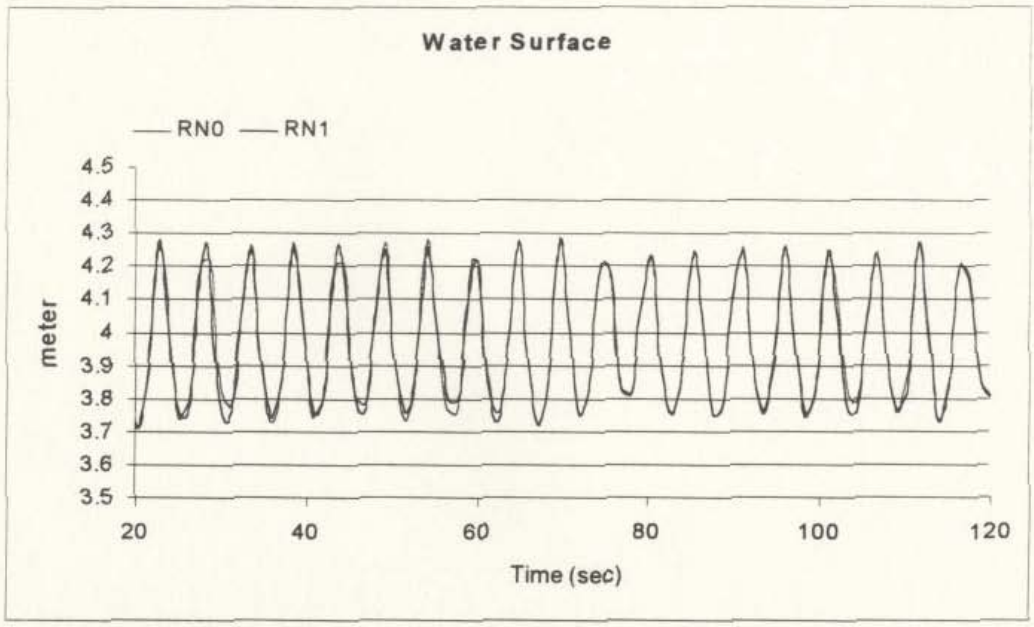

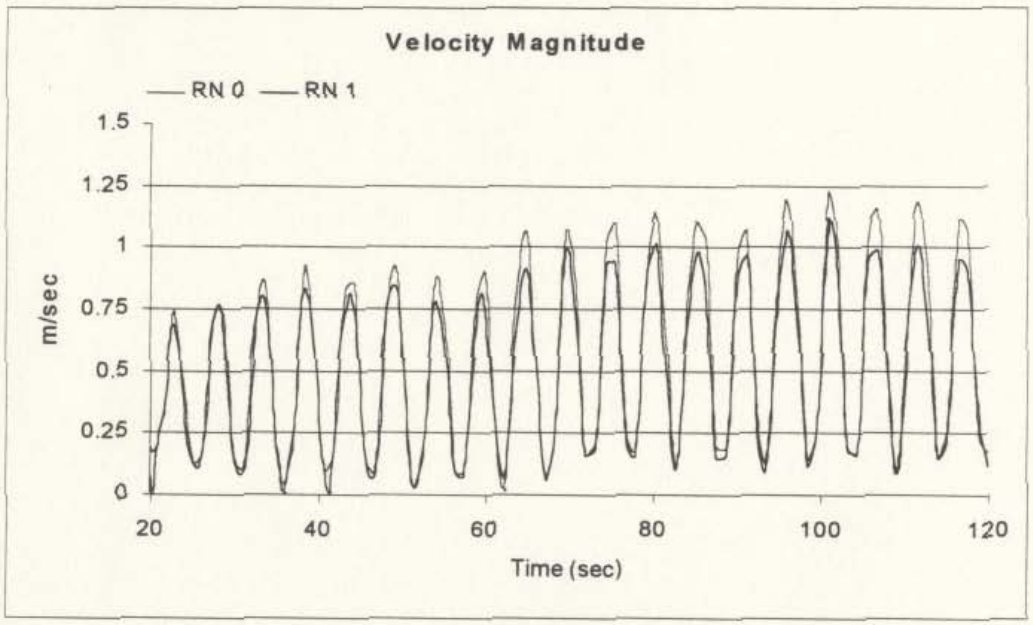

Figure 4.12 Water Surface Profile and Surface Velocity Magnitude Time Series for One Reef at x:+15.0m

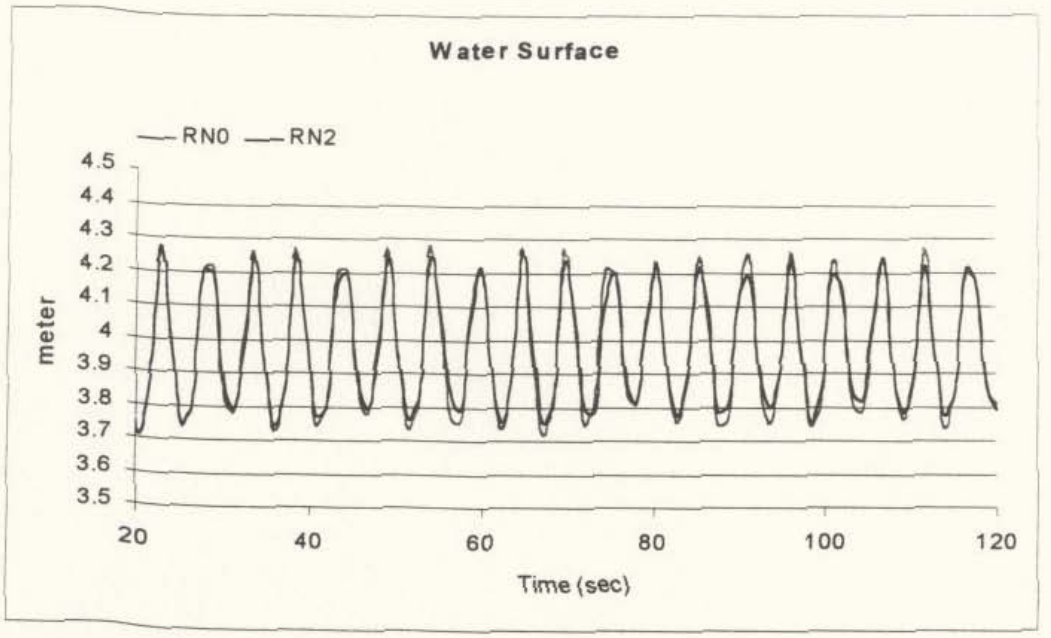

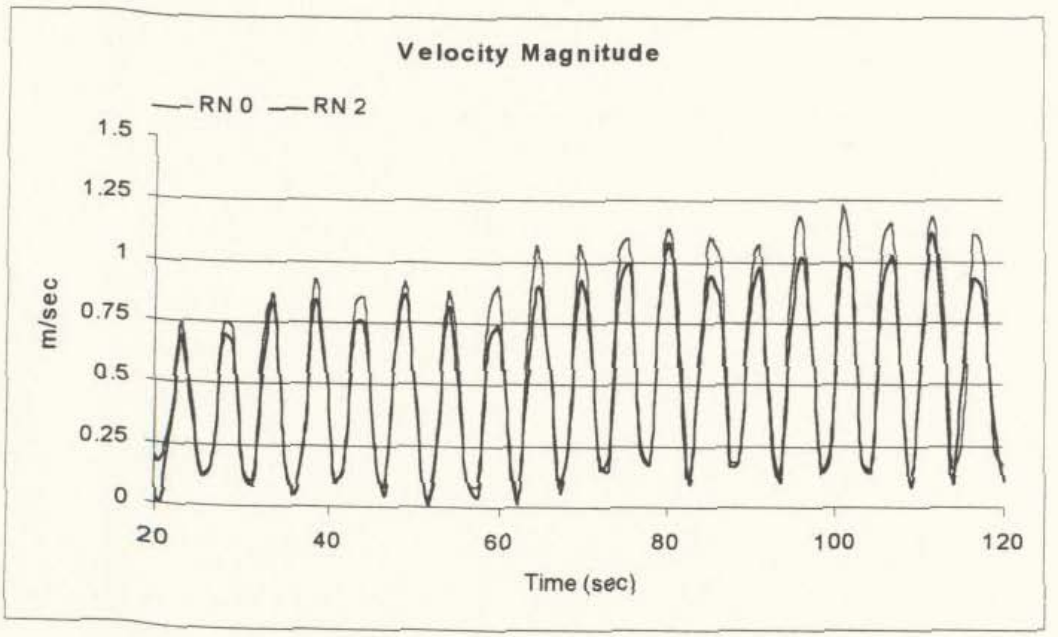

Figure 4.13 Water Surface Profile and Surface Velocity Magnitude Time Series for Two Reefs at x:+15.0m

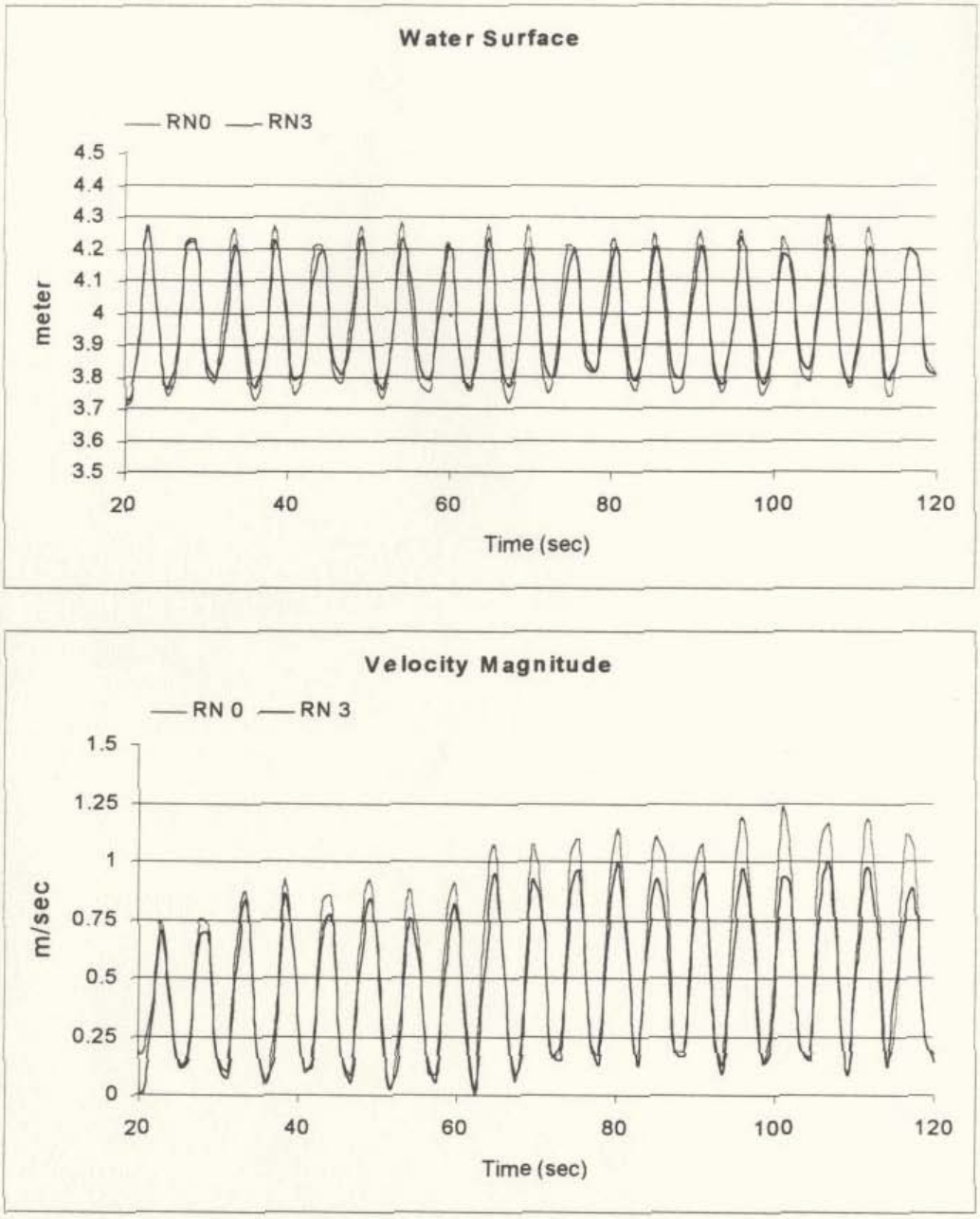

Figure 4.14 Water Surface Profile and Surface Velocity Magnitude Time Series for Three Reefs at x:+15.0m

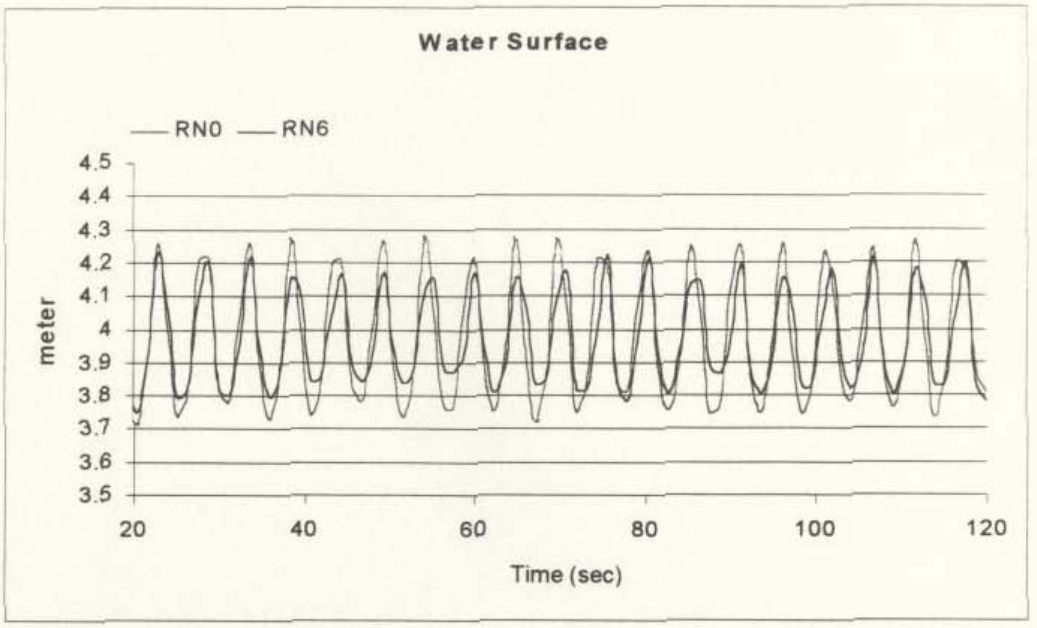

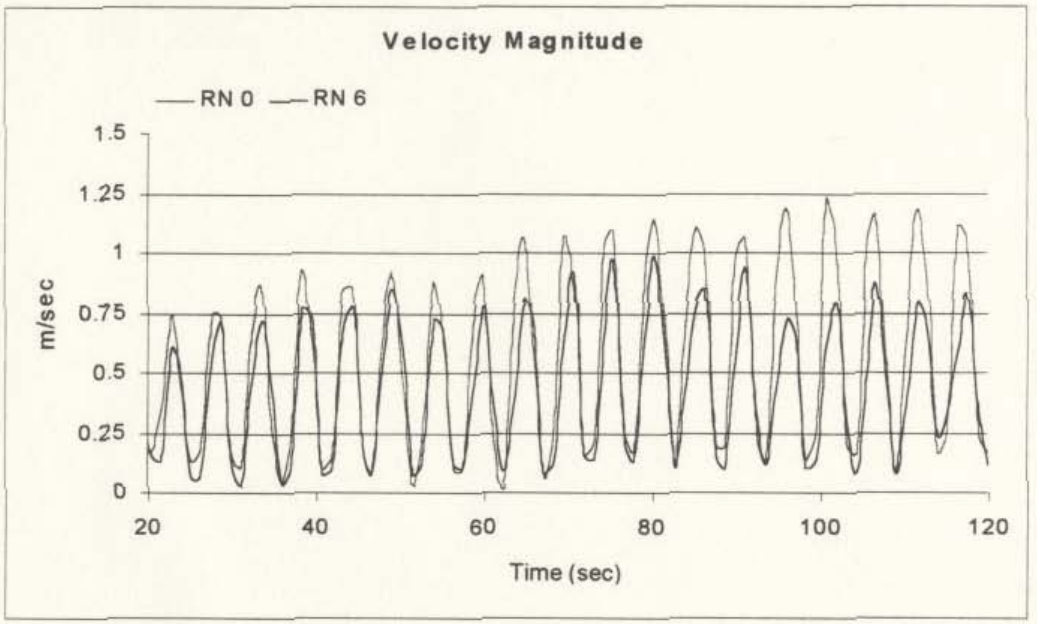

Figure 4.15 Water Surface Profile and Surface Velocity Magnitude Time Series for Six Reefs at x:+15.0m

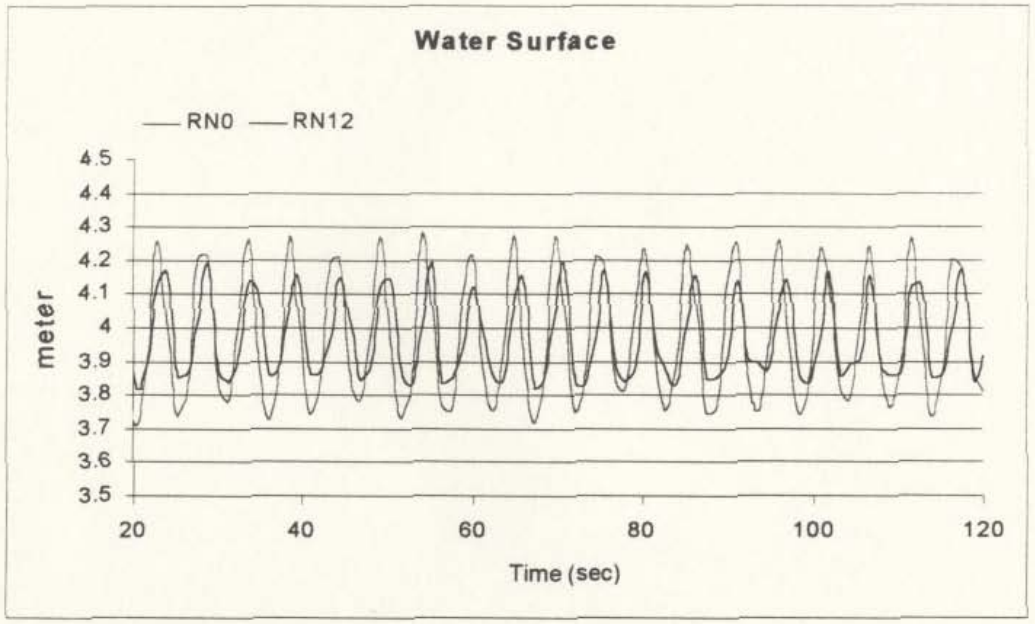

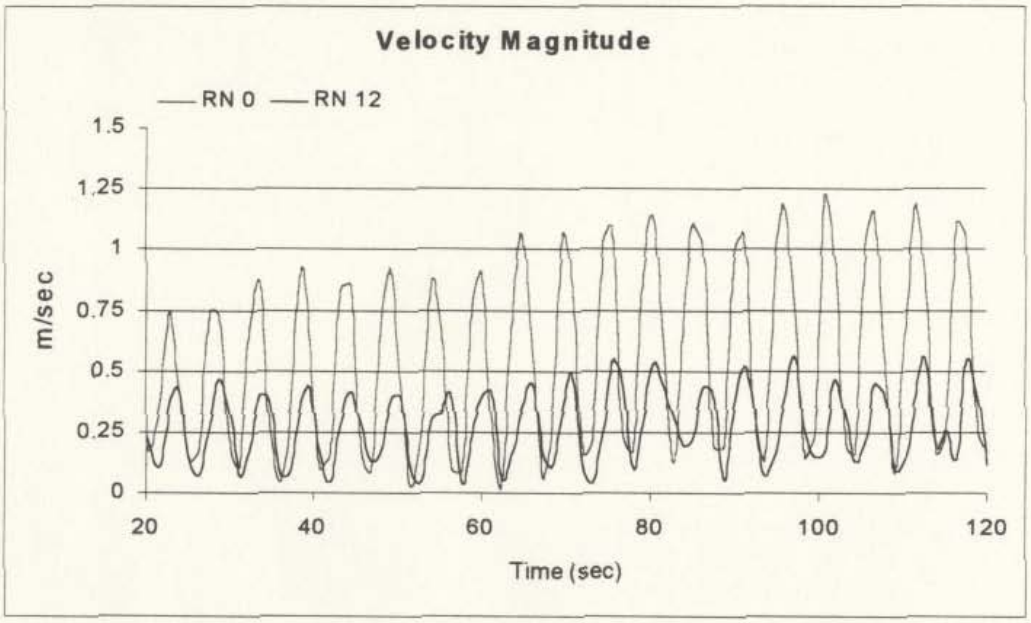

Figure 4.16 Water Surface Profile and Surface Velocity Magnitude Time Series for Twelve Reefs at x:+15

When the reefs are less than six, the waves travel over the reefs as if there is no obstruction and hence do not break at the reef location. This is due to the fact that the reefs are placed deep below the water surface and as such do not influence in reducing the energy of the wave located around the sea surface. However, as shown in Figures 4.10 and 4.11, where six and twelve reefs are installed, the waves break over the reefs and dissipate the wave energy considerably: this leads to the reduction of wave amplitude profiles.

In Figures 4.12 to 4.16, the water surface history plots at +15 meters from the toe of beach (inside the left hand end of the basin produced in between the reefs and shore) are compared before and after installation of the reefs. The red line represents the water surface without reefs, while the black line represents the water surface time history when the reefs, either, one, two, three, six, or twelve are installed. The reductions are noticeable when the number of reefs installed are twelve; (a phase shift can also be noticed). Since the model used for numerical analysis is only two dimensional, the crossflow generated in the lateral direction by the three-dimensional porous hemispherical reef is not properly modelled in analysis.

The FLOW3D computation resulted in an increase of all the flow variables as a results of fluid accumulation. In the results shown above, the mean accumulated value was subtracted (or added) on a cycle by cycle basis to maintain the horizontal nature of mean fluid surface.

Figures 4.12 to 4.16 also give the surface velocity variation within the basin (at x = +15.0 m) for one, two, three, six and twelve reefs. It is seen that the velocities at this

location (just near the reef on the shoreward side) decrease considerably for twelve reefs, which would facilitate the settlement of benthic diatoms and congregation of fish.

The two-dimensional model results show that the wave amplitudes are reduced inside the wave basin produced by reefs when the number of reefs are greater than six, even though the reduction is not significant. This reduction would create quiescent areas inside the basin between the reef and the coast leading to the congregation of fishes, settling down of biomass and the development of a productive aquaculture habitat.

However it must be cautioned that this reduction of velocities should not lead to the settlement of fine marine sediments which would lead to siltation and the consequent closure of reefs. The reduction of velocity must be such as to keep the mean average velocity above the critical settling velocity of marine sediments.

As water moves through the reefs, the incoming wave energy is dissipated by turbulence; furthermore, pressure waves, which can be detected by fish, are produced as water exits through the holes on the top and sides of the hemispherical balls. Turbulent water, which exits/enters through the holes on the top and sides, moves upward/ downward and modifies the incoming/outgoing wave field.

This movement of water is found to be effective in attracting fish swimming near the sea surface. Typical flow over one wave period, around the reefs, is given in Figures 4.17 to 4.22. It is seen that the waves break over the reefs when the number of reef units installed are more than six (Figures 4.21 and 4.22). The shades of colors represent the varying velocity magnitudes in the vicinity of reefs. As seen in the figure the energy dissipation, due to turbulence around each structure, leads to almost quiescent local areas (points A, B, and C, shown in Figure 4.3) in and around the lower hemispherical reefs

where fish can settle down and spawn. The area where the velocities are low are represented by the blue color.

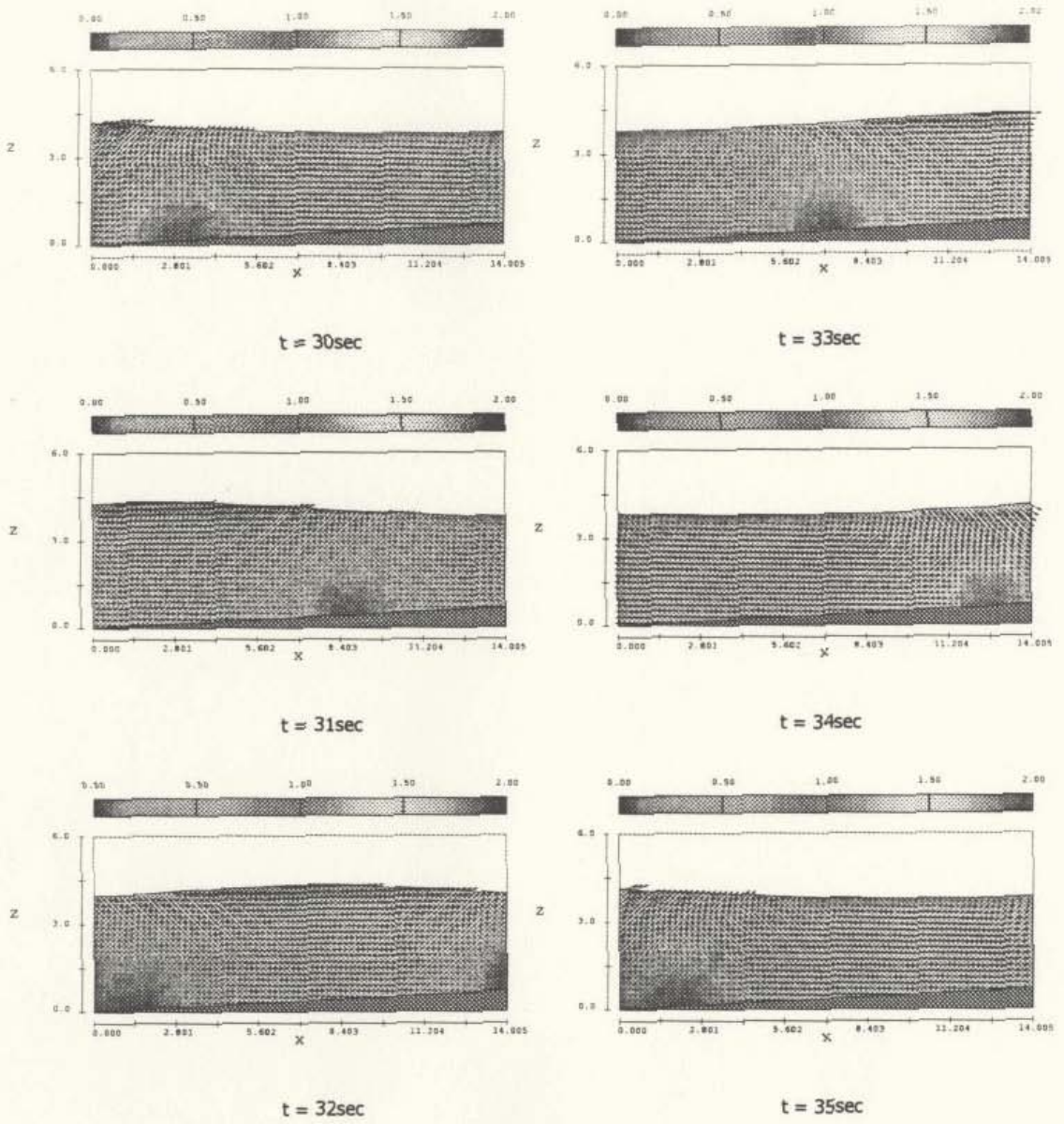

Figure 4.17 Velocity Magnitudes for a Beach without Reefs at Various Times

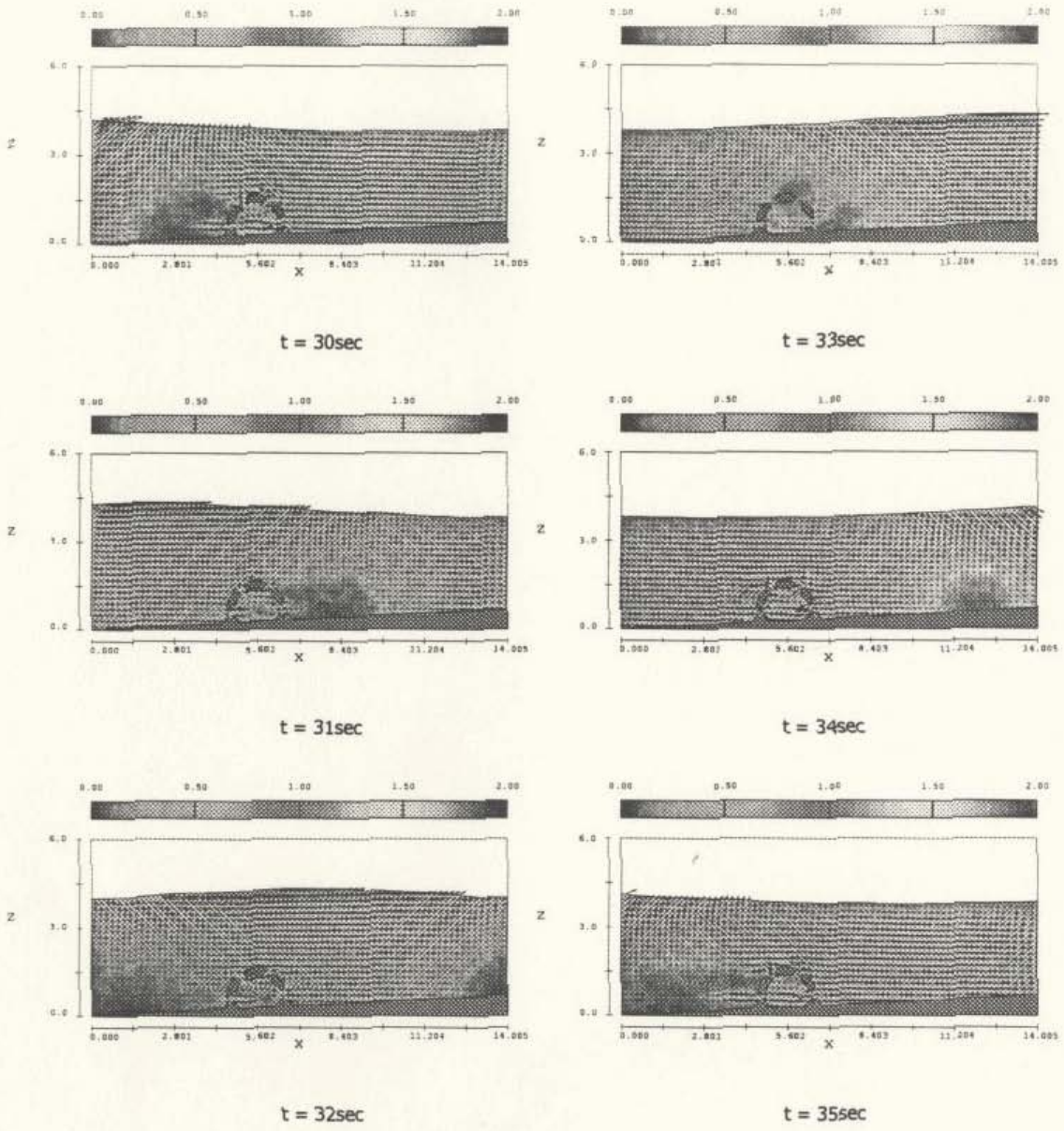

Figure 4.18 Velocity Magnitudes for a Beach with One Reef at Various Times

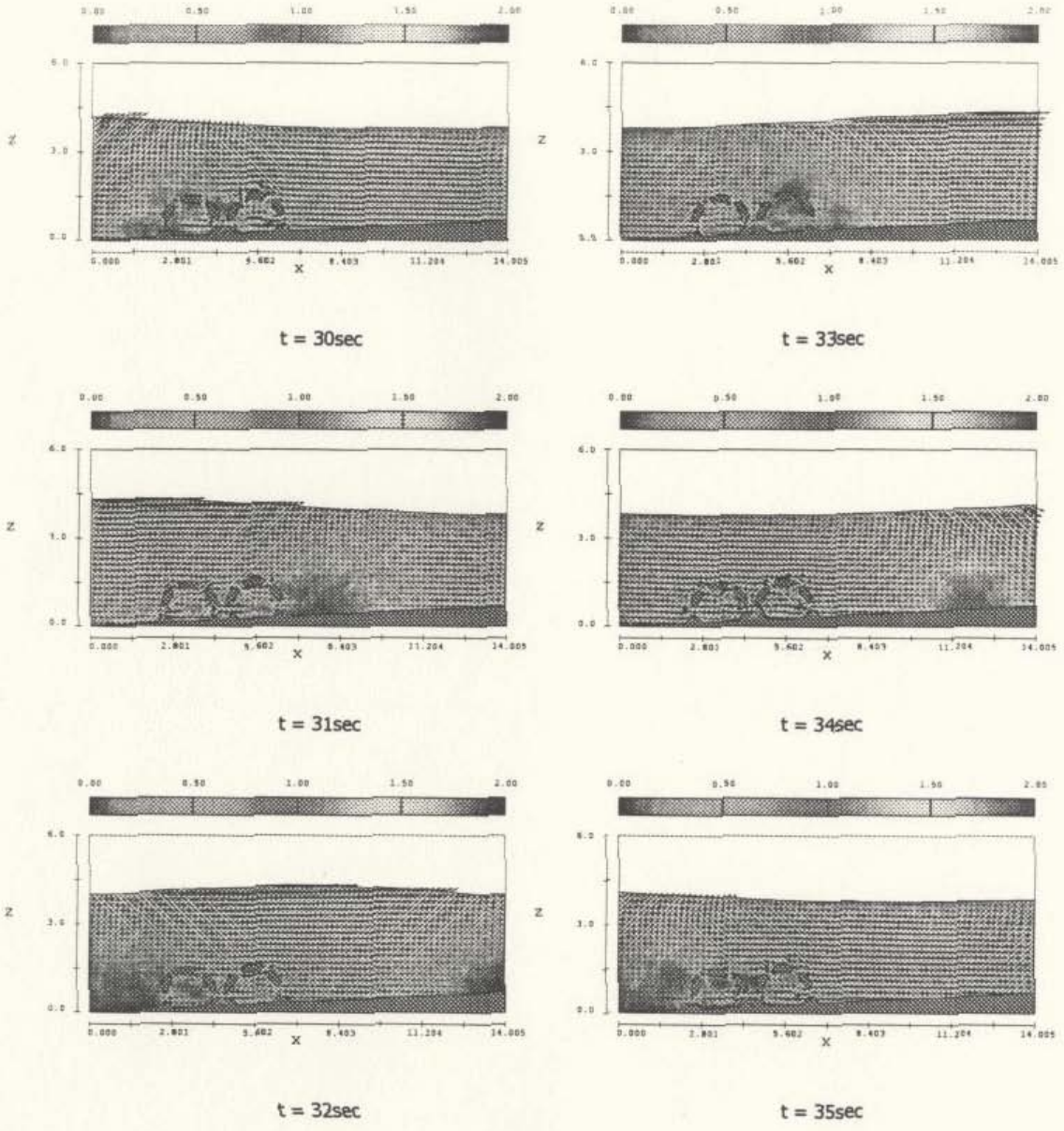

Figure 4.19 Velocity Magnitudes for a Beach with Two Reefs at Various Times

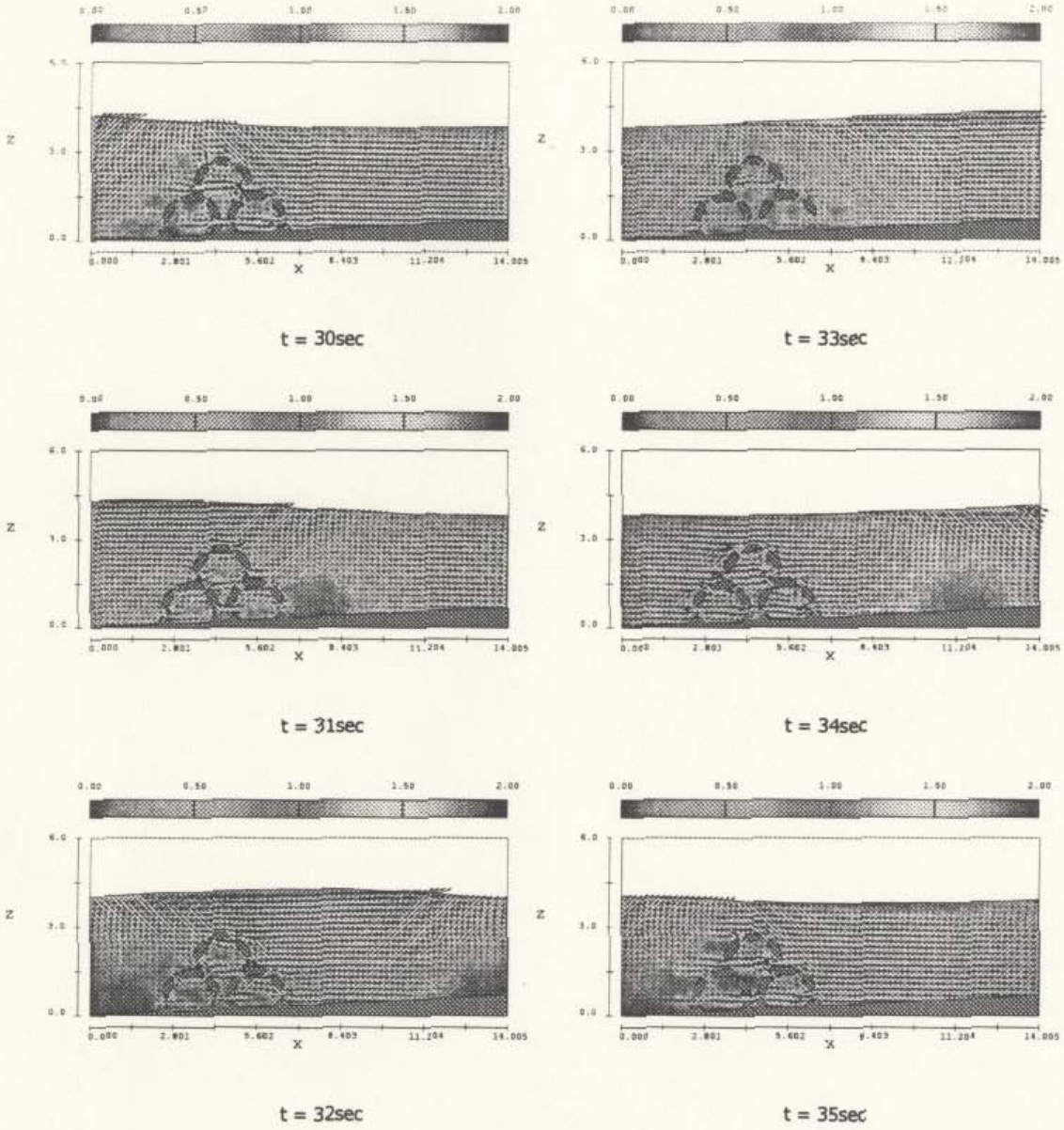

Figure 4.20 Velocity Magnitudes for a Beach with Three Reefs at Various Times

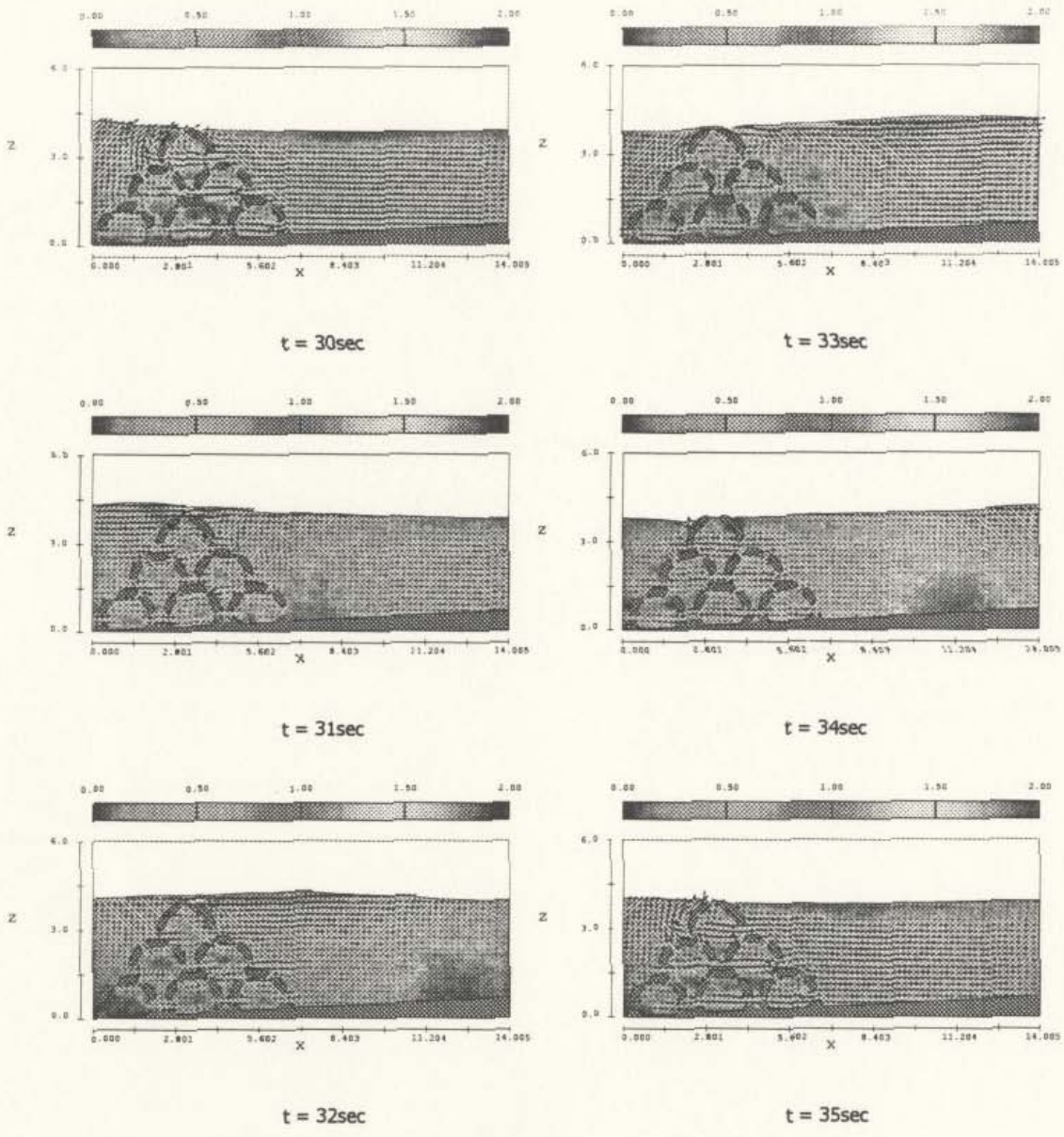

Figure 4.21 Velocity Magnitudes for a Beach with Six Reefs at Various Times

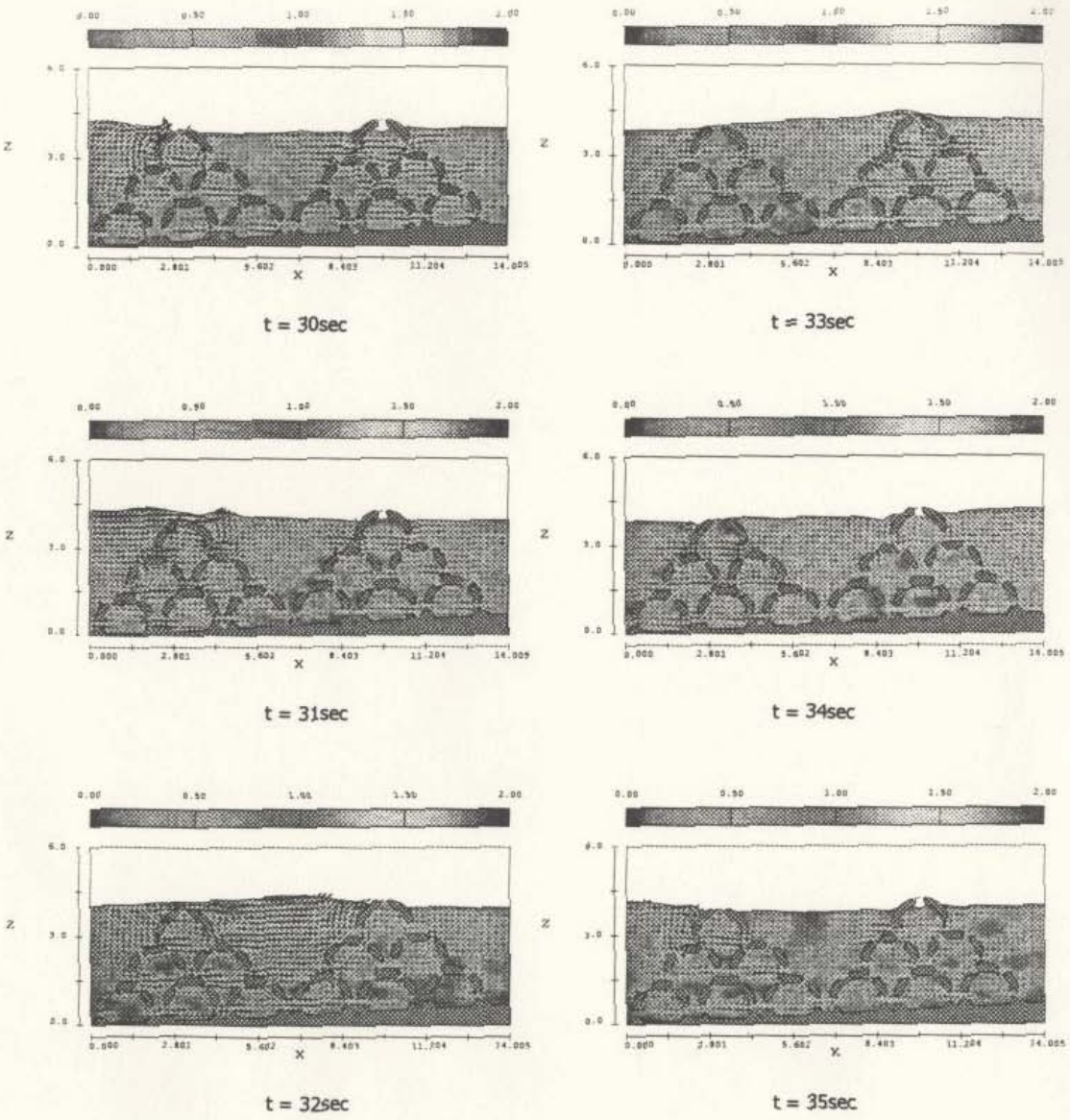

Figure 4.22 Velocity Magnitudes for a Beach with Twelve Reefs at Various Times

It should also be noted that the generated reduced fluid flow would lead to the deposition of sediments containing food organisms; as well it would also lead to the growth of seaweeds. This would attract bottom-feeding animals such as flatfish, sea urchins and lobsters. These benthic animals tend to congregate and populate the partially quiescent areas on the leeward side of these structures. As stated by Mottet (1986) the possibility of silting at the bottom of the hemispherical reef (due to very low velocities), that will inhibit the growth of benthic diatoms and prevent the attachment of seaweed spores, must be judiciously minimized.

From a computation of the Keulegan-Carpenter (KC) numbers (U_{max} x T/D) for the flow inside the reefballs, it was observed that the KC numbers fluctuated in the ranges of 5.5 to 11.25 for locations A, B, and C (Figs. 4.23 to 4.27). Hence the flow can be characterized as inertia-dominated for lower values of KC < 6 and inertia & drag dominated for the higher values of 6 < KC < 11.25. Since the flow is not highly turbulent (KC > 25) the turbulence effects are not very dominant in these regions. Hence the use of k-ε turbulence model is justified.

Time series for velocity magnitudes before and after reef installation, for one, two, three, six and twelve reefs at points A, B and C within the reef in the bottom layer (indicated in Figure 4.3), are shown in Figures 4.23 to 4.27. It is seen that the water velocities decrease considerably especially in the twelve reefs installation at all the three locations (A, B, and C) facilitating the attachment of marine organisms and their subsequent growth, especially at locations B and C.

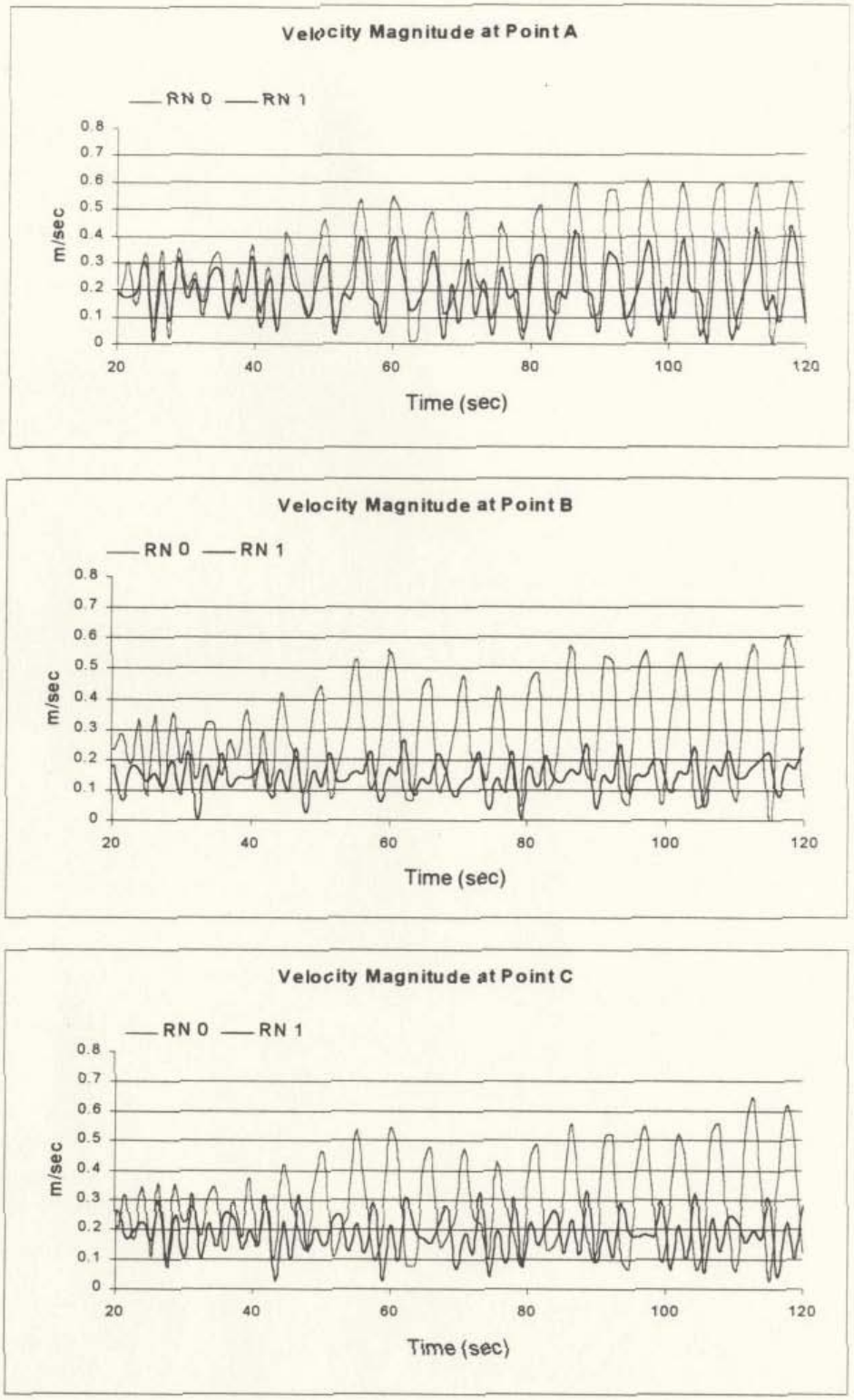

Figure 4.23. Velocity Magnitudes Time Series for One Reef at Points A, B, and C

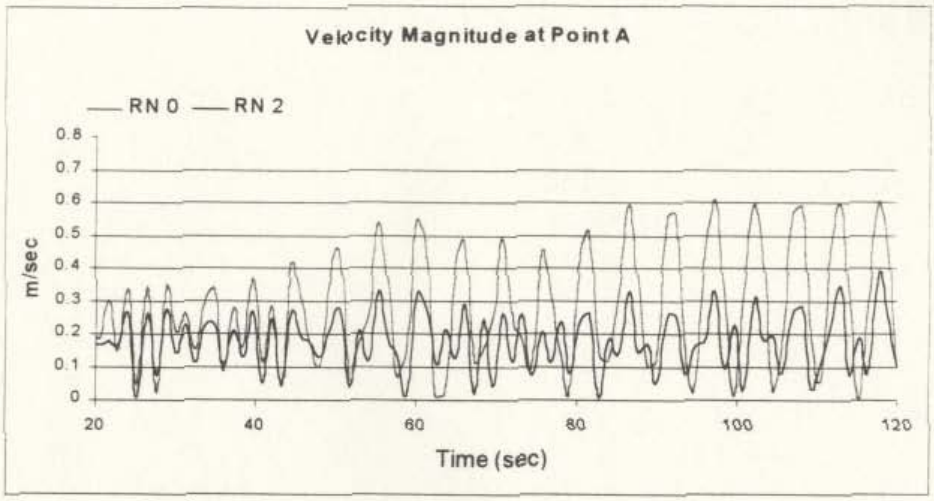

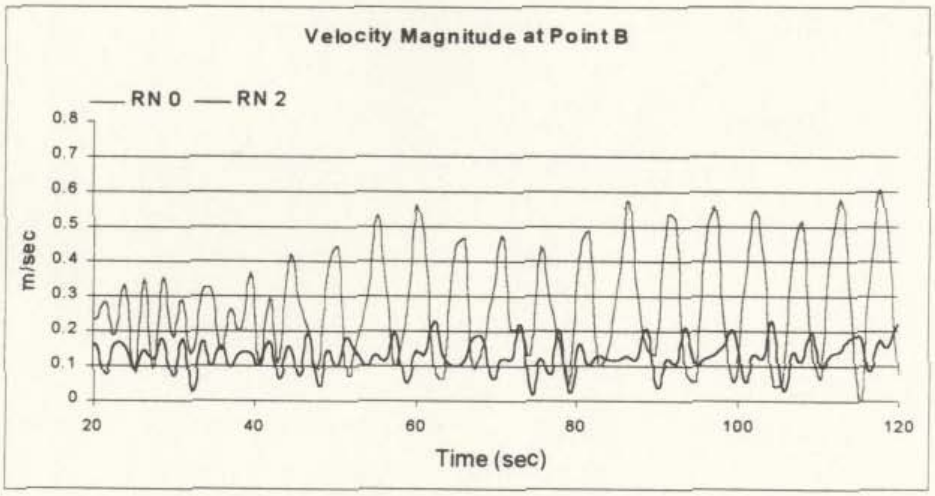

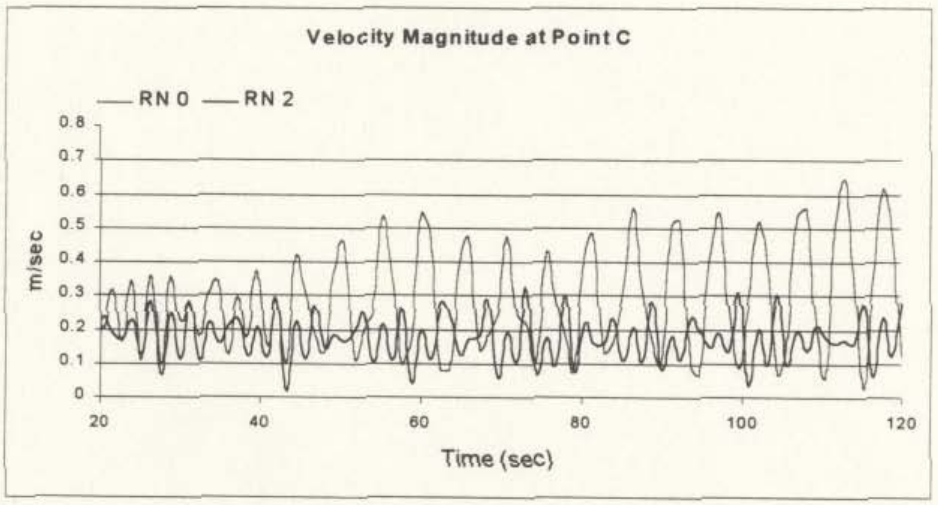

Figure 4.24. Velocity Magnitudes Time Series for Two Reefs at Points A, B, and C

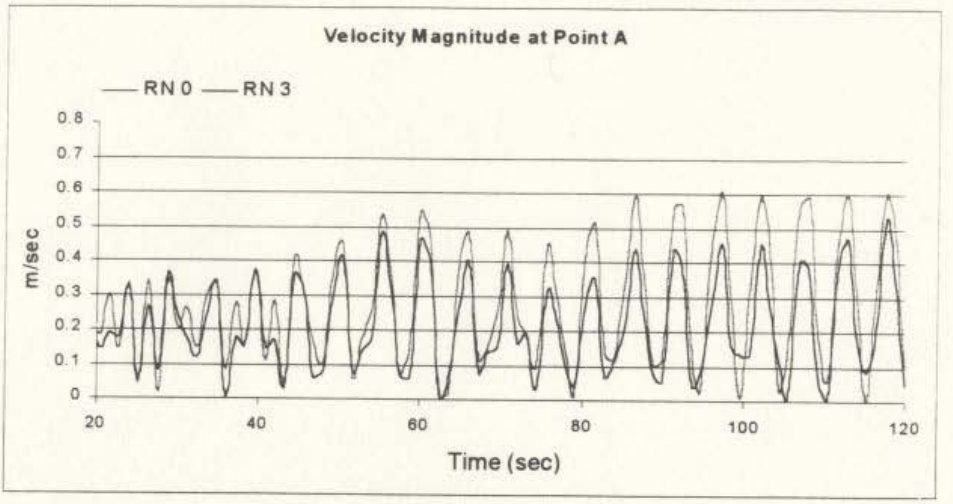

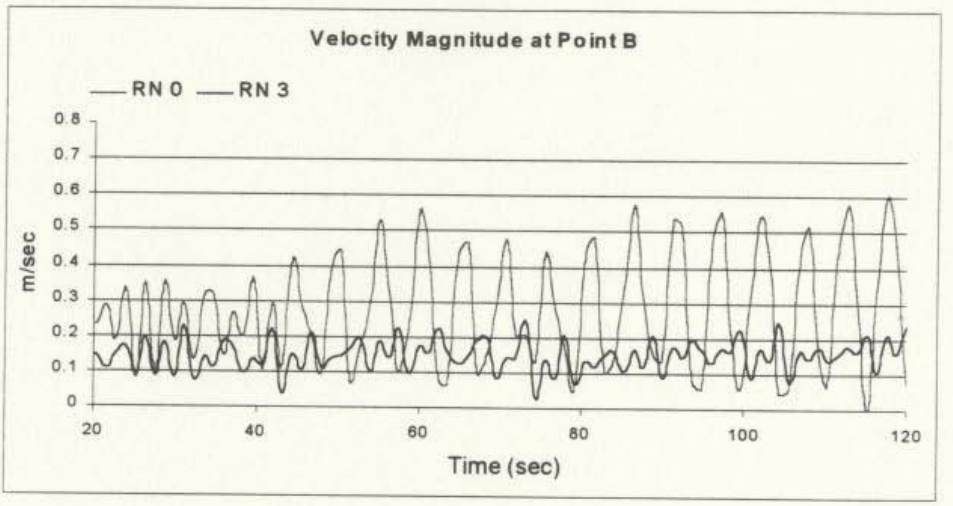

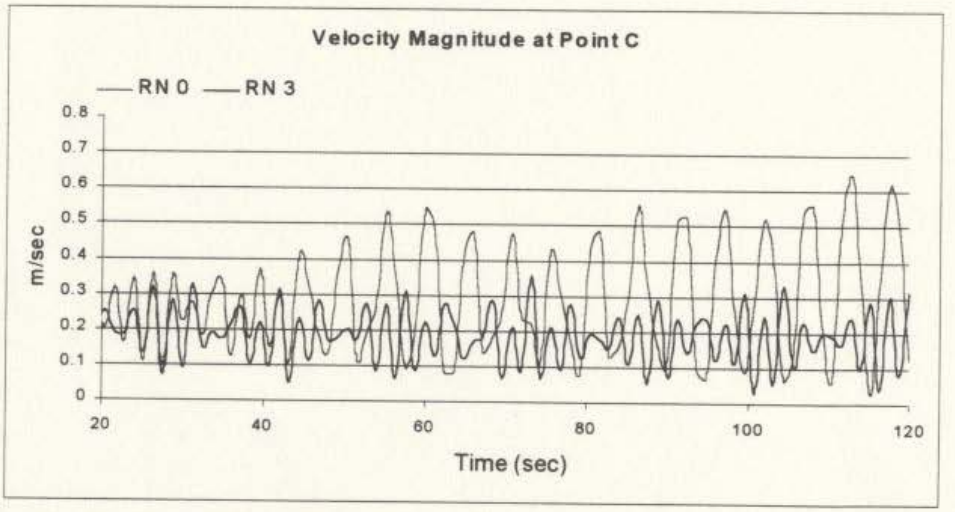

Figure 4.25. Velocity Magnitudes Time Series for Three Reefs at Points A, B, and C

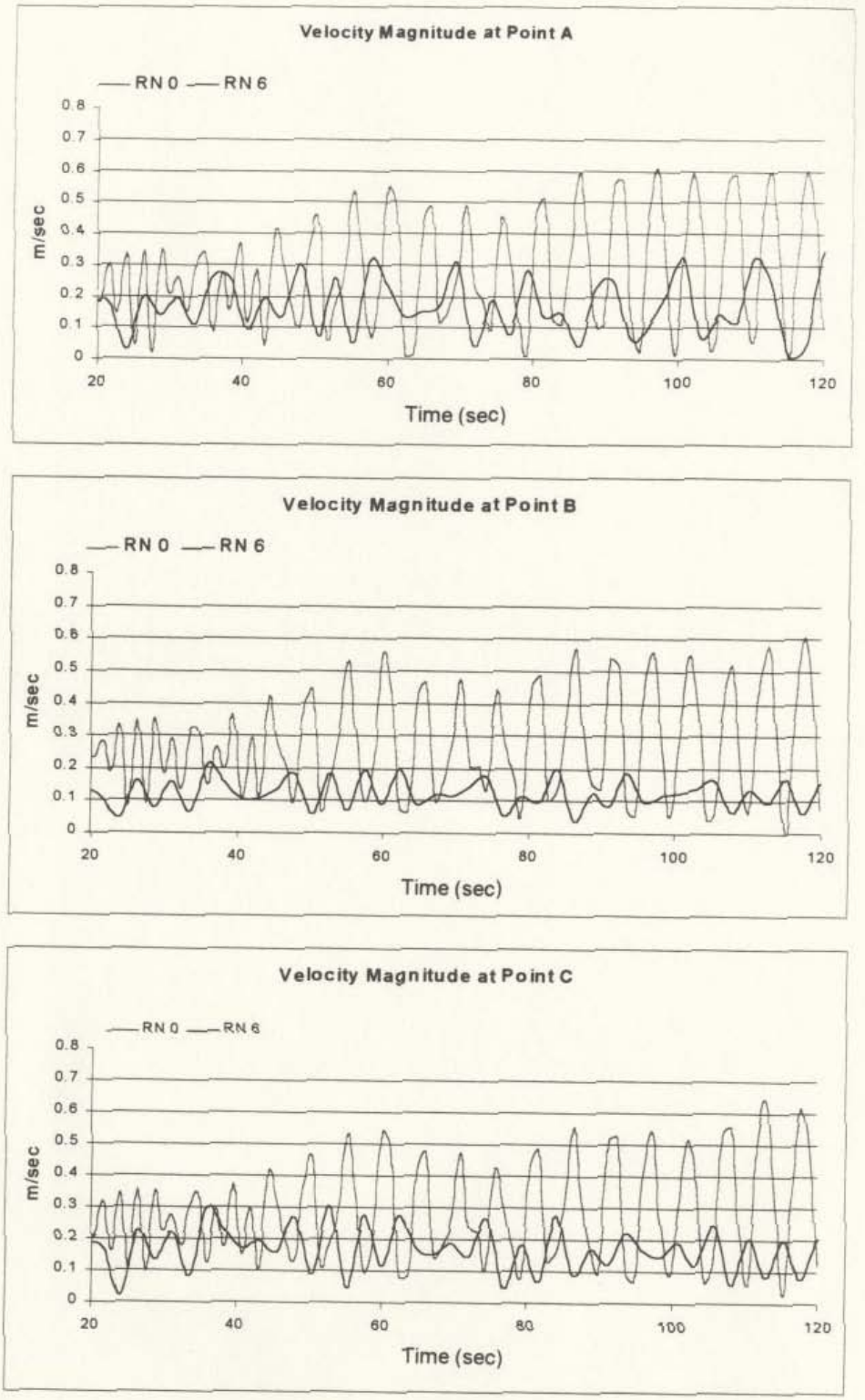

Figure 4.26. Velocity Magnitudes Time Series for Six Reefs at Points A, B, and C

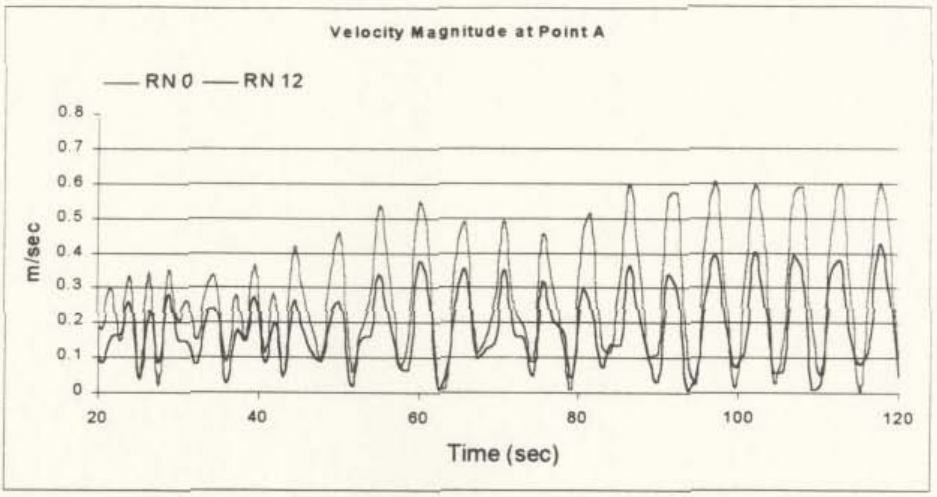

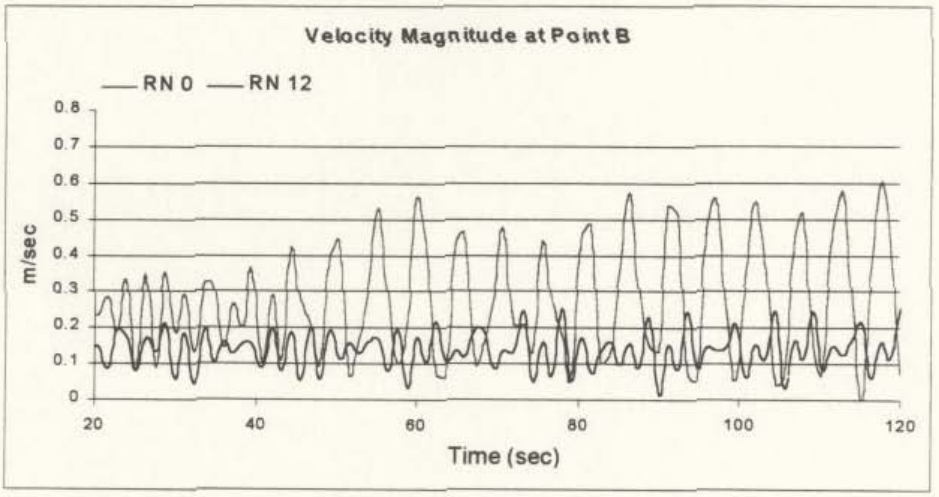

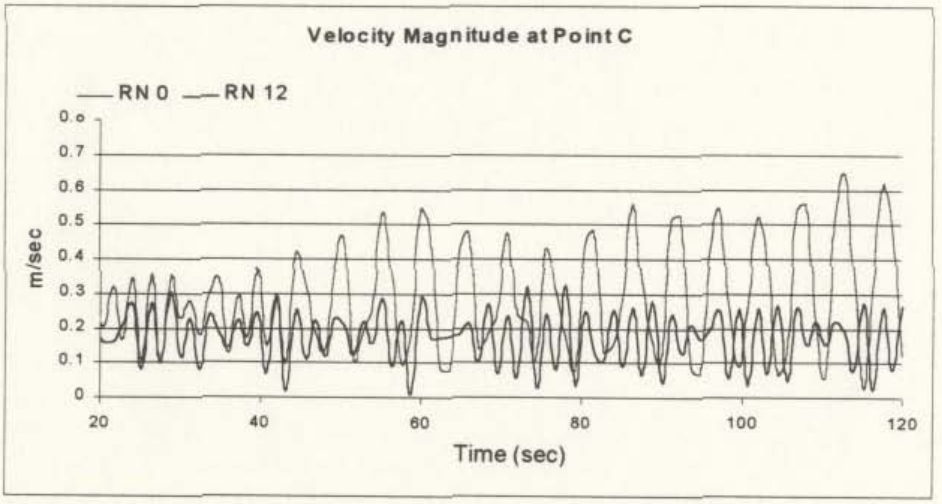

Figure 4.27 Velocity Magnitudes Time Series for Twelve Reef at Points A, B, and C

4.4. Summary

The numerical analysis of the two-dimensional model of an artificial reef with hemispherical hollow units has been presented here. It can be concluded that increasing the number of installed reefs will reduce the waveheight and velocity magnitudes considerably. However, if the number of installed reefs are below six, the energy is not dissipated much; this might be due to the placement of the reef units below the water surface.

Since the model used for numerical analysis is only two dimensional, the crossflow generated in the lateral direction by the three-dimensional porous hemispherical reef is not properly modelled in analysis. Therefore, a three dimensional model study was also carried out, and the results are presented in the next chapter.

Chapter 5
Three Dimensional Modelling of Artificial Reefs with Hollow Hemispherical Blocks

5.1. Introduction

The results of the three dimensional modelling of the hollow hemispherical reefs is presented in this chapter. As stated before, in the two-dimensional model, the lateral flow in the reef vicinity was neglected. Therefore, to model the lateral flow, a three-dimensional analysis was carried out. The three dimensional model was essentially an extension of the two dimensional model in the lateral direction (y axis). However, due to the limitation of the software, the effects of refraction or diffraction of the incoming wave could not be properly investigated in the analysis, since the numerical model could consider only a small transverse section in the vicinity of reefs. Similar to the two-dimensional model, the waveheight as well as the velocity at salient points in the reefs' vicinity of the three dimensional model is compared to those of the model without reefs.

The results of twelve reefs as used in the two dimensional model is also compared to fifteen and twenty-four reefs configuration (of three-dimensional model).

5.2. Numerical Model

In general, the results of three-dimensional model are similar to those of two-dimensional model. The reef was located upward from the toe of the beach (5% slope) as shown in Figure 4.1, given earlier. However, since the computational range of the number of cells provided by the software was limited, the grids were rearranged to obtain an optimum computational accuracy.

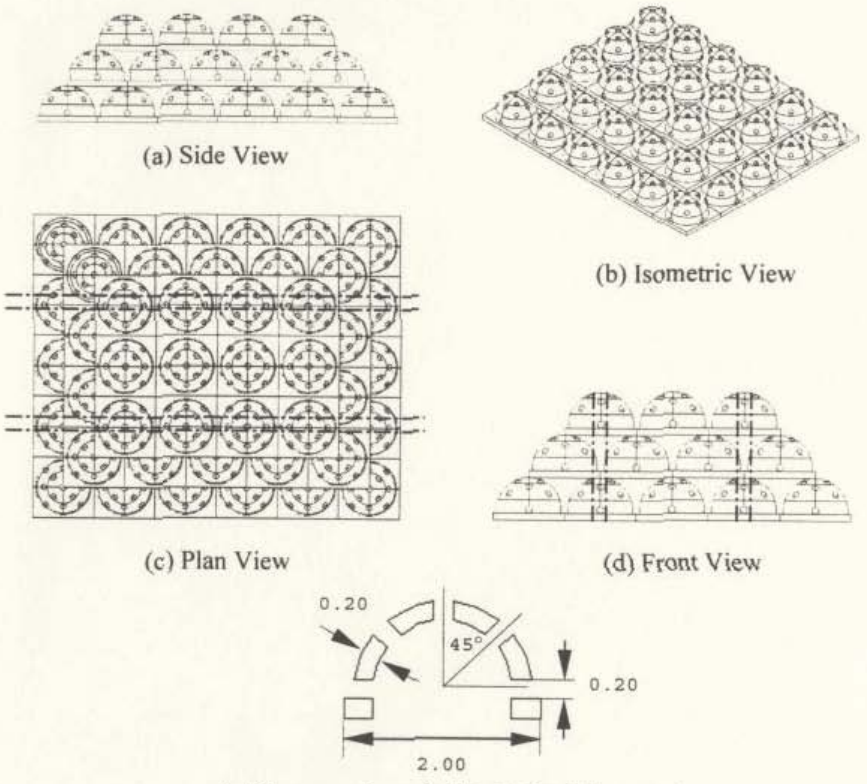

(a) Side View

(b) Isometric View

(c) Plan View

(d) Front View

(e) Cross-section of a Single Reef (in meter)

Figure 5.1 Typical Three Dimensional Reef Arrangement

The designation of 'twelve', 'fifteen', and 'twenty four' represent the number of reefs (used in building of reef) that could be seen from their side view. For example, in Figure 5.1, the total number of reef units used in the model were more than 15; however, from the side view as shown in Figure 5.1(a), the number of reefs were only 15

Table 5.1 Number of cell used in computational domain

Along the Horizontal (x axis) : 140 m	**Number of Cells**	**Total Cells**
-50.0m to -48.0m	10	
-48.0m to +0.0m	29	
+0.0m to +20.0m	100	
+20.0m to +68.0m	29	
+68.0m to +70.0m	10	
+70.0m to +90.0m	20	**198**
Along the Lateral (y axis) : 6.0 m		
+0.0m to +6.0m	30	**30**
Along the Vertical (z axis) : 4.0 m		
+0.0m to +4.0m	20	**20**

Due to the limitation of the software and the symmetrical nature of the reefs, the computational domain was limited only to a 4.0 m width, while the length and height were similar to the two dimensional model; viz., 140.0 m and 6.0 m, respectively. The computational grid consisted of 198 cells in horizontal direction (x axis). In the horizontal direction, the cell sizes were varied. Cells in the vicinity of reefs and in the vicinity of some other salient points (the right hand end and left hand end of fluid domain) were denser than in other areas and have same density to obtain the computational accuracy. The wave height generated in the left hand end of fluid domain (at location x: -50.0 m)

was compared to the results obtained from the linear wave theory; therefore to obtain better results, the grids in this regions were made denser than in other areas.

In the vicinity of reefs (from +0.0 m to + 20.0 m), 100 cells (each cell equal to 0.20 m wide, which gave nearly 10 cells within one hemispherical reef) were used to represent the reefs smoothly. While in the areas between -50.0m to -48.0m and 68.0 m to 70.0m, the number of cell were 10, in the area between -48.0m to 0.0m and +20.0m to +68.0m were 29, and 20 cells were used in the areas between +70.0m to +90.0m For lateral (y axis) and vertical (z axis) directions, the number of cells used were 20 and 30, respectively. Total cells used in all three directions were 118,800. Table 5.1 above shows the total number of cells used in the computational domain given in Figure 5.1. Figure 5.2 below shows the computational grid for the three dimensional model:

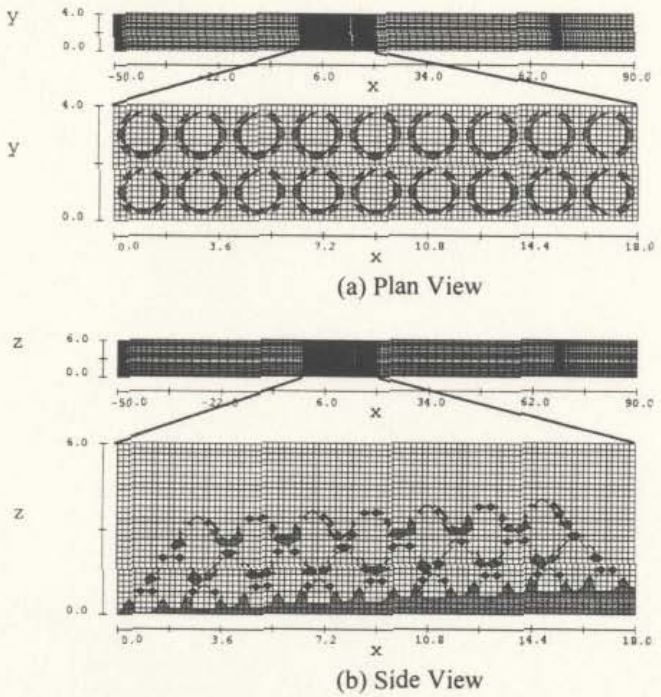

(a) Plan View

(b) Side View

Figure 5.2. Computational Grid used for Three-dimensional Model with Twenty-four Reef Units

Similar to the previous two-dimensional model, the reef unit of interest (with its cross section), as shown in Figure 5.3, was considered in this study. The velocity magnitudes within this third reef located in the bottom layer, were examined at points A, B, and C.

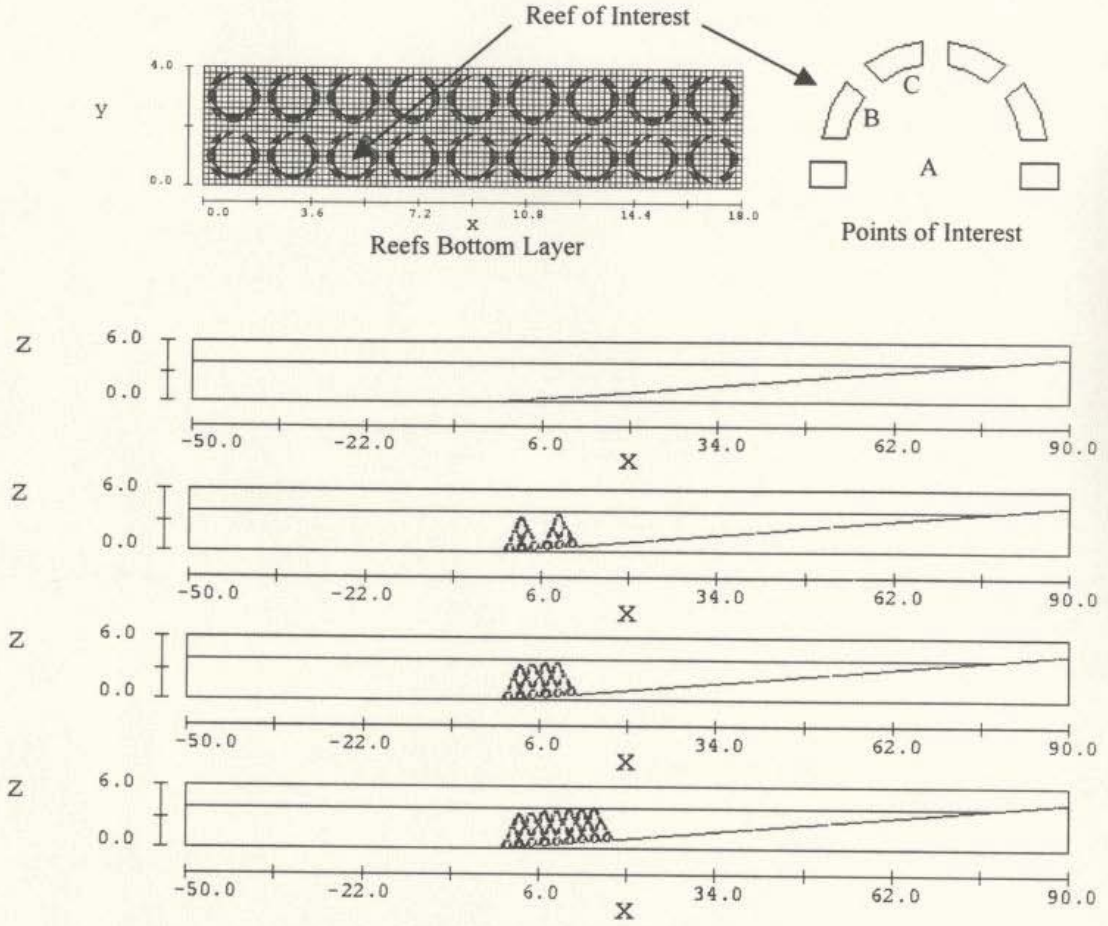

Figure 5.3 Points of Interest within the Reef Units

Initially, the velocities obtained from a sinusoidal wave with 1.0 m height and 5 seconds period (at a deep-water location) was applied for all the reef configurations as the left boundary condition. The water depth was set at 4.0 m, and the sea considered to

be at rest. Symmetry boundary conditions were used at the lateral boundaries and a rigid wall boundary condition was used at the end of the right computational domain.

The numerical calculations were carried out on a 500 MHz personal workstation DEC Alpha with 768 MB memory. Since the three-dimensional model consumed a large memory and execution time (almost 24 hours for each simulation), the final time for model was limited to 60 seconds. The first step was to simulate the wave profile without any reef, and then to compare the wave profile with that obtained for the installation of twelve, fifteen, and twenty-four reefs. One meter waves with wave periods of 3.5 seconds and 4.0 seconds were also considered in the model with twenty-four reefs. Similar to the two-dimensional model, the k-ε turbulence model was utilized by setting a parameter in the FLOW3D input file. A typical input file containing all physical property data, mesh and obstacle descriptions, boundary and initial conditions as well as computational parameters controlling the operation and output for a three dimensional model using FLOW-3D is given in Appendix C.

5.3. Results and Discussion

The surface wave profiles resulting from a wave of height 1.0m with 5 seconds period, at y = +2.0 m (in the middle of computational domain), are shown in Figures 5.4 to 5.7 for the beach without the reef, as well as that with twelve, fifteen and twenty four reef units. For a 5 seconds wave period, the wave length was 27.94 m at 4.0 m depth. The waves seem to break over the reefs when the number of reef units are equal to or greater than fifteen. By comparing the results, it is seen that the addition of a number of reef units would reduce the wave height, considerably.

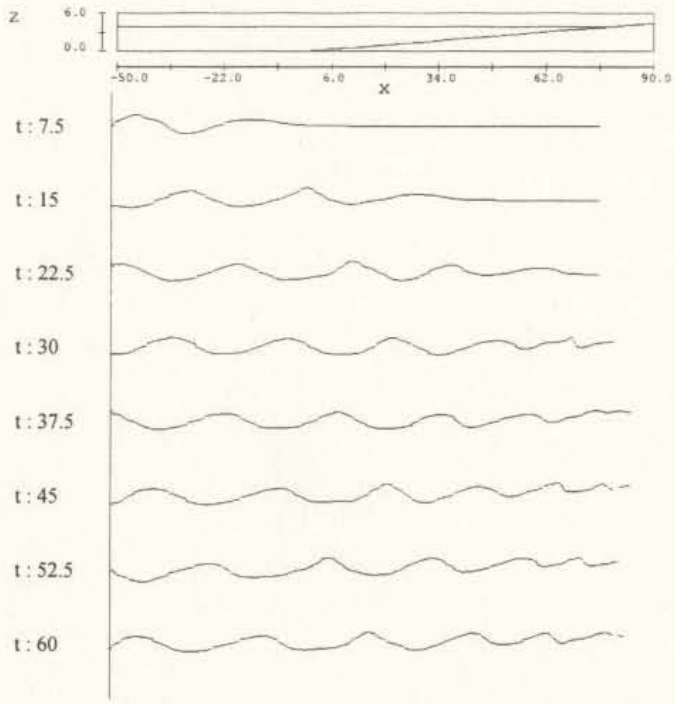

Figure 5.4. Wave Profile without Reefs, T: 5.0 sec

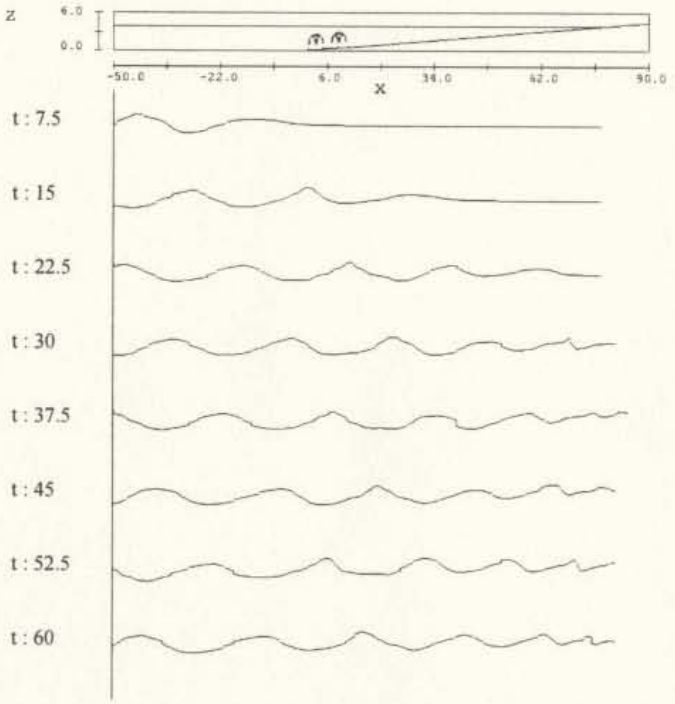

Figure 5.5. Wave Profile with Twelve Reefs, T: 5.0 sec

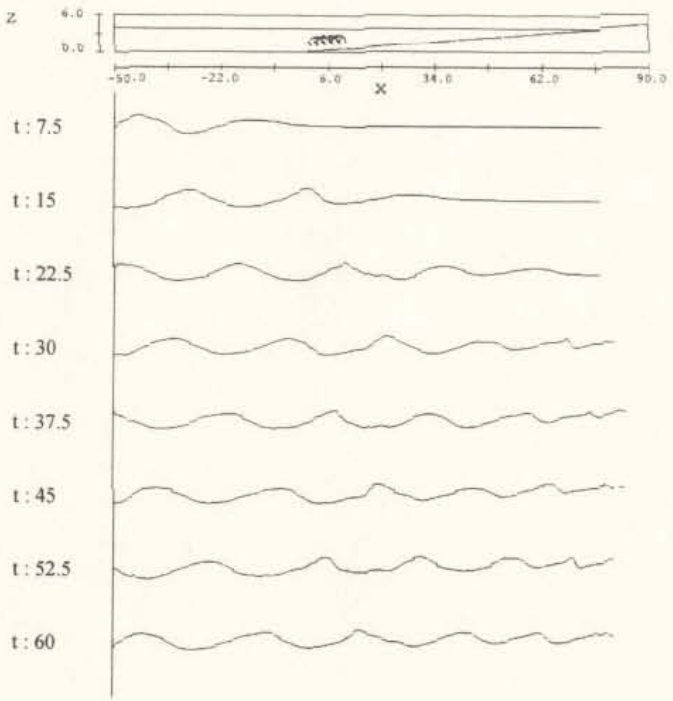

Figure 5.6. Wave Profile with Fifteen Reefs, T: 5.0 sec

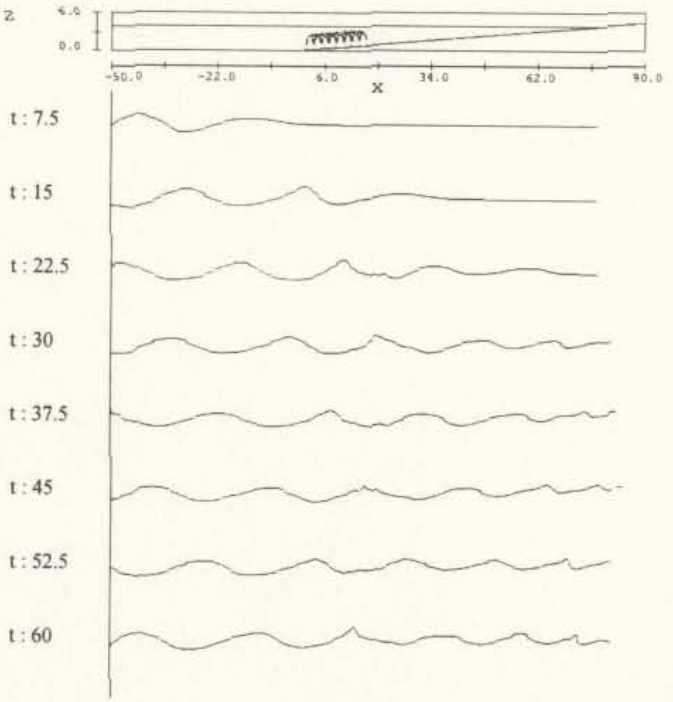

Figure 5.7. Wave Profile with Twenty-four Reefs, T: 5.0 sec

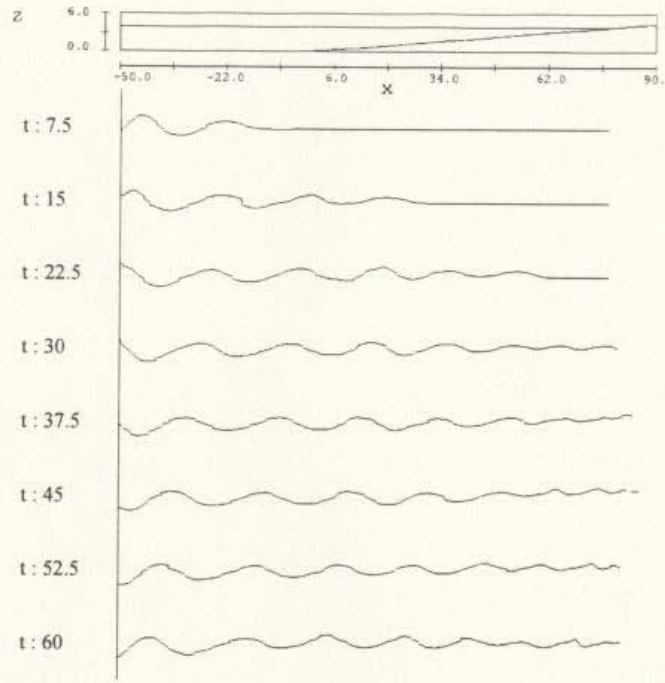

Figure 5.8 Wave Profile without Reefs, T: 4.0 sec

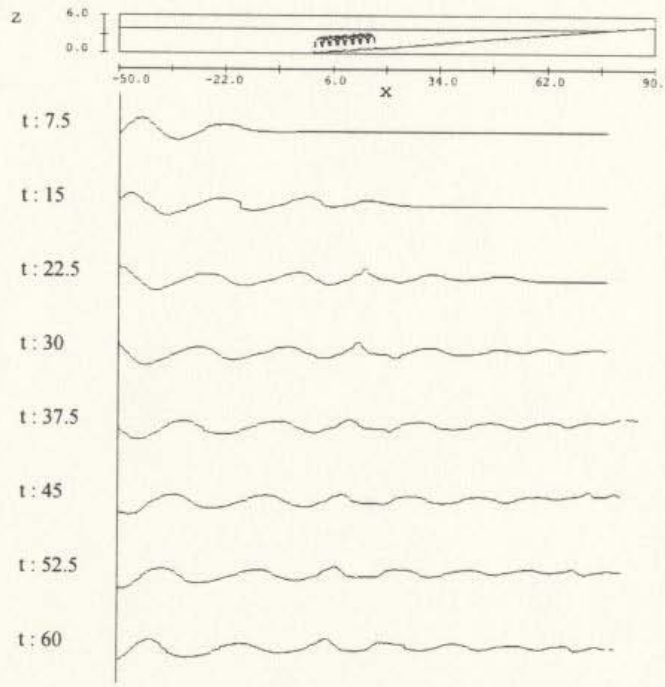

Figure 5.9 Wave Profile with Twenty-four Reefs, T: 4.0 sec

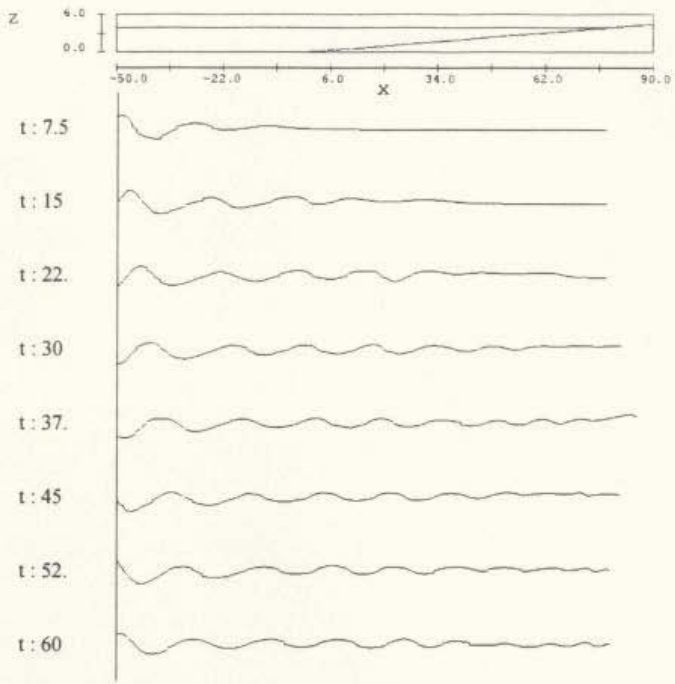

Figure 5.10. Wave Profile without Reefs, T; 3.5 sec

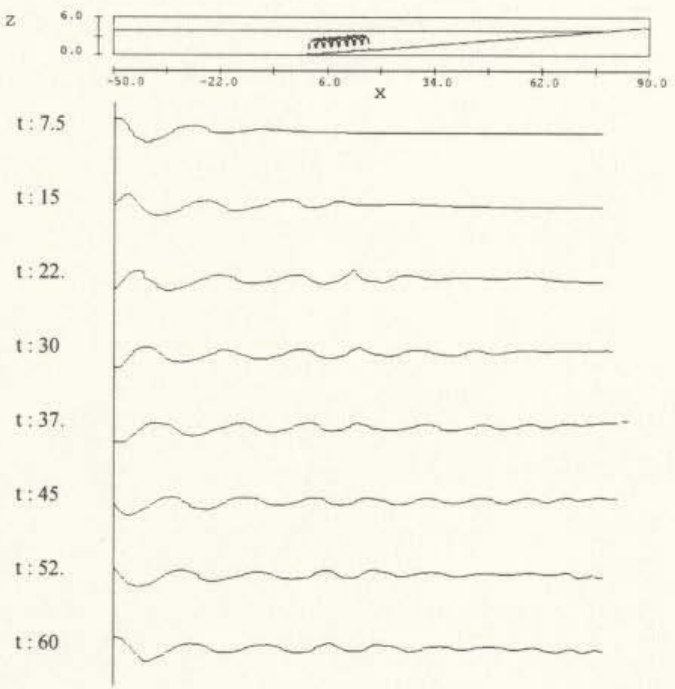

Figure 5.11 Wave Profile with Twenty-four Reefs, T: 3.5 sec

Figures 5.8 and 5.9 above show the surface wave history of the beach without reefs and that with twenty-four reefs for a 4 seconds period, while results for a 3.5 seconds period are given in Figures 5.10 and 5.11. Comparing these results with those for a 5 seconds period, it is seen that the wave heights in the basin were reduced considerably for the waves with 4 seconds and 3.5 seconds period.

Furthermore, Figure 5.12 shows the water level histories of the beach with variation in number of reef units (twelve, fifteen and twenty-four; represented by black line) compared to a beach without reefs (represented by red line) for a 5 seconds wave period at x = +18.0m (just after the reefs). Figure 5.12 shows that the reduction in wave height is much less when the number of reef units per unit width is equal to or less than fifteen. It is also seen than there is a considerable phase shift (more than 60°) in the wave when the reef units are twenty-four.

In addition, the water surface history comparison for the beach without reefs and with twenty four reefs at same location (x: +18.00 m) for different wave periods; i.e: 5 seconds, 4 seconds and 3.5 seconds, respectively, are shown in Figure 5.13

Comparing these results with those of the two-dimensional model, the wave heights were reduced much less (by 16-17%) for twenty-four unit reefs compared with 40% for two-dimensional model with twelve reefs (Figure 4.16) as shown in Figure 5.12. This might be due to the assumption of the reefs used in the two models. In the two dimensional model, the reefs were assumed as semi circular cylindrical shapes, while in the three-dimensional model the reefs were hemispherical in shape. Hence, if in the three dimensional model the reefs were also modelled as those with semi circular hollow shapes and extended laterally, the results would almost be the same.

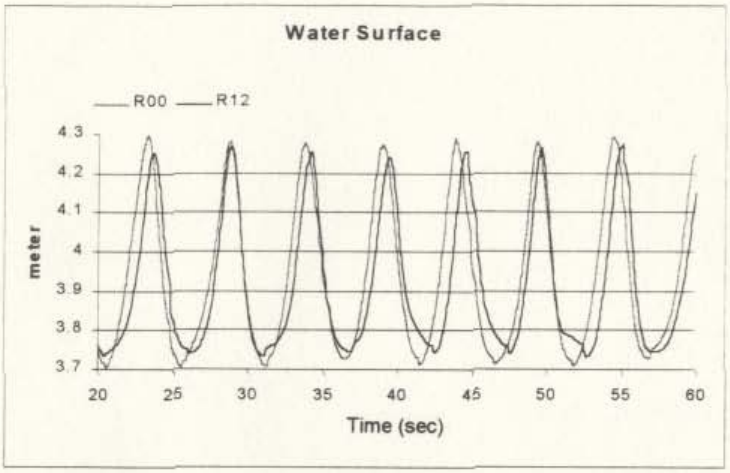

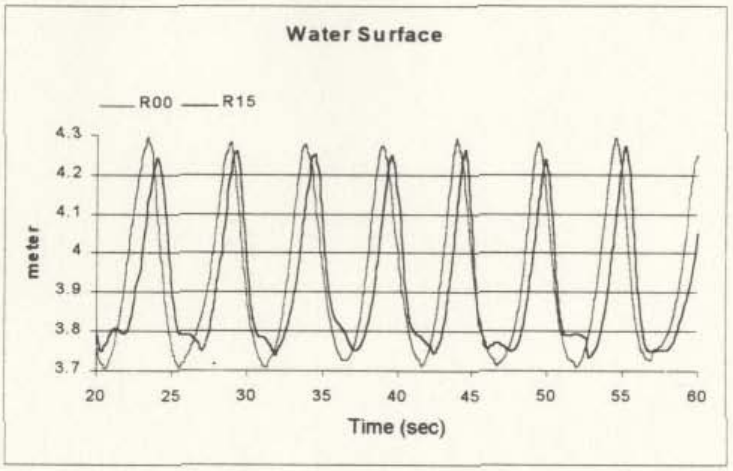

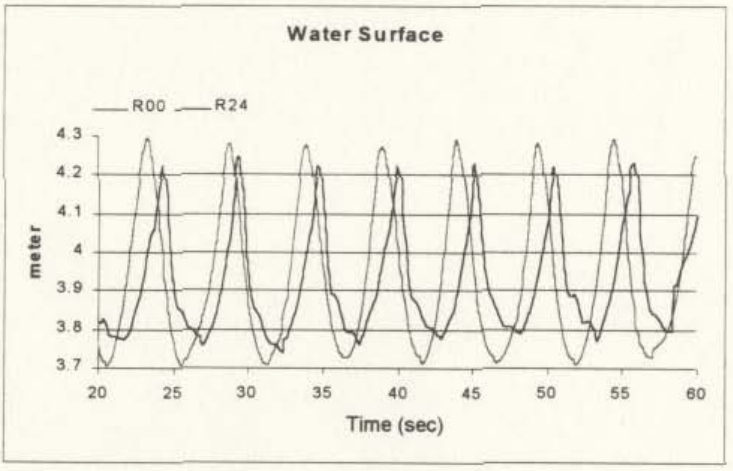

Figure 5.12 Surface Wave History for Three Different Reefs at x: +18.0m
Ho: 1.0m, L: 27.94m, T: 5 seconds

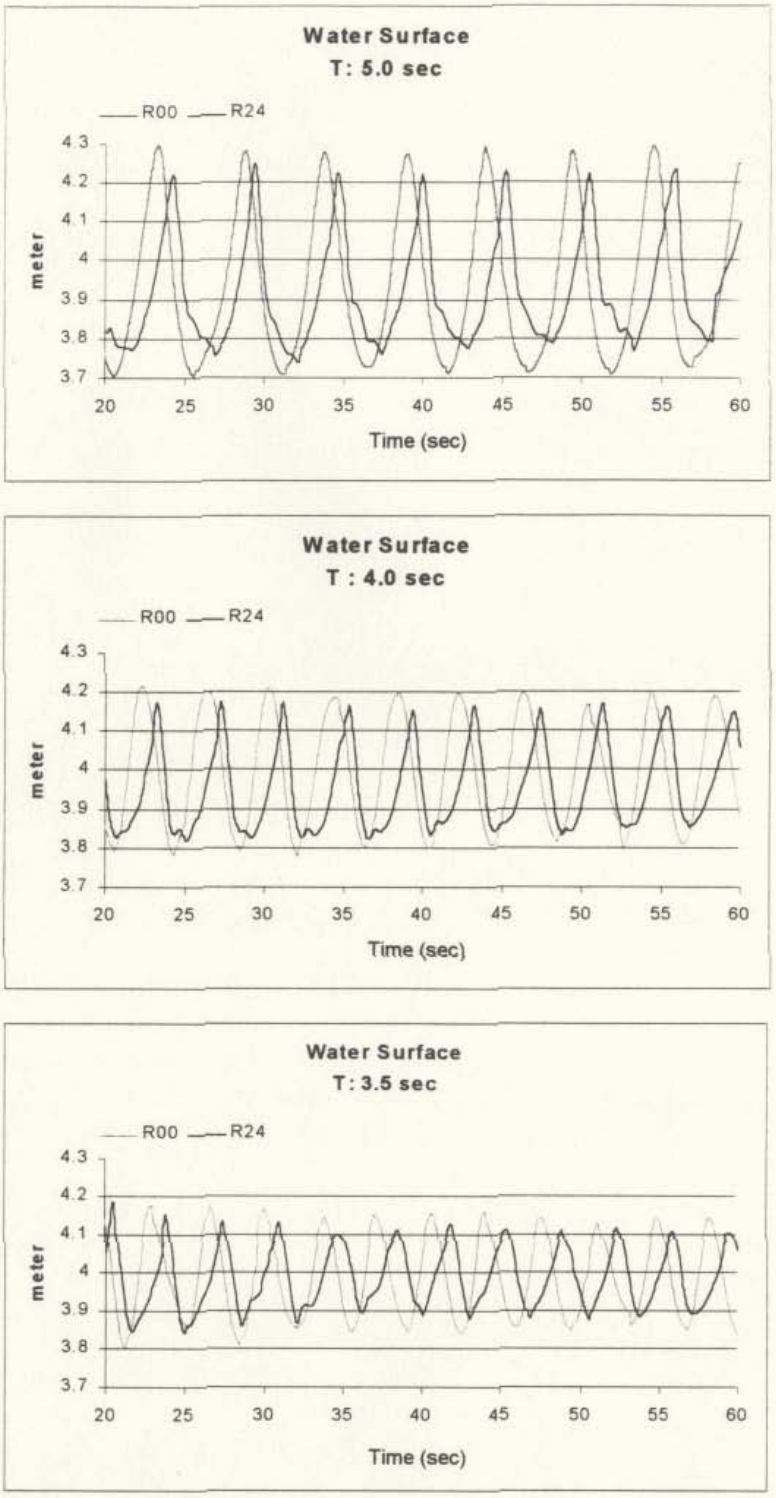

Figure 5.13. Surface Wave History for Three Different Periods at x: +18.0m

For the model with fifteen reefs, the wave phases were shifted more compared to the model of twelve reefs. The wave heights were also reduced slightly, and were almost same as the model with twelve reefs. However, the wave energy reduction was significant in the model with twenty-four reefs where a wave of 27.94m length, at 4.0m depth, traveled over the reefs (of base length 18.0m). The average reduction was 16.7%. This fact has also been shown in Figures 5.4 to 5.7 above

Therefore, for the same wave period the longer the wave travel occurs over the reefs (or wider the reefs), the greater the wave energy dissipated over the reefs. Moreover, the energy dissipation was not due to the breaking of waves as observed in the two-dimensional model (as described in Chapter 4), but mostly due to the flow separation that occurs over the reefs. In addition, the wave energy dissipation also occurs due to the diffraction of waves around the reefballs.

Furthermore, as the wavelengths get reduced due to the increase in wave frequency (reduction of wave period), the wave heights are also reduced considerably. For a 5 seconds period, the wave height at a location just after the reef (x: +18.0m), was reduced by 16.7% on average, while for 4 and 3.5 seconds period the reductions were was 17.5% and 20%, respectively. Finally, it can be concluded that the greater the reef length over which a single wave travels, greater the wave energy dissipated.

Typical velocity magnitudes over a wave cycle in the vicinity of model without reefs and for the model with twelve, fifteen, and twenty-four reefs, respectively, are shown Figures 5.14 to 5.17. The shades of color represent the velocity magnitudes in the reefs' vicinity. These figures have been plotted in a three dimensional manner in Figures 5.18 to 5.21.

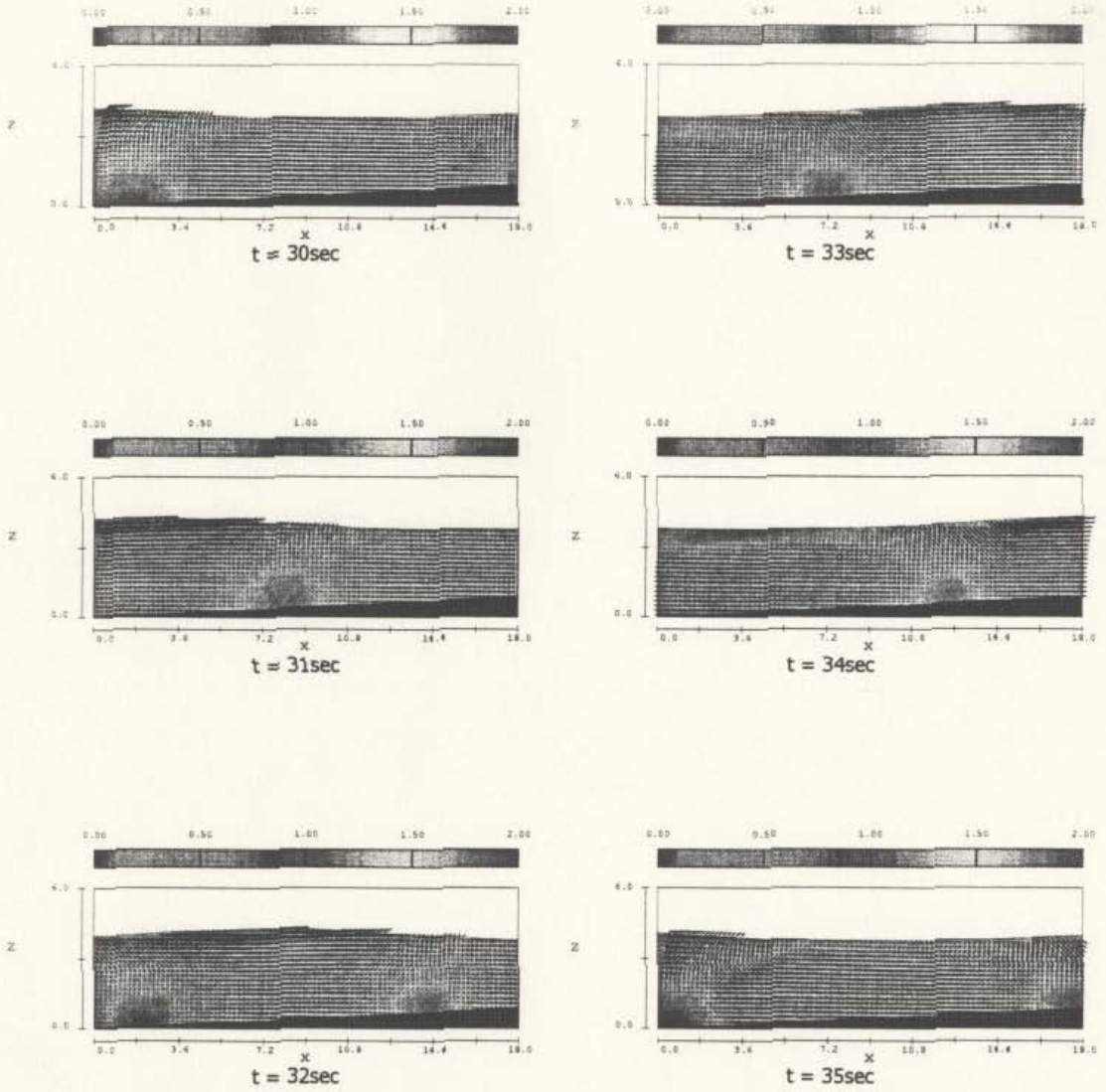

Figure 5.14 Time Series of Velocity Magnitudes for a Beach without Reefs; at y= +2.0m

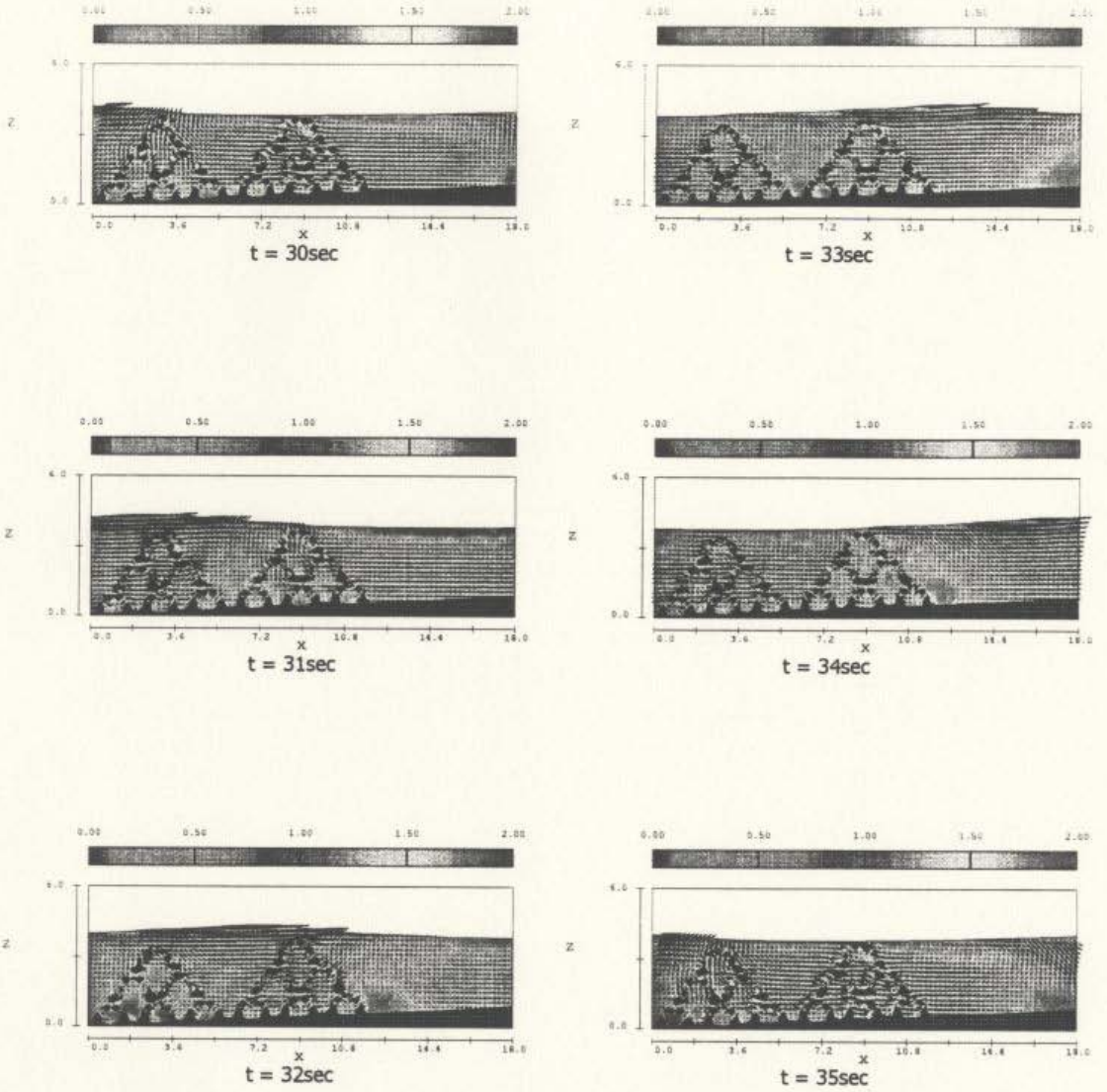

Figure 5.15 Time Series of Velocity Magnitudes for a Beach with Twelve Reefs; at y= +2.0m

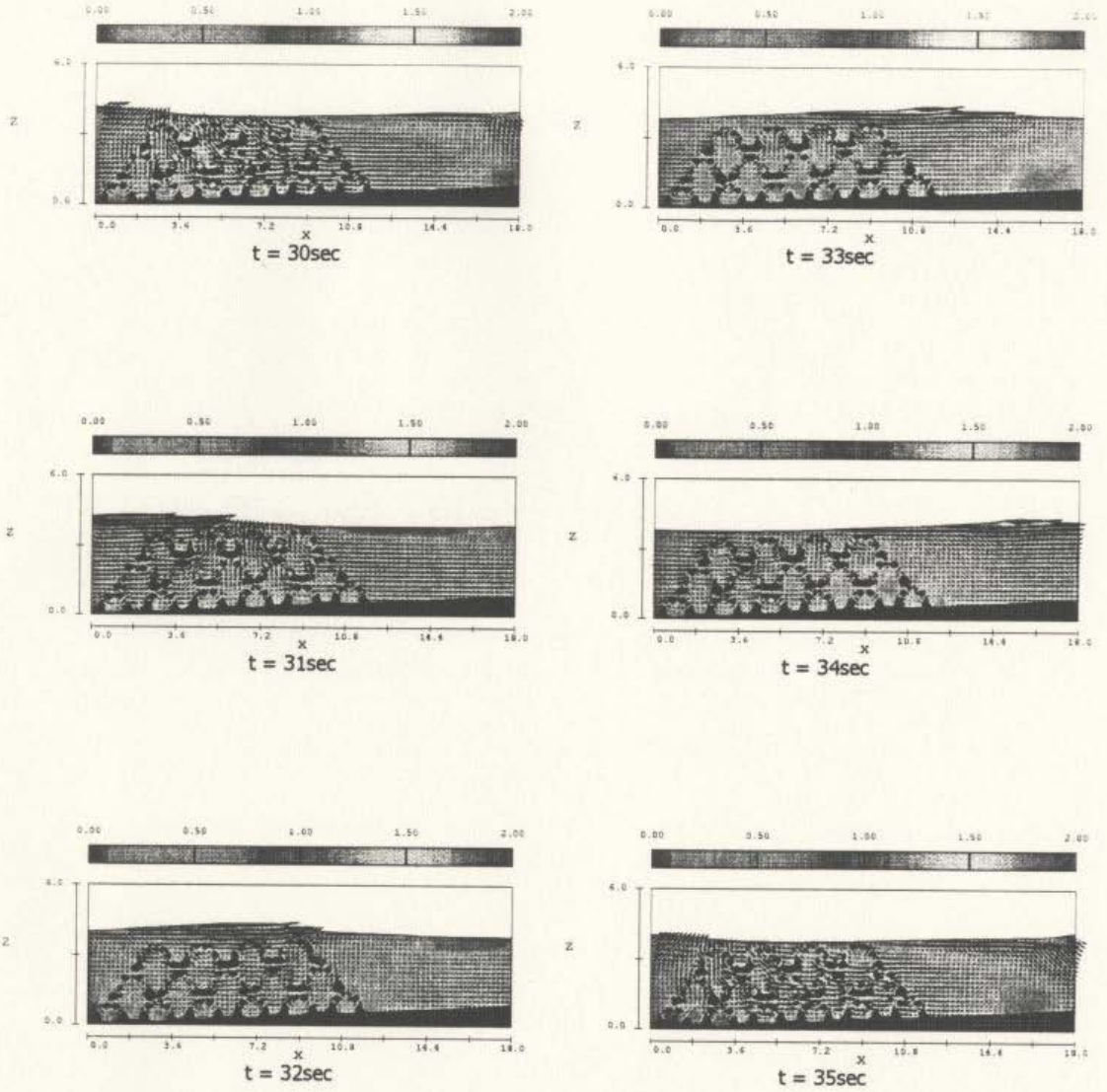

Figure 5.16 Time Series of Velocity Magnitudes for a Beach with Fifteen Reefs; at y= +2.0m

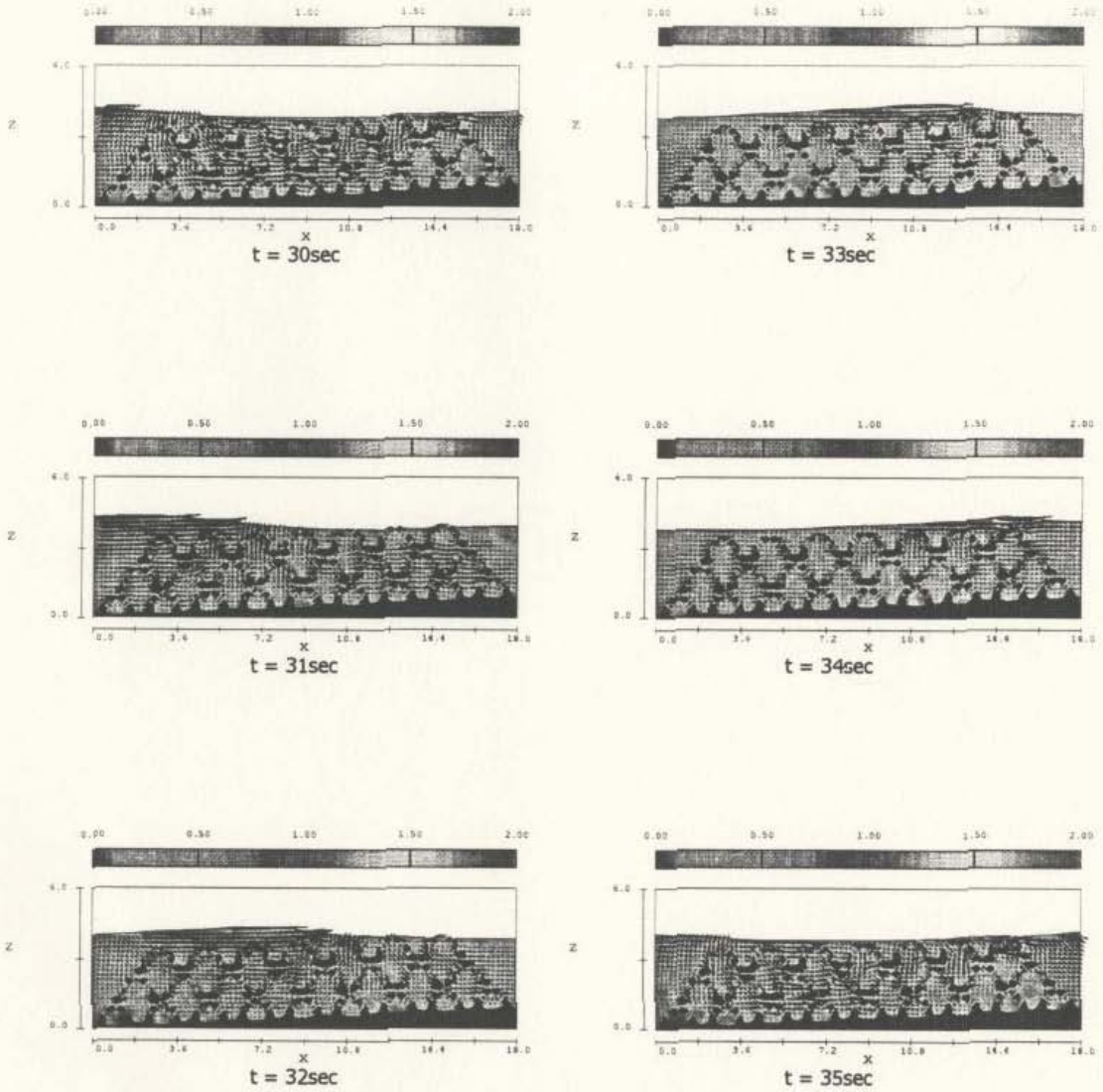

Figure 5.17 Time Series of Velocity Magnitudes for a Beach with Twenty-four Reefs; at y= +2.0m

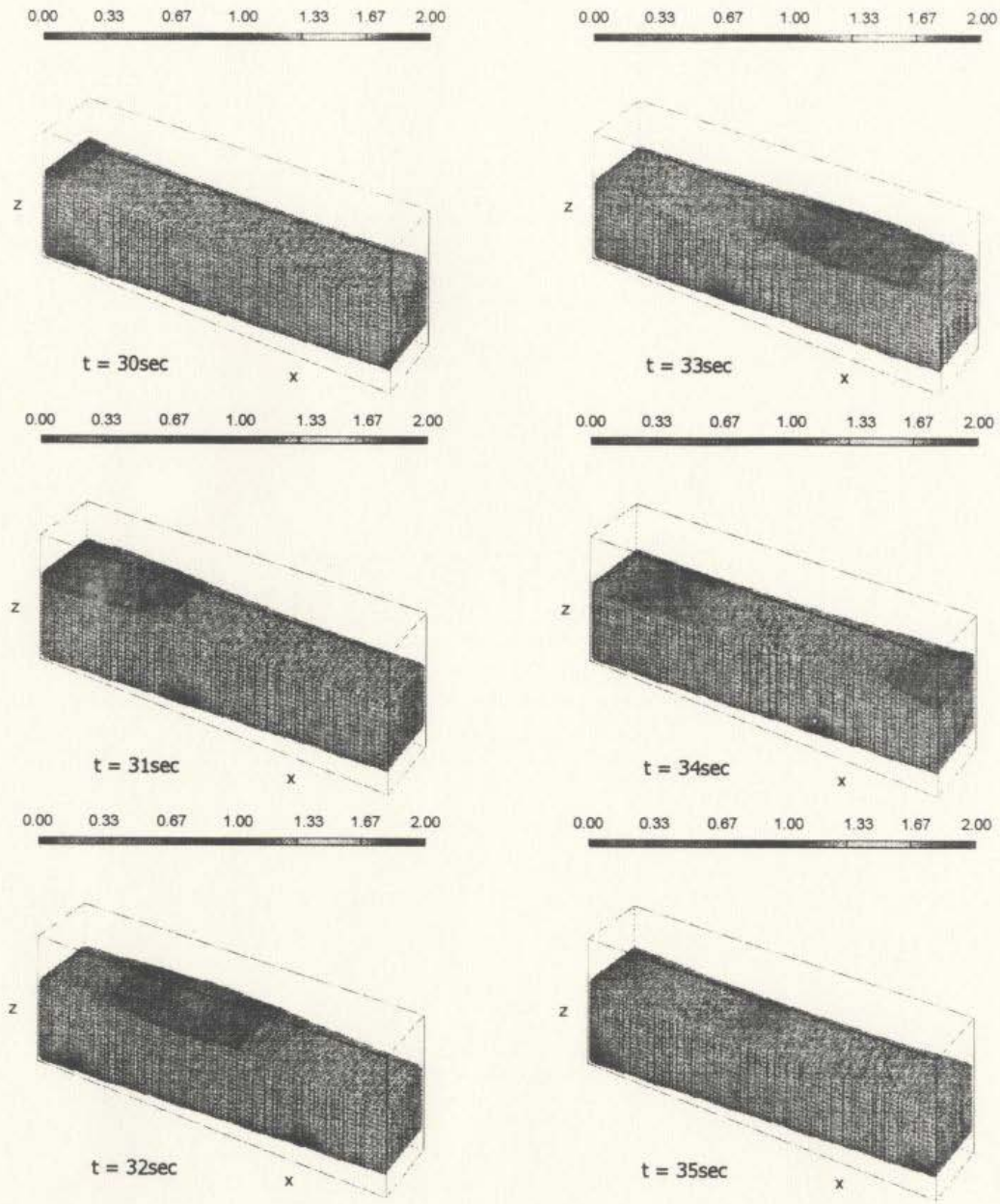

Figure 5.18 Time Series of Velocity Magnitudes for the Beach without Reefs shown Three Dimensionally

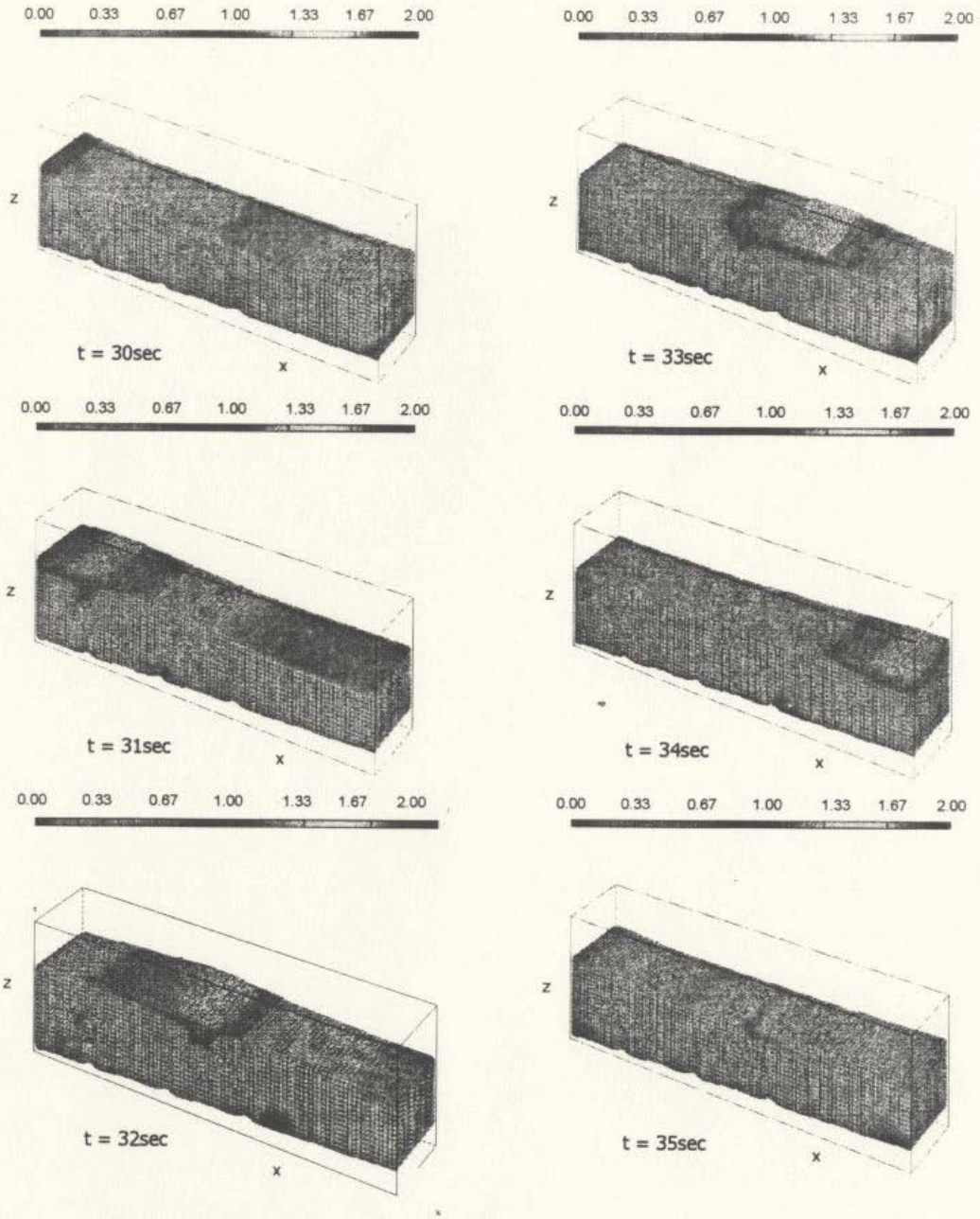

Figure 5.19. Time Series of Velocity Magnitudes for the Beach with Twelve Reefs shown Three Dimensionally

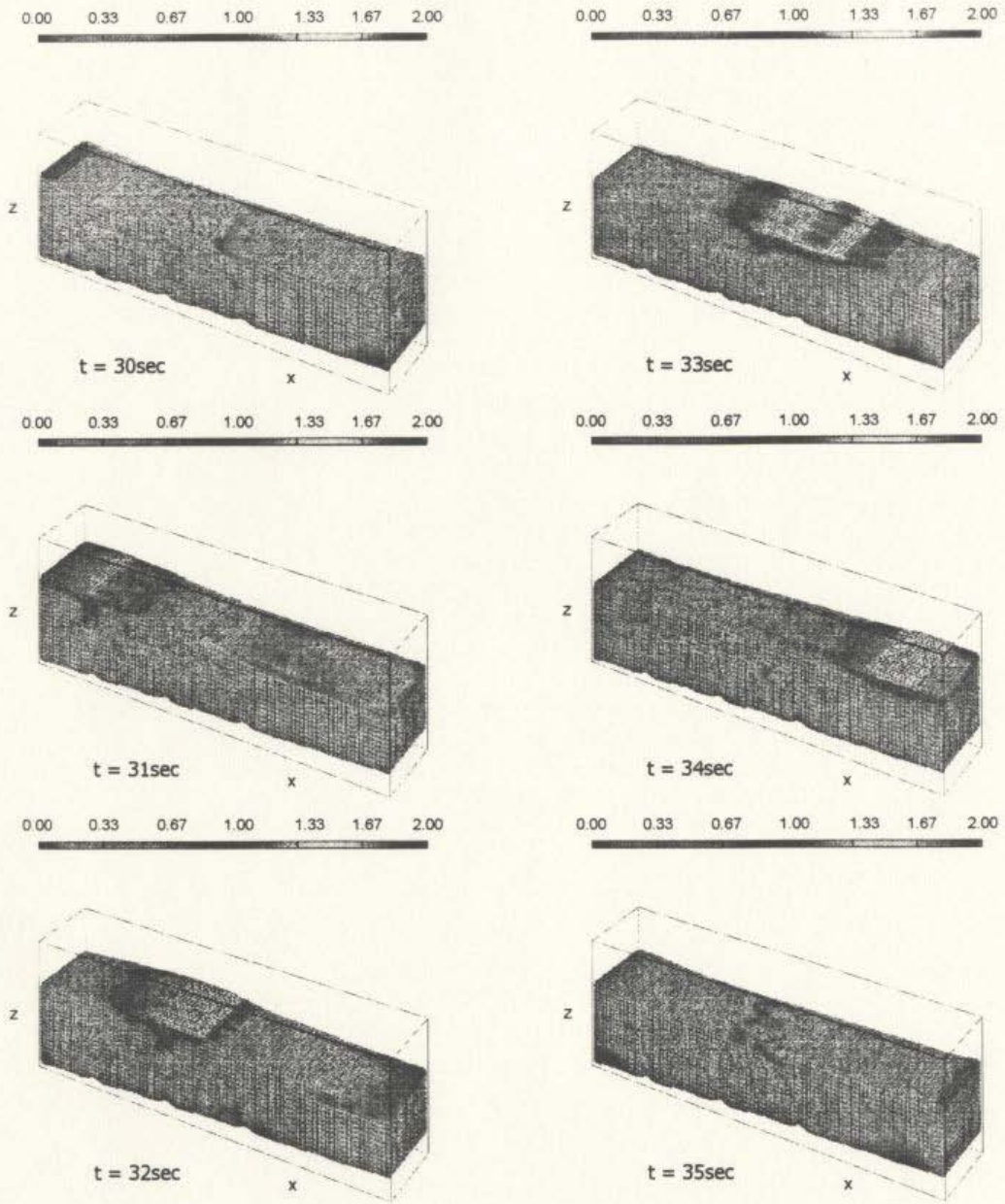

Figure 5.20 Time Series of Velocity Magnitudes for the Beach with Fifteen Reefs shown Three Dimensionally

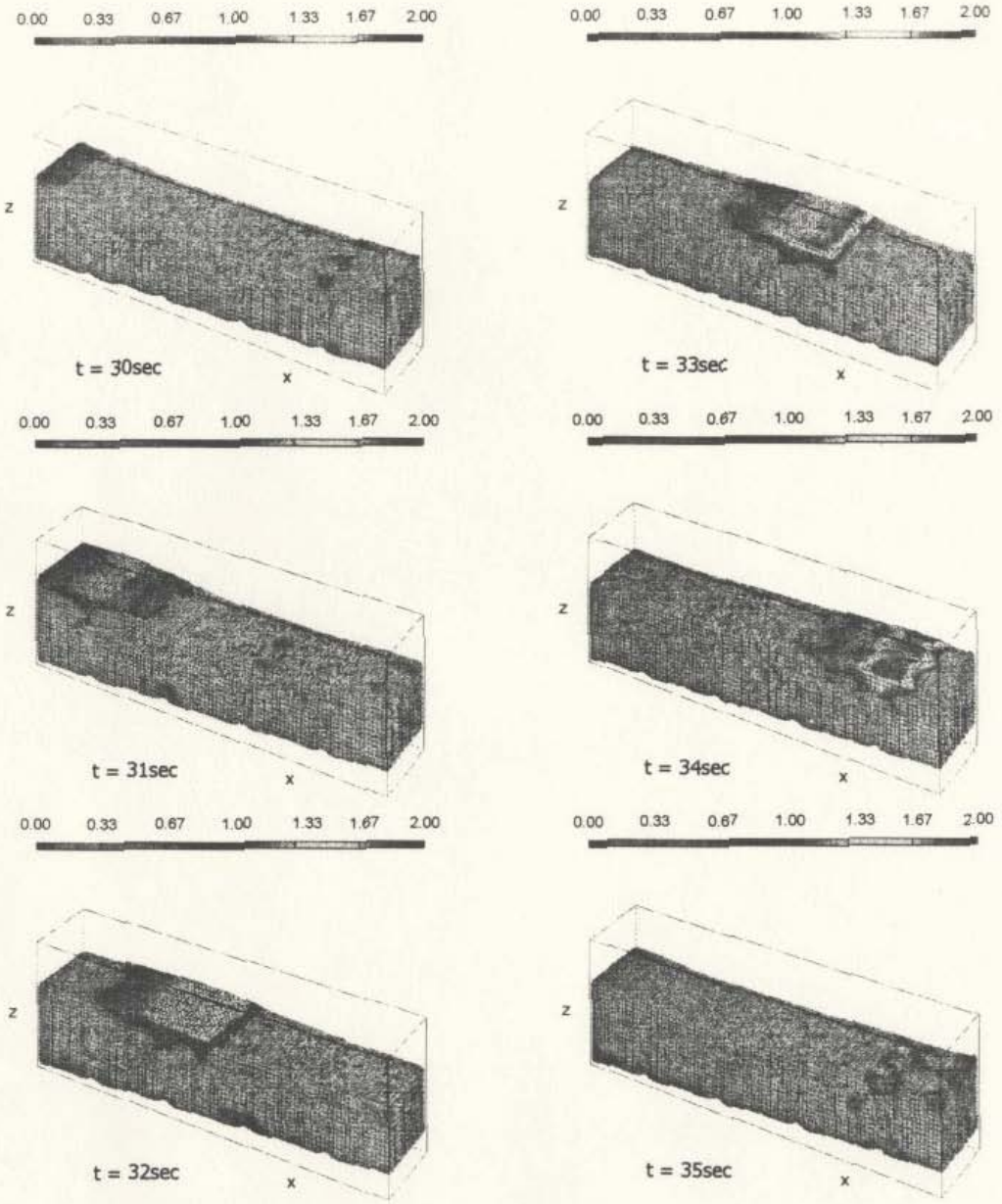

Figure 5.21 Time Series of Velocity Magnitudes for the Beach with Twenty-four Reefs shown Three Dimensionally

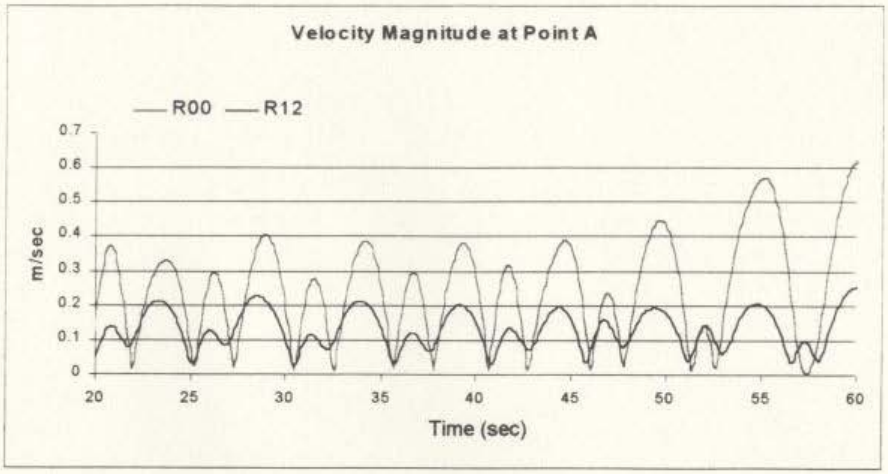

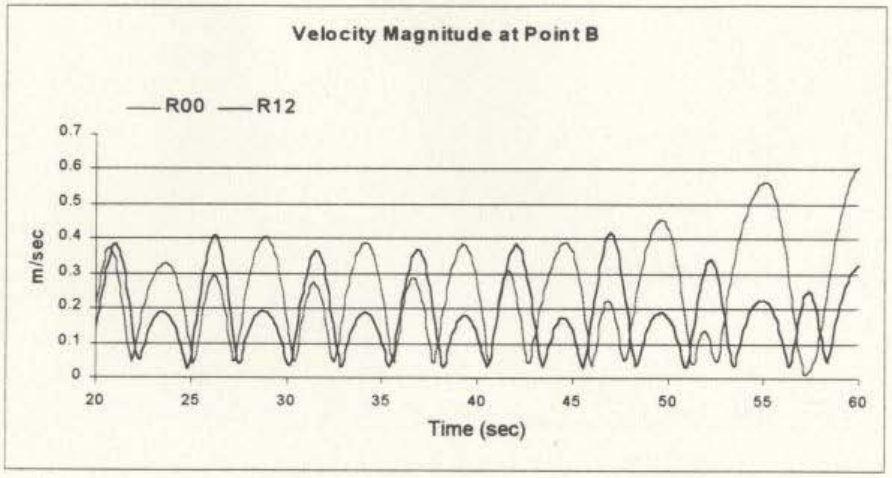

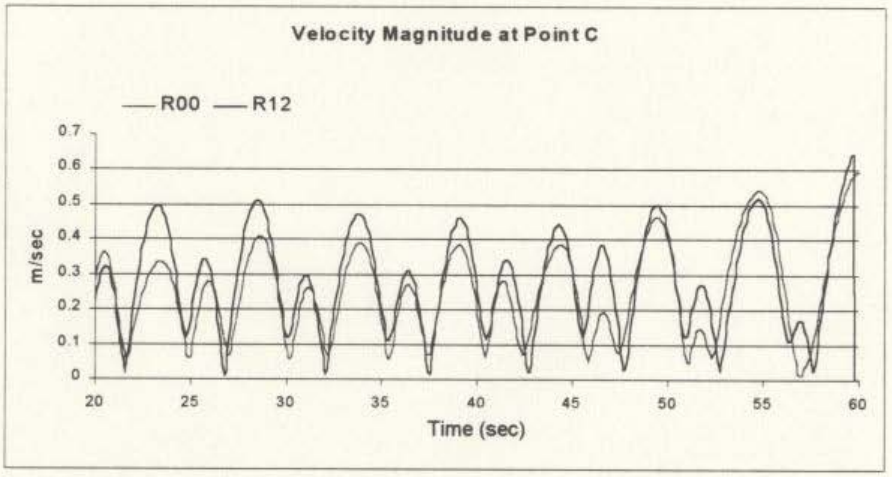

Figure 5.22 Velocity Magnitude Time Series for Twelve Reefs at Points A, B, and C

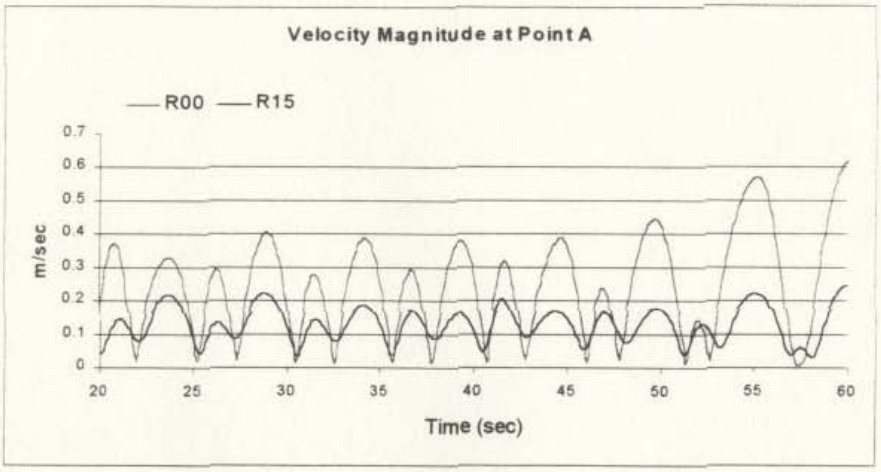

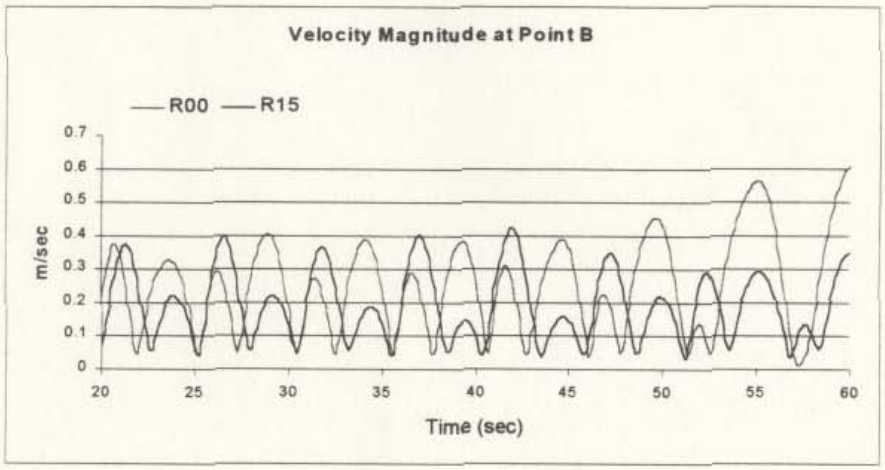

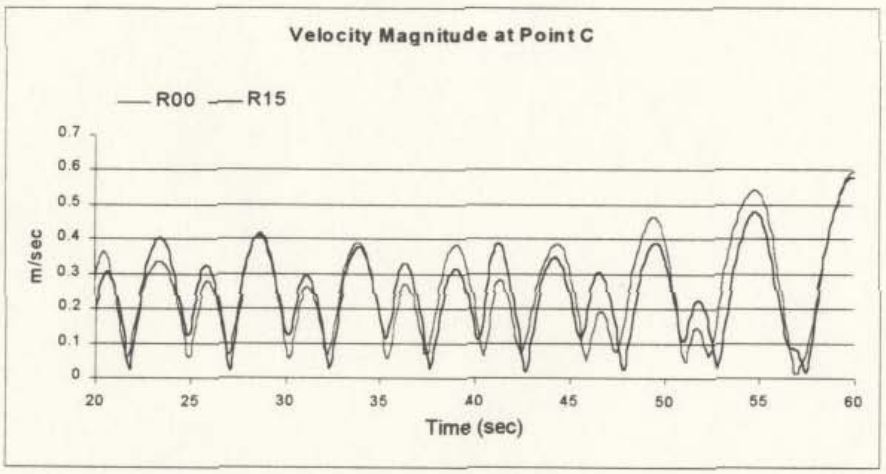

Figure 5.23. Velocity Magnitude Time Series for Fifteen Reefs at Points A, B, and C

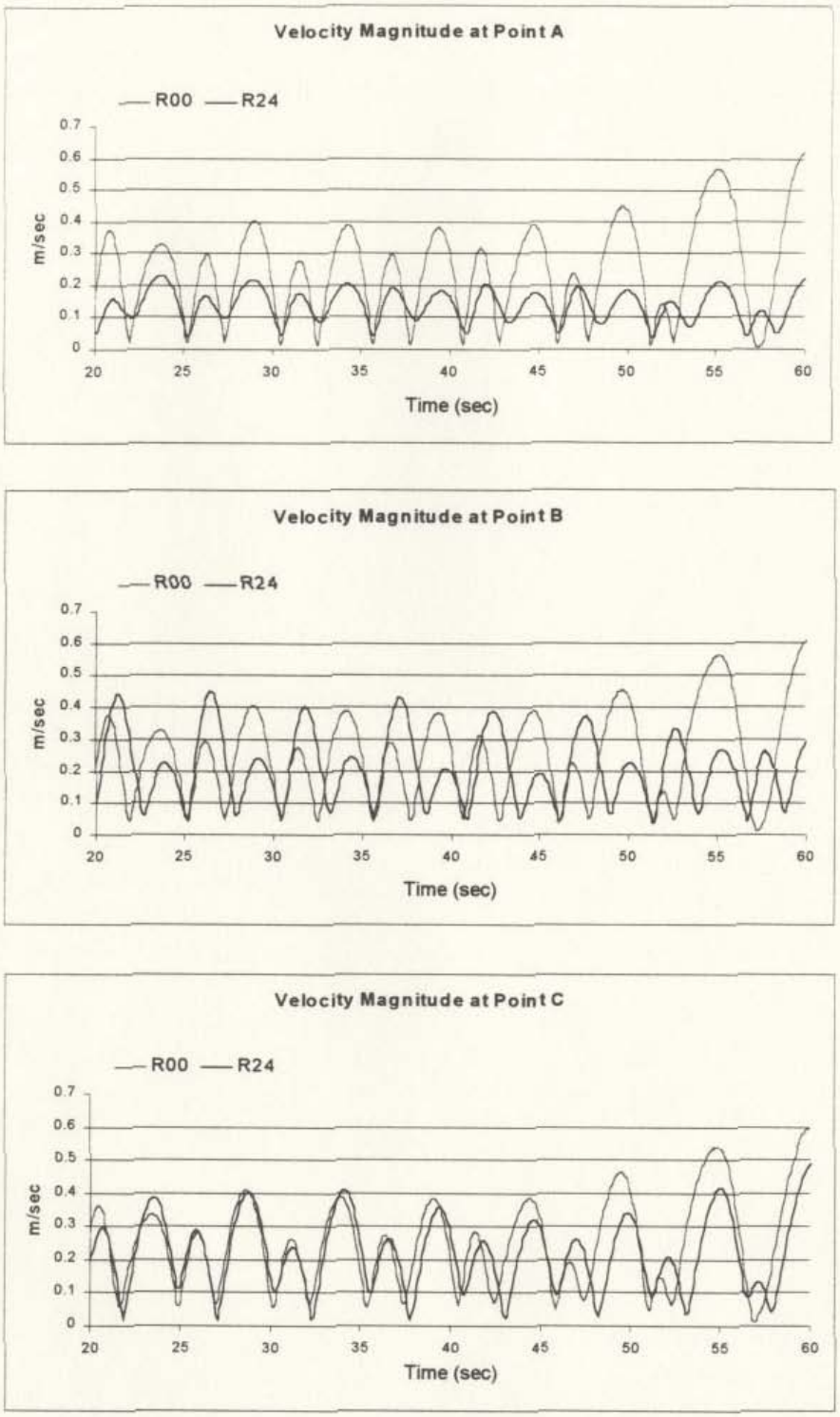

Figure 5.24 Velocity Magnitude Time Series for Twenty-four Reefs at Points A, B, and C

As it has been pointed out earlier, turbulence and vortex shedding occuring behind the structures are the important hydraulic characteristics required for energy dissipation and for the congregating of fish around the reefs. Figures 5.14 to 5.17 show the distribution of turbulence and vortex shedding in the vicinity of reefs.

Low velocities, as represented by dark blue color, were found within the reefs, as well as in the regions behind the reefs. As mentioned before, these regions provide the space for fish to congregate and spawn. More over, Figures 5.22 to 5.24 show the velocity magnitude plots at points A, B, and C (shown in Figure 5.3). It is seen from these figures that at point A (sea bottom) velocities decrease considerably; this is contrary to the observation made for the two-dimensional model where the largest decrease was observed at C. The decrease at C is minimal while that at B is greater than that at C. The velocities seems to fluctuate between a maximum and a minimum in the two adjacent wave cycles, probably due to the alternate exiting and entering of waves through the holes located on the reef units.

5.4. Summary

The results of a three-dimensional modelling of the artificial reef made of hollow hemispherical balls have been presented in this chapter. It was observed that the energy dissipation was not due to the breaking wave as observed in the case of two-dimensional model, but due to the turbulence, flow separation and diffraction of waves occurring around the reefs. Therefore, the wider the crest of the reef or the longer the wave travels over the reefs, the greater is the energy dissipation that occurs in the basin. Numerical results presented by Tsujimoto, et. al (1999) as well as field observation made by Ohnaka and Yoshizawa (1994) seem to confirm these results of the study.

Chapter 6
Conclusions and Recommendations for Future Study

6.1. Conclusions

After an introduction to the utilization of artificial reefs in the coastal and offshore areas, a brief review of artificial reefs, their deployment around the globe, purpose, materials used, the design and engineering aspects based on environment and ecology have been presented in chapter two. Emphasis has been placed on highlighting the factors that influence the engineering and design aspects of artificial reefs.

A brief overview of the Volume of Fluid method and its numerical implementation in the computational fluid dynamic software package FLOW3D for the modelling of artificial reefs is given in chapter three. The Volume of Fluid method was used in the study to obtain the optimum reef configuration.

Chapter four gives the results of two-dimensional modelling of the fluid flow in and around the hollow hemispherical units that constitute the artificial reef. Chapter five models the beach and artificial reef structure in a three dimensional manner and presents

the salient results obtained from this study. The following conclusions were drawn from this study.

1. Based on the results of two-dimensional analyses, it can be concluded that increasing the number of installed reefs will reduce the waveheights and velocity magnitudes, considerably. However, if the numbers of installed reefs are below six, the energy is not dissipated much. This is due to the fact that below six reef units the surface wave energy region is not influenced much by the presence of reefs
2. The reduction of wave amplitudes and velocity magnitudes, around the vicinity of artificial reefs, makes the region to be most conducive for the congregation of fishes, growth of biomass and spawning of fish.
3. Since the model used for numerical analysis was only two dimensional, the crossflow generated in the lateral direction by the hollow three-dimensional porous hemispherical reef units was not properly modelled in the two-dimensional analysis. Therefore, a three dimensional numerical model study was carried out. It was observed from the results of the three dimensional model, that the energy dissipation was not due to the breaking of waves as observed in the two dimensional model, but due to turbulence and flow separation at the crest and around the reefs.
4. Moreover, it was observed that wider the crest of the reef (equal or more than one wavelength) greater the wave energy dissipation. Numerical investigation by Tsujimoto, et. al (1999) as well as field observations by Ohnaka and Yoshizawa (1994) have confirmed the results of the three-dimensional model obtained in this study.

5. Overall, the numerical analyses have shown that the installation of reefs would produce turbulence and vortex shedding in the vicinity of reefs. These phenomena are important hydraulic characteristics required to aggregate fish. Therefore, provision of suitable reef configurations will provide a conducive environment and suitable locations for the fish to congregate and spawn; in addition it will also provide areas wherein the benthic diatoms and seaweed spores can attach and grow.

6.1. Recommendation

Since the limitations of the computer software allowed the use of only a limited lateral space in the reef vicinity, the analysis for comparison of three-dimensional arrangement of reefs as longitudinal against lateral, to obtain an optimum reef configuration, could not be carried out. Despite the fact that the longitudinal arrangement of reefs has been shown to be more efficient in dissipating energy for submerged roubble mound breakwaters (Goda and Takagi, 1998), the analyses for various configurations of hollow hemispherical reef blocks need to be carried out to verify and confirm the above results.

The wave characteristics approaching the shoreline such as diffraction and refraction also need to be considered in the analysis to give a better comprehension of the reef effects in dissipating wave energy. This study also could not be carried out due to computer software limitations. The possibility of siltation and erosion around the reef barrier need to be investigated and eliminated by the provision of a suitable configuration.

Furthermore, studies to determine the optimum form of the hemispherical shapes such as external appendages (to produce turbulence and flow separation), need for and influence of identified number of holes within a reef unit, and the combination of normal and inverted forms of reef groups to produce better wave field in the reef vicinity also should be carried out.

References

1. Ahrens, J.P. (1987). Characteristics of Reef Breakwaters. *Technical Report CERC - 87-17.* 46 p.

2. Ambrose, R.F., and Swarbrick, S.L., (1989). "Comparison of Fish Assemblages on Artificial and Natural Reefs off the Coast of Southern California", *Bulletin of Marine Science.* Vol. 44, No.2, pp.718-733.

3. Anderson, I, (1997). "Let's Go Surfin' ", *New Scientist* Vol. 151, pp.26-27.

4. Anderson, T.W., DeMartini, E.E., and Roberts, D.A., (1989). "The Relationship Between Habitat Structure, Body Size and Distribution of Fishes at A Temperate Artificial Reefs", *Bulletin of Marine Science,* Vol. 44, No.2, pp.681-697.

5. Aono, T., and Cruz, E.C. (1996). "Fundamental Characteristic of Wave Transformation around Artificial Reefs", *Proceedings of 25th Coastal Engineering Conference,* pp. 2298 - 2311.

6. Battjes, J.A., (1974). "Surf Similarity", *Proceedings of 14th Coastal Engineering Conference,* pp. 466-480

7. Bayle-Sempere, J.T., Ramos-Espla, A.R., and Charton, J.G., (1994). "Intra-annual Variability of an Artificial Reef Fish Assemblage in The Marine Reserve of Tabarca (Alicante, Spain, SW Mediterranean)", *Bulletin of Marine Science,* Vol. 55, Nos.2-3, pp.824-835.

8. Baynes, T.W., and Szmant, A.M., (1989)."Effect of Current on The Sessile Benthic Community Structure of An Artificial Reef", *Bulletin of Marine Science,* Vol. 44, No.2, pp.545-566.

9. Bell, M., Moore, C.J., and Murphey, S.W., (1989). "Utilization of Manufactured Reef Structures in South Carolina's Marine Artificial Reef Program", *Bulletin of Marine Science,* Vol. 44, No.2, pp.818-830.

10. Bombace, G., Fabi, G., Fiorentini, F., and Speranza, (1994). "Analysis of The Efficacy of Artificial Reefs Located in Five Different Areas of The Adriatic Sea", *Bulletin of Marine Science,* Vol. 55, Nos.2-3, pp.559-580.

11. Bombace, G., (1989). "Artificial Reefs in The Mediterranean Sea", *Bulletin of Marine Science,* Vol. 44, No.2, pp.1023-1032.

12. Bohnsack, J.A., Harper, D.E., McClellan, D.B., and Hulsbreck, M., (1994). "Effects of Reef Size on Colonization and Assemblage Structure of Fishes at Artificial reefs off Southeastern Florida, USA", *Bulletin of Marine Science,* Vol. 55, Nos.2-3, pp.796-823.

13. Bohnsack, J.A., Johnson, D.L., and Ambrose, R.F., (1991). "Ecology of Artificial Reef Habitats and Fishes", *Artificial Habitats for Marine and Freshwater Fisheries*, W. Seaman Jr., and Lucian M. Sprague, (eds.), Academic Press, Inc., 285 p.

14. Bohnsack, J.A, and Sutherland, D.L., (1985). "Artificial Reef Research: A Review With Recommendations for Future Priorities", *Bulletin of Marine Science*, Vol. 37, No.1, pp.11-39.

15. Bohnsack, J.A., and Talbott, F.H., (1980). "Species-packing by Reef Fishes on Australian and Carribean Reefs: An Experimental Approach", *Bulletin of Marine Science*, Vol. 30, pp.710-723.

16. Bortone, S.A., Martin, T., and Bundrick, C.M., (1994). "Factors Affecting Fish Assemblage Development on A Modular Artificial reef in A Northern Gulf Mexico Estuary", *Bulletin of Marine Science*, Vol. 55, Nos.2-3, pp.319-332.

17. Branden, K.L, Pollard, D.A., and Reimers, H.A., (1994). "A Review of Recent Artificial Reef Developments in Australia", *Bulletin of Marine Science* Vol.55, Nos.2-3, pp. 982-994.

18. Brock, R.E., and Norris, J.E., (1989). "An Analysis of The Efficacy of Four Artificial Reef Design in Tropical Waters", *Bulletin of Marine Science*, Vol. 44, No.2, pp.934-941.

19. Bruno, M.S. (1993). "Laboratory Testing of an Artificial Reef Erosion Control Device", *Coastal Zone '93*, pp.2147 -2158.

20. Carleton, J.H., and Sammarco, P.W., (1987). "Effects of Substratum Irregularity on Success of Coral Settlements: Quantification by Comparative Geomorphological Techniques", *Bulletin of Marine Science*, Vol. 40, No.1, pp.85-98.

21. Carter, R.W.G., (1988). *Coastal Environment: An Introduction to the Physical, Ecological and Cultural Systems of Coastlines*, Academic Press, London, 617p.

22. Coastal Enginering Research Centre (CERC), (1984), *Shore Protection Manual*, Vol 1 and II, US Army Corps of Engineers.

23. Chang, K., (1985), "Review of Artificial Reefs in Taiwan: Emphazing Site Selection and Effectiveness", *Bulletin of Marine Science*, Vol. 37, No.1, pp.143-150.

24. Chandler, C.R., Sanders Jr, R.M., and Landry Jr, A.M., (1985). "Effects of Three Substrate Variables on Two Artificial reef Fish Communities", *Bulletin of Marine Science*, Vol. 37, No.1, pp.129-142.

25. Chou, L.M. (1997). "Artificial Reefs of Southeast Asia - Do They Enhance or Degrade the Marine Environment", *Environmental Monitoring & Assessment*, Vol.44, pp.45 - 52.

26. Clark, S., and Edwards, A.J., (1994). "Use of Artificial Reef Structures to Rehabilitate Reef Flats Degraded by Coral Mining in the Maldives". *Bulletin of Marine Science*, Vol. 55, No. (2-3), pp.724-744.

27. Collins, K.J., Jensen, A.C., Lockwood, A.P.M, and Lockwood, S.J. (1994a). "Coastal Structures, Waste Materials and Fishery Enhancement". *Bulletin of Marine Science* Vol.55, Nos.2-3, pp.1240 - 1250.

28. Collins, K.J., Jensen, A.C., Lockwood, A.P.M., and Turnpenny, A.W.H. (1994b) "Evaluation of Stabilized Coal-Fired Power Station Waste for Artificial Reef Construction". *Bulletin of Marine Science* Vol.55, Nos.2-3, pp. 1251 - 1262.

29. Craig, O, (1992). "Surfers Demand a Reef of Their Own". *New Scientist*, 13 June edition, p.19.

30. Creter, R.E., (1994). "Offshore Erosion Controls Take on New Dimensions". *Sea Technology*, September Edition, pp. 23-26.

31. Delmendo, M.N., (1991). "A Review of Artificial Reefs Development and Use of Fish Aggregating Devices (FADs) in The ASEAN Region". *Symposium on Artificial Reefs and Fish Aggregating Device as Tools for the Management and Enhancement of Marine Fisheries Resources*. RAPA - FAO Report: 1991/11, pp.116-141.

32. Downing, N., Tubb, R.A., El-Zahr, C.R., and McClure, R.E., (1985). "Artificial Reefs in Kuwait, Northern Arabian Gulf". *Bulletin of Marine Science* Vol.37, No.1, pp. 157 - 178.

33. Fitzhardinge, R.C., and Bailey-Brock, J.H., (1989). "Colonization of Artificial Reef Material by Corals and Other Sessile Organism". *Bulletin of Marine Science*, Vol. 44, No.2, pp.567-579.

34. Flow Science, Inc., (1997). FLOW-3D® Excellence in Flow Modelling Software, FLOW3D *version 7.1: User's Manual*, Los Alamos, NM. 97 p.

35. Goda, Y., and Takagi, H., (1998). "Lateral Versus Longitudinal Artificial Reef System", *Abstract of 26th International Conference of Coastal Engineering*, Copenhagen Denmark, Paper No. 240, pp.480 - 481.

36. Gomez-Buckley, M.C and Haroun, R., (1994). "Artificial Reefs in The Spanish Coastal Zone", *Bulletin of Marine Science* Vol.55, Nos.2-3, pp. 1021 - 1028.

37. Gross, M.G., (1987). *Oceanography: A View of the Earth*, Prentice Hall Inc., N.J., 406 p.

38. Grove, R.S., Nakamura, M., Kakimoto, H., and Sonu, C.J. (1994). "Aquatic Habitat Technology Innovation in Japan", *Bulletin of Marine Science*, Vol.55, Nos.2-3, pp.276 - 294.

39. Grove, R.S., Nakamura, M., and Sonu, C.J., (1991). "Design and Engineering of Manufactured Habitats for Fisheries Enhancement", *Artificial Habitats for Marine and Freshwater Fisheries*, W. Seaman Jr., and Lucian M. Sprague, (eds.), Academic Press, Inc., pp. 109-152

40. Grove, R.S., Sonu, C.J., and Nakamura, M., (1989). "Recent Japanese Trends in Fishing Reef Design and Planning", *Bulletin of Marine Science*, Vol. 44, No. 2, pp. 984-996.

41. Hardjono (1991), "Indonesia's Experience of Fish Aggregating Devices (FAD's)", *Symposium on Artificial Reefs and Fish Aggregating Device as Tools for the Management and Enhancement of Marine Fisheries Resources*, RAPA - FAO Report: 1991/11, pp.164-195.

42. Harris, L.E. (1995). "Engineering Design of Artificial Reefs", *Ocean '95*, pp.1139-1148.

43. Hayakawa, N., Hosoyamada, T., Yoshida, S., and Tsujimoto, G. (1998). "Numerical Simulation of Wave Field around The Submerged Breakwater with SOLA-SURF Method", *Abstract of 26th International Conference of Coastal Engineering*, Copenhagen Denmark, Paper No. 78 pp.156-157

44. Hilbertx, W.H. and Goreau, T.J., (1996), "Reef Restoration using Sea-Water Electrolysis in Jamaica", 8th *International Coral Reef Symposium*, Panama City.

45. Hirt, C.W., and Nichols, B.D., (1981). "Volume of Fluid (VOF) Method for the Dynamics of Free Boundaries", *Journal of Computational Physics* Vol. 39, pp. 201-225.

46. Hixon, M.A., and Brostoff, W.N., (1985). "Substrate Characteristics, Fish Grazing and Epibenthics Reef Assemblages off Hawaii", *Bulletin of Marine Science*, Vol. 37, No.1, pp.200-213.

47. Hudson R.Y, Herrmann, F.A., Sager, R.A., Whalin, R.W., Keulegan, G.H., Chatham, C.E. and Hales, L.Z. (1979). *Coastal Hydraulic Models*, Special Report 5, U.S. Army Coastal Engineering Research Center, Ft. Belvoir, VA.

48. Ino, K. (1974). "Historical Review of Artificial Reef Activities in Japan", *Proceeding of an International Conference on Artificial Reefs*, Colunga, L and Stone, R (eds.), Texas A&M University, pp. 21-23.

49. Kakimoto, H., (1991). "Systematic Construction of Artificial Habitats for Fisheries", *Japan-US Symposium on artificial Habitats for Fisheries Proceedings*, Southern California Edison Co. 345 p.

50. Kawasaki, K and Iwata, K. (1998). "Numerical Analysis of Wave Breaking Due to Submerged Breakwater in Three Dimensional Wave Field", *Abstract of 26th International Conference of Coastal Engineering*, Copenhagen, Denmark, Paper No. 79, pp. 158-159.

51. Lin, J., and Su, W., (1994). "Early Phase of Fish Habitation Around a New Artificial Reefs off Southwestern Taiwan", *Bulletin of Marine Science*, Vol. 55, Nos.2-3, pp.1112-1121.

52. Lindquist, D.G., and Pietrafesa, L.J., (1989). "Current Vortices and Fish Aggregations: The Current Field and Associated Fishes around a Tugboat Wreck in Onslow Bay, North Carolina", *Bulletin of Marine Science*, Vol. 44, No.2, pp.533-544.

53. McGurrin, J.M., Stone, R.B., and Sousa, R.J., (1989). "Profiling United States Artificial Reef Development", *Bulletin of Marine Science*, Vol. 44, No. 2, pp. 1004-1013.

54. McGurrin, J.M., and Reeff, M.J., (1986). "Artificial Reef Development and Deployment", *Marine Technology Society Journal*, Vol. 20, No.3, pp. 3-9.

55. Moreno, I., Roca, I., Renones, O., Coll, J., and Salamanca, M. (1994). "Artificial Reefs Program in Balearic Waters (Western Mediteranean)", *Bulletin of Marine Science*, Vol. 55, No. 2-3, pp. 667-671.

56. Mottet, M.G. (1985). "Enhancement of The Marine Environment for Fisheries and Aquaculture in Japan", *Artificial Reefs: Marine and Freshwater Applications*, ed. F.M. D'itri, Lewis Publishers, Inc., 2nd ed., pp. 13-112.

57. Nakamura, M., (1985). "Evolution of Artificial Fishing Reef Concept in Japan", *Bulletin of Marine Science*, Vol. 37, No. 1, pp. 271-278.

58. Nakayama, A., Horikosi, N., and Kobayashi, H., (1993). "The Planning and Design of Multipurpose Artificial Barrier Reefs", *Proceedings Coastlines of Japan - Volume II*, Yoshimi Nagao (ed.), pp.183 - 197.

59. Newman, K.L., (1989). "Effect of Artificial Reefs on Nearshore Currents", *Proceedings of International Association for Hydraulic Research (IAHR) XXIII Congress*, pp. B147 - B164

60. Nichols, B.D., Hirt, C.W., and Hotchkiss, R.S. (1980). "SOLA-VOF: A Solution Algorithm for Transient Fluid Flow with Multiple Free Boundaries", *Los Alamos Scientific Laboratory Report*, LA-8355, 119 p.

61. Ogawa, Y. (1982). "The Present Status and Future Prospect of Artificial Reefs: Development Trends of Artificial Reef Units", *Japanese Artificial Reef Technology: Translation of Selected Recent Japanese Literature and An Evaluation of Potential Applications in The United States*, ed. S.F. Vik, Technical Report 604, Aquabio, Inc., Belleair Bluffs Florida, pp. 23-41

62. Ohnaka, S., and Yoshinawa, T. (1994). "Field Observation on Wave Dissipation and Reflection by an Artificial Reef with Varying Crown Width", *Hydro-Port '94 International Conf. On Hydro-Technical Engineering for Port and Harbor Construction*, pp.365 - 376.

63. Otake, S., Imamura, H., Yamamoto, H., and Kondou, K., (1991). "Physical and Biological Conditions around an Artificial Upwelling Structure", *Japan-US Symposium on artificial Habitats for Fisheries Proceedings.* Southern California Edison Co. 345 p.

64. Pamintuan, I.S., Alino, P.M., Gomez, E.D., and Rollon, R.N. (1994). "Early Succesional Pattern of Invertebrates in Artificial Reefs Established at Clear and Silty Areas in Bolinao, Pangasinan, Northern Philipinnes", *Bulletin of Marine Science* Vol.55, Nos.2-3, pp. 867 - 877.

65. Patankar, S.V., (1980). *Numerical Heat Transfer and Fluid Flow*, MC-Graw Hill Book, Co., 197p.

66. Pollard, D.A., and Matthews, J., (1985). "Experience in The Construction and Siting of Artificial Reefs and Fish Aggregation Devices in Australian Waters, with Notes on and a Bibliography of Australian Studies", *Bulletin of Marine Science,* Vol. 44, No. 2, pp. 299-304.

67. Reefball Deveopment Group (RBDG), (1997). Internet Brochure, http: //www.reefball.org.

68. Relini, G., and Relini L.O., (1989a). "Artificial Reefs in The Liguarian Sea (Northwestern Mediterranean): Aim and Results", *Bulletin of Marine Science.* Vol. 44, No. 2, pp. 744-751.

69. Relini, G. and Relini, L.O., (1989b). "Artificial Reefs in The Liguarian Sea: A Report on The Present Situation", *Report of The First Session of The Working Group on Artificial Reefs and Mariculture.* FAO Fisheries Report No. 428, pp.114-119

70. Richardson, J.E., (1996). Surf Similarity, *Flow Science Technical Note #44,* FSI-96-00-TN44. Los Alamos, NM, 8 p.

71. Roehl, E.J., (1997). "The Stability of Manufactured Artificial Reefs", *MSc. Thesis* - Florida Institute of Technology, Melbourne, Florida, U.S., 102 p.

72. Sabeur, Z.A., Allsop N.W.H., and Dennis, J.M., (1996)."Wave Dynamics at Coastal Structures: Development of A Numerical Model for Free Surface Flow", *Proceeding of 25th Coastal Engineering Conference 1996,* pp. 389 - 402.

73. Sampaolo, A., and Relini, G., (1994). "Coal Ash for Artificial Habitats in Italy", *Bulletin of Marine Science* Vol.55, Nos.2-3, pp. 1277 - 1294.

74. Seaman Jr., W, and Sprague, L.M., (1991). "Artificial Habitat Practices in Aquatic Systems", *Artificial Habitats for Marine and Freshwater Fisheries,* W. Seaman Jr., and Lucian M. Sprague, (eds.), Academic Press, Inc., 285 p.

75. Shinn, E.A., and Wicklund, R.I., (1989). "Artificial Reef Observations from A Manned Submersible off Southeast Florida", *Bulletin of Marine Science* Vol.44, No.2, pp. 1041 - 1050.

76. Shulman, M.J., (1984). "Resource Limitation and Recruitment Patterns in a Coral Reef Assemblage" *Journal of Experimental Marine Biology and Ecology*, Vol 74, pp. 85-109

77. Sinanuwong, K., (1991). "Artificial Reefs in Thailand", *Symposium on Artificial Reefs and Fish Aggregating Device as Tools for the Management and Enhancement of Marine Fisheries Resources*, RAPA - FAO Report: 1991/11, pp.340-363.

78. Smith, E.R., and Kraus, N.C. (1991). "Laboratory Study of Wave Breaking over Bars and Artificial Reefs", *Journal of Waterway, Port, Coastal and Ocean Engineering*, ASCE, Vol.117, No.4, pp.307 - 325.

79. Smith, E.R., and Kraus, N.C. (1990), Laboratory Study on Macro Features of Wave Breaking over Bars and Artificial Reefs, *CERC Technical Report 90-12*.

80. Sonu, C.J., and Grove, R.S., (1985), "Typical Japanese Reef Modules", *Bulletin of Marine Science*, Vol. 37, No. 1, pp. 348-355.

81. Sorensen, R.M., (1993). *Basic Wave Mechanics: for Coastal and Ocean Engineers*, John-Wiley and Sons, Inc.New York, NY. 284 p.

82. Spanier, E., Tom, M., and Pisanty, S., (1985). "Enhancement of Fish Recruitment by Artificial Enrichment of Man-made Reefs in The Southeastern Mediterranean", *Bulletin of Marine Science* Vol.37, No.1, pp. 356 - 363.

83. Stone, R.B., Mc Gurrin, J.M, Sprague, L.M., and Seaman, W., (1991), "Artificial Habitats of the World: Synopsis and Major Trends", *Artificial Habitats for Marine and Freshwater Fisheries*, W. Seaman Jr., and Lucian M. Sprague, (eds), Academic Press, Inc., 285 p.

84. Stone, R.B., (1985). "History of Artificial Reef Use in the United States", *Artificial Reefs: Marine and Freshwater Applications*, ed. F.M. D'itri, Lewis Publishers, Inc., 2nd ed., pp. 3-9.

85. Takeuchi, T., (1991). "Design of Artificial Reefs in Consideration of Environmental Characteristics", *Japan-US Symposium on Artificial Habitats for Fisheries Proceedings, Southern California Edison Co.*, M. Nakamura, Robert S. Grove, Charles J., Sonu, (eds), pp.195 - 203.

86. Tsujimoto, G., Kakuno, S., Shigematsu, T., Kurata, K., and Hosoyamada, T., (1999). "Numerical Simulation of Turbulent Flows around A New Type of Reef Breakwater with Perforations by The k-ε Turbulence Model", *Coastal Structures '99 (Abstract)*, pp. 158-159.

87. Versteeg, H.K., and Malalasekera, W., (1995). *An Introduction to Computational Fluid Dynamics: The Finite Volume Methods*, Longman Scientific & Technical Ltd., Essex, 256 p.

88. Walsh, W.J., (1985) "Reef Fish Community Dynamics on Small Artificial Reefs: The Influence of Isolation, Habitat Structure, and Biogeography". *Bulletin of Marine Science* Vol.36, No.2, pp. 357 - 376.

89. White, A.T., Ming, C.L., de Silva, M.W.R.N, and Guarin, F.Y. (1990) *Artificial Reefs for Marine Habitat Enhancement in Southeast Asia*, ASEAN/USCRMP, Manila, Philippines, 45 p.

90. Wiegel, R.L, (1964). *Oceanographical Engineering*, Prentice Hall, 532 p.

91. Yoshioka, K., Kawakami, T., Tanaka, S., Koarai, M., and Uda, T., (1993). "Design Manual for Artificial Reefs", *Proceeding Coastlines of Japan - Volume II*, Yoshimi Nagao (ed.), pp.93 - 107.

Appendix A
FLOW3D Structure
(Flow Science, 1997)

FLOW3D consists of five modules: PEEK (utility program) to monitor computational process and to interact with the solver while it is being run. PREP3D (preprocessor) to process the input file before the solver is executed. HYDR3D (hydrodynamic solver) to solve the hydrodynamic model. FLSCON (postprocessor) to process computational results, and DISPLAY (graphics display program) to show the results in a graphics format as well as to create postcript files. These modules are outlined in Figure A.1.

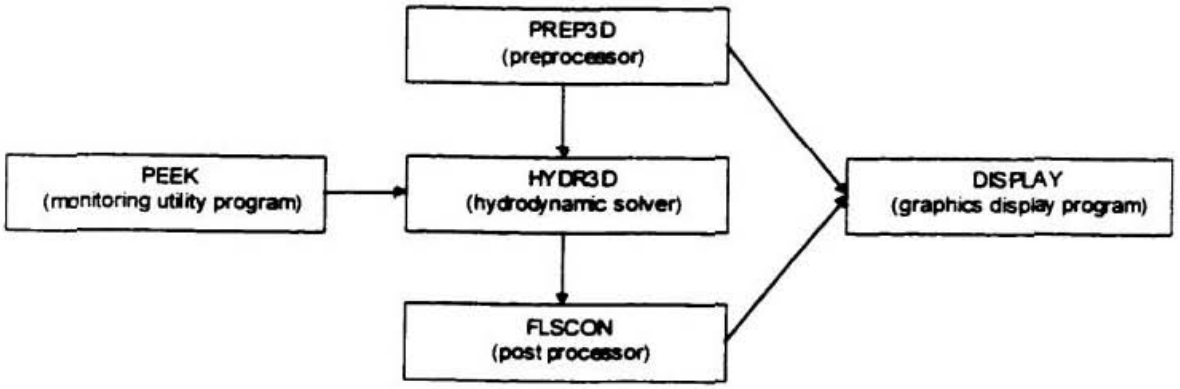

Figure A.1. FLOW3D Modules

Input file for FLOW3D is 'prepin.inp'. This file contains all physical property data, mesh and obstacle description, boundary condition and specified initial conditions, as well as all computational parameters controlling the operation and output of the code. Some files are generated by FLOW3D as output files from modules above or as transfer data files between modules. There are two type of running modes in FLOW3D: regular (non-restart, where t=0) and non-regular (restart, where t>0). Figure A.2 shows the file structure for regular run.

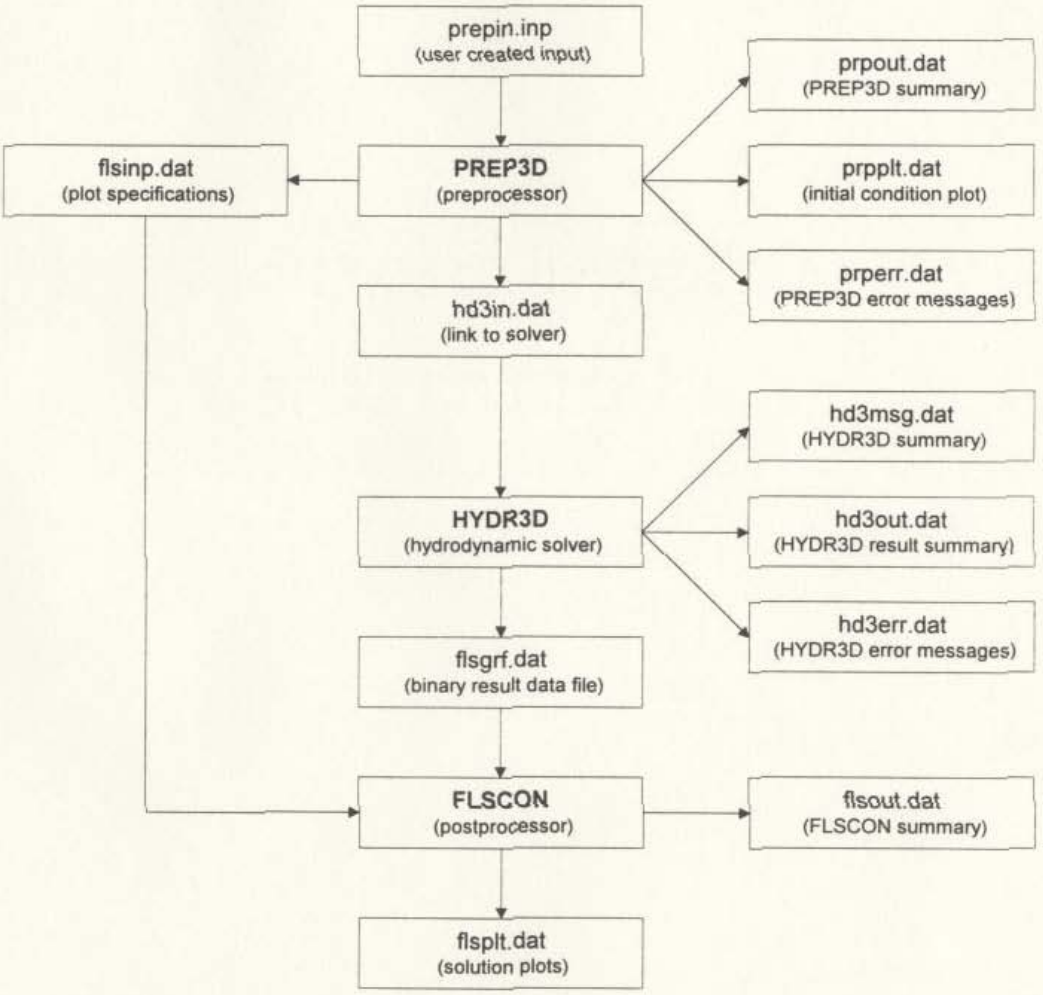

Figure A.2 File structure for regular run (non restart; t = 0)

In a regular run, the model is started with initial conditions, and time t is set starting from 0. However, it is not necessary to repeat the starting computation time from t = 0 when the user needs to extend the time execution from last computation. The computation can be carried out using non-regular run, and the starting time is based on the availability of data from the previous run. The old files from previous run, especially 'flsgrf.dat' are needed to access the initial conditions data for the restart run. File structure for non-regular run is given in Figure A.3.

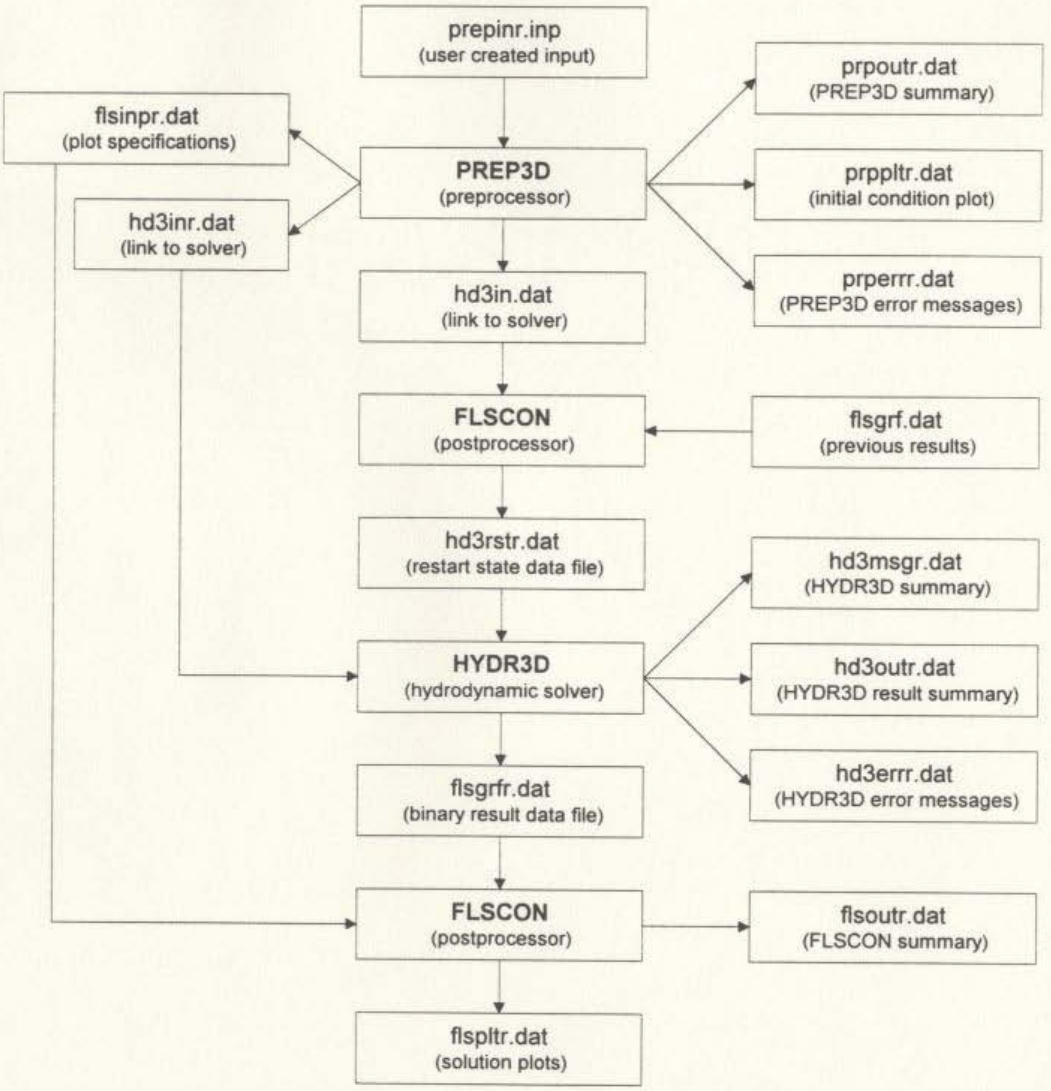

Figure A.3 File structure for non regular run (restart; t > 0)

FLOW3D input files, 'prepin.dat' where extension files 'dat' can be any character string to identify the input file, contains several namelists blocks to describe problem model. Typical input files used in this study are given in Appendix B and C, while Table A.1 below describes the namelist used on input file:

Table A.1 Namelist in 'prepin.dat'

Namelist	Description
XPUT	computational parameter and general problem description
LIMITS	specification of computational limits and print window limits
PROPS	specification of fluid properties
BCDATA	boundary condition specification
MESH	definition of computational mesh
OBS	definition of solid obstacle geometry
FL	initialization of fluid state within mesh at beginning of simulation
BF	definition of 2D baffle element (not used in this study)
TEMP	specification of initial fluid temperature distribution (not used in this study)
GRAFIC	specification of graphic output request
PARTS	specification of mass or marker particles

Furthermore, since the Volume of Fluid method uses FLOW3D, the flowchart is assumed to be similar to the flowchart of SOLA-VOF (Solution Algorithm - Volume of Fluid) method given by Nichols, et al. (1980). A flow chart of this method is given Figure A.4. Typically, this flowchart is similar to the flowchart in hydrodynamic solver module (HYDR3D) in FLOW3D.

The following lists describe each subroutine with a brief description of its major function (Nichols, et al, 1980).

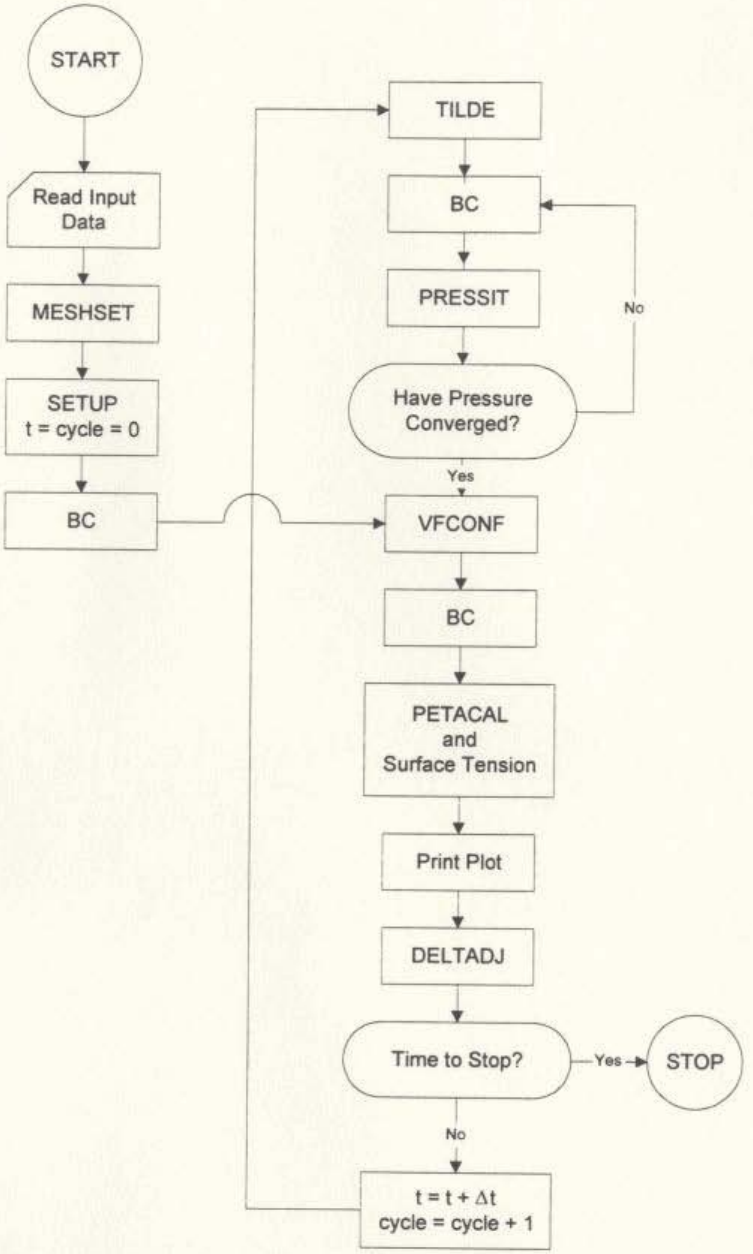

Figure A.4 Flow chart for SOLA-VOF

TILDE: (Temporary Velocity Calculation)

1. Computes an explicit solution for each of the momentum equation, i.e., new values of velocities are obtained from the time n values of pressure, advective, and diffusive accelerations. These TILDE values are advanced to time n+1 in the pressure iteration

BC (Boundary Condition)

1. Sets the values of appropriate variables at rigid free-slip, no-slip, continuative outflow, periodic, and specified pressure or velocities boundary
2. Sets the values of appropriate variables around the boundaries established by free surfaces.
3. Allows for special boundary condition inclusions, such as inflow boundaries
4. Sets average F and p values in obstacle cells adjacent to fluid cells.

MESHSET (Mesh Setup)

1. Generates the computing mesh from the input data established in namelist MESH
2. Evaluates all of the necessary geometric variables that are used throughout the code.

SETUP (General Setup)

1. Initializes constants necessary to the calculation
2. Computes the scaling factors and centering shifts required for graphics output.
3. Computes the initial hydrostatic pressure distribution to initialize the pressure array, [p (i,j) or p (i,j,k)].
4. Initializes marker particle number
5. Sets up the initial velocity with U(i,j) = UI and V(i,j) = VI everywhere in the mesh for two-dimensional model.

PRESSIT (Pressure Iteration)

1. Iterates the velocity and pressure field such that mass is conserved in each cell of the mesh.
2. Computes a free-surface cell pressure adjustment based on the applied surface pressure; mass conservation in the surface is not iterated, it is set by application of the free-surface boundary conditions.

VFCONV (Volume Fraction convection)

1. Computes the solution of the VOF function
2. Computes and stores for printout any errors in volume (i.e.. loss or gain) during the calculation of step (1) above.

PARMOV (Particle movement)

1. Computes the movement of marker particle in the fluid velocity field
2. Provides the necessary bookkeeping to allow marker particles to exit the mesh or to be replaced by newly input particles.

PETACAL (PETA Interpolation factor calculation)

1. Determines the slope of the surface in the surface cells
2. Determines the cell flag NF(i,j) to indicate the interpolation neighbour of the surface cell.
3. Computes the surface pressure PS(i,j) caused by surface tension in surface cells. if the surface tension flag is set.

DELTADJ (Time step adjustment)

1. Computes maximum allowable δt for stability
2. Adjusts δt according to number of iterations and maximum allowed for stability

Appendix B
Two Dimensional Input Files for FLOW 3D

A typical input file (`prepin.inp`) used to model the hemispherical hollow reefs is given in this appendix. The file contains all physical property data, mesh and obstacle description, boundary and initial conditions, as well as all computational parameters controlling the operation and output of the code. The explanation of each command line will be given together in the lists as 'remark'. Namelist blocks are typed in bold to distinguish with other namelists.

```
Twelve hollow reef 1.m diameter smooth surface opening one hole on top
 $xput
  remark='units are mks',
  twfin=120.0,      remark='set termination time'
  gz=-9.81,         remark='vertical gravitational acceleration'
  ipdis=1,          remark='uniform hydrostatic pressure'
  itb=1,            remark='free surface modelling flag'
  prtdt=1000.0,     remark='limit in hd3out output file'
  iadiz=1,iadix=1,remark='pressure   iteration   use   line   implicit
methods',
  epsadj=1.,        remark='multiplier for calculated pressure iteration
                            convergence',
  nmat=1,           remark='number of materials',
  pltdt=1.,         remark='time  interval  (in  second)  between  spatial
plot
```

```
                        in flsgrf/flsplt output files',
  ifvis=3,          remark='k-e turbulence model, set viscosity flag',
  dum1=1.2566,      remark='dum1 is wave angular frequency, T=5 sec',
  dum2=0.2248,      remark='dum2 is wave number, L=28m',
  dum3=0.5,         remark='dum3 is wave amplitude, H=1.0m',
 $end
 $limits
  irpr=1,           remark='print window maximum x cell index'
  jbkpr=1,          remark='print window maximum y cell index'
  ktpr=1,           remark='print window maximum z cell index'
 $end
 $props
  rhof=1030.0,      remark='water density',
  mui=0.0012,       remark='water coefficient dynamic viscocity',
 $end
 $bcdata
  flhtl=4.0,        remark='water depth',
  wl=6,             remark='left-specified velocity boundary condition',
  wr=2,             remark='right-rigid wall boundary ',
  wt=1,             remark='top-symmetry plane boundary condition',
  wb=1,             remark='bottom-symmetry plane boundary condition',
  wbk=1,            remark='back-continuative boundary condition',
  wf=1,             remark='front-continuative boundary condition',
 $end
 $mesh
nxcelt=192,         remark='total cell in horizontal (x) direction'
   px(1)=-50., nxcell(1)=50,   remark='50 cells used in between -50 to
0'
   px(2)=0.,   nxcell(2)=65,  remark='65 cells used in between 0 to 13'
   px(3)=13.,   nxcell(3)=77,   remark='77 cells used in between 13 to
90'
   px(4)=90.,

   nycelt=1,              remark='total cell in lateral (y) direction'
   py(2)=1.0,             remark='only   one   cell   used   in   lateral
direction'

   nzcelt=30,             remark='total cell in vertical (z) direction'
   pz(1)=0.0,  nzcell(1)=30,   remark='50 cells used in between 0 to 6'
   pz(2)=6.0,
 $end
 $obs
 nobs=3,           remark='number of defined obstacles'

 remark='the following commands define shoreline slope',
 iob(1)=1, cx(1)=-0.05, cz(1)=1.0,

 remark='define virtual reefs for cottom and middle reefs layer',
 remark='the following command define the outer circle of the reefs',
 ivrt(2)=1,
 iofo(1,2)=11,
 cx2(11)=1., cz2(11)=1.,    cc(11)=-1.0,
```

```
zl(11)=0.125,

remark='the following command define the inner circle of the reefs',
iofo(2,2)=12,
ioh(12)=0,
cx2(12)=1., cz2(12)=1.,    cc(12)=-0.5625,
zl(12)=0.125,

remark='define reefs holes',
iofo(3,2)=13,  ioh(13)=0,
zl(13)=-0.125,  zh(13)=0.125,
xl(13)=-1.1,    xh(13)=-0.74,
roty(13)=60.,
iofo(4,2)=14,  ioh(14)=0,
zl(14)=-0.125,  zh(14)=0.125,
xl(14)=-1.1,    xh(14)=-0.74,
roty(14)=120.,


remark='the following commands define reef foundation; height=0.25m',
iofo(12,2)=18,
 cx(18)=-2., cc(18)=-0.405, cz(18)=1.0,
 zl(18)=-0.125,    zh(18)=0.125,
 xh(18)=0.,
 trnx(18)=-0.875, trnz(18)=-0.25,
iofo(13,2)=19,
 cx(19)=2.,  cc(19)=-0.405, cz(19)=1.0,
 zl(19)=-0.125,  zh(19)=0.125, xl(19)=0.,
 trnx(19)=-0.875, trnz(19)=-0.25,
iofo(14,2)=20,
 cx(20)=-2., cc(20)=-0.405, cz(20)=1.0,
 zl(20)=-0.125,  zh(20)=0.125,
 xh(20)=0.,  trnx(20)=0.875,
 trnz(20)=-0.25,
iofo(15,2)=21,
 cx(21)=2.,  cc(21)=-0.405, cz(21)=1.0,
 zl(21)=-0.125,  zh(21)=0.125,
 xl(21)=0.,  trnx(21)=0.875,
 trnz(21)=-0.25,

remark='define second virtual reefs for top reef layer',

remark='the following commands define outer circle of the reef'
 ivrt(3)=1,                    ,
 iofo(1,3)=2,
 cx2(2)=1., cz2(2)=1.,    cc(2)=-1.0,
 zl(2)=0.125,

remark='the following commands define inner circle of the reef',
 iofo(2,3)=3, ioh(3)=0,
 cx2(3)=1., cz2(3)=1.,    cc(3)=-0.5625,
 zl(3)=0.125,
```

```
 remark='the following commands define top holes of the reef',
  iofo(3,3)=4, ioh(4)=0,
  zl(4)=-0.125, zh(4)=0.125,
  xl(4)=-1.1,  xh(4)=-0.74,
  roty(4)=90.,

 remark='copy, translate and rotate virtual reefs',
  icpy(1)=2,  ctrnx(1)=1.180,   ctrnz(1)=0.434,   croty(1)=-2.862,
  icpy(2)=2,  ctrnx(2)=3.377,   ctrnz(2)=0.544,   croty(2)=-2.862,
  icpy(3)=2,  ctrnx(3)=5.574,   ctrnz(3)=0.654,   croty(3)=-2.862,
  icpy(4)=2,  ctrnx(4)=7.772,   ctrnz(4)=0.764,   croty(4)=-2.862,
  icpy(5)=2,  ctrnx(5)=9.969,   ctrnz(5)=0.874,   croty(5)=-2.862,
  icpy(6)=2,  ctrnx(6)=12.166,  ctrnz(6)=0.984,   croty(6)=-2.862,
  icpy(7)=2,  ctrnx(7)=2.218,   ctrnz(7)=1.688,   croty(7)=-2.862,
  icpy(8)=2,  ctrnx(8)=4.416,   ctrnz(8)=1.798,   croty(8)=-2.862,
  icpy(9)=2,  ctrnx(9)=8.810,   ctrnz(9)=2.017,   croty(9)=-2.862,
  icpy(10)=2, ctrnx(10)=11.007, ctrnz(10)=2.127,  croty(10)=-2.862,
  icpy(11)=3, ctrnx(11)=3.157,  ctrnz(11)=2.941,  croty(11)=-2.862,
  icpy(12)=3, ctrnx(12)=9.849,  ctrnz(12)=3.271,  croty(12)=-2.862,
  $end
 $fl
  flht=4.0,     remark='define water depth'
 $end
 $bf
 $end
 $temp
 $end
 $grafic
   contpv(1)='p', remark='contoured velocity magnitude under the
                          vectors',
   nvplts(1)=1    remark=,velocity vector only plot once'

   remark='define coordinat plots',
   xv1(1)=0.,            xv2(1)=12.,
   zv1(1)=0.,            zv2(1)=6.,

   remark='the  following  command  define  location  for  water  level
probe',
   xloc(2)=-50., yloc(2)=0., zloc(2)=4.,
   xloc(3)=-25., yloc(3)=0., zloc(3)=4.,
   xloc(4)=0.,   yloc(4)=0., zloc(4)=4.,
   xloc(5)=15.,  yloc(5)=0., zloc(5)=4.,
   xloc(6)=70.,  yloc(6)=0., zloc(6)=4.,

   remark=''the following command  define location for velocity probe',
   iloc(7)=79,  jloc(7)=2, kloc(7)=3,
   iloc(8)=76,  jloc(8)=2, kloc(8)=6,
   iloc(9)=79,  jloc(9)=2, kloc(9)=7,
 $end
 $parts
 $end
```

Appendix C

Three Dimensional Model Input Files for FLOW3D

In a three dimensional model, since the reef units are too complex to be handled by FLOW3D obstacle generation, the reefs models were created using CAD software, and exported as stereolithography file (.STL). Furthermore, the STL files will be embedded in the input files. Comparing with two-dimensional model, this method will reduce the command line in obstacle description, considerably.

```
Twenty four hollow reef smooth surface with opening one hole on top
 $xput
  remark='units are mks',
  twfin=60.0,      remark='set termination time',
  gz=-9.81,        remark='coefficient      of      vertical      gravity
acceleration',
  ipdis=1,         remark='uniform hydrostatic pressure',
  itb=1,           remark='free surface tracking enabled',

  apltdt=0.5,      remark=time interval for animation plot',
  prtdt=1000.0,    remark='limit in hd3out',
  hpltdt=0.1,      remark='set interval for history plot',
  pltdt=0.5,       remark='time  interval  (in  second)  between  spatial
plot
                          in flsgrf/flsplt output files',

  iadiz=1,         remark='pressure    iteration    use    line    implicit
methods',
```

```
  iadix=1,
  iadiy=1,
  epsadj=1.,        remark='multiplier for calculated pressure iteration
                    convergence',
  nmat=1,           remark='number of materials',
  ifvis=3,          remark='k-e turbulence model, viscocity flag'

  dum1=1.2566,      remark='dum1 is wave angular frequency, T=5 sec',
  dum2=0.2248,      remark='dum2 is wave number, L=28m',
  dum3=0.5,         remark='dum3 is wave amplitude, H=1.0m',
 $end
 $limits
  irpr=1,           remark='print window maximum x cell index',
  jbkpr=1,
  ktpr=1,
 $end
 $props
  rhof=1030.0,      remark='water density',
  mui=0.0012,       remark='water coeffient dynamic viscocity',
 $end
 $bcdata
  flhtl=4.0,        remark='water depth',
  wl=6,             remark='left-specified velocity boundary condition',
  wr=2,             remark='right-rigid wall boundary ',
  wt=1,             remark='top-symmetry plane boundary condition',
  wb=1,             remark='bottom-symmetry plane boundary condition',
  wbk=1,            remark='back-continuative boundary condition',
  wf=1,             remark='front-continuative boundary condition',
 $end
 $mesh
   nxcelt=198,     remark='total cell at x direction',
   px(1)=-50, nxcell(1)=10, remark='10 cells used in between -50 to -
48'
   px(2)=-48, nxcell(2)=29, remark='29 cells used in between -48 to 0'
   px(3)=0,   nxcell(3)=100,remark='100 cells used in between 0 to 20'
   px(4)=20,  nxcell(4)=29, remark='29 cells used in between 20 to 68'
   px(5)=68,  nxcell(5)=10, remark='10 cells used in between 68 to 70'
   px(6)=70,  nxcell(6)=20, remark='20 cells used in between 70 to 90'
   px(7)=90,

   nycelt=20,      remark='total cell at y direction'
   py(1)=0.0,
   py(2)=4.0,

   nzcelt=30,      remark='total cell at z direction'
   pz(1)=0.0,
   pz(2)=6.0,
 $end
 $obs
  avrck=-2.1,      remark='adjust cell volume fraction so ratio does not
                   exceed 2.1'
  nobs=6,          remark='number of obstacle',
```

```
 remark='the following commands define shoreline',
 iob(1)=1, cx(1)=-0.05, cz(1)=1.0,

 remark='import the reefs from cad data (STL files)',

 remark='the following command is used to import first reef group',
  iob(2)=2,
    igen(2)=3,  ioh(2)=1,
    trnx(2)=-1., trny(2)=-3., trnz(2)=-0.2,    roty(2)=-2.862,


 remark='the following command is used to import second reef group'
  iob(3)=3,
    igen(3)=3,  ioh(3)=1,
    trnx(3)=5.,  trny(3)=-3., trnz(3)=0.1,     roty(3)=-2.862,


 remark='the following command is used to import middle reef group'
  iob(4)=4,
    igen(4)=3,  ioh(4)=1,
    trnx(4)=-1.,  trny(4)=-3., trnz(4)=-0.2,   roty(4)=-2.862,

 remark='the following command is used to import third reef group'
  iob(5)=5,
    igen(5)=3,  ioh(5)=1,
    trnx(5)=11.,  trny(5)=-3., trnz(5)=0.4,    roty(5)=-2.862,

 remark='the following command is used to import second middle reef
         group'
  iob(6)=6,
    igen(6)=3,  ioh(6)=1,
    trnx(6)=5.,  trny(6)=-3., trnz(6)=0.1,     roty(6)=-2.862,
$end
$fl
 flht=4.0,   remark='water depth'
$end
$bf
$end
$temp
$end
$grafic
 anmtyp(1)='vel',
 anmtyp(2)='p',
 contpv(1)='p', remark='contoured velocity magnitude under the
                        vectors',
 nvplts(1)=1     remark=,velocity vector only plot once'

 remark='define coordinat plots',
  xv1(1)=0.,            xv2(1)=18.,
  zv1(1)=0.,            zv2(1)=6.,
```

```
      remark='define location for water level probe',
      remark='at x:-50m,-24m,0m,18m,70m, y:0.5m,1.5m,2m, 2.5m,3.5m',
    iloc(2)=2,     jloc(2)=4,     kloc(2)=22,
    iloc(3)=26,    jloc(3)=4,     kloc(3)=22,
    iloc(4)=41,    jloc(4)=4,     kloc(4)=22,
    iloc(5)=130,   jloc(5)=4,     kloc(5)=22,
    iloc(6)=179,   jloc(6)=4,     kloc(6)=22,

    iloc(7)=2,     jloc(7)=9,     kloc(7)=22,
    iloc(8)=26,    jloc(8)=9,     kloc(8)=22,
    iloc(9)=41,    jloc(9)=9,     kloc(9)=22,
    iloc(10)=130,  jloc(10)=9,    kloc(10)=22,
    iloc(11)=179,  jloc(11)=9,    kloc(11)=22,

    iloc(12)=2,    jloc(12)=11,   kloc(12)=22,
    iloc(13)=26,   jloc(13)=11,   kloc(13)=22,
    iloc(14)=41,   jloc(14)=11,   kloc(14)=22,
    iloc(15)=130,  jloc(15)=11,   kloc(15)=22,
    iloc(16)=179,  jloc(16)=11,   kloc(16)=22,

    iloc(17)=2,    jloc(17)=14,   kloc(17)=22,
    iloc(18)=26,   jloc(18)=14,   kloc(18)=22,
    iloc(19)=41,   jloc(19)=14,   kloc(19)=22,
    iloc(20)=130,  jloc(20)=14,   kloc(20)=22,
    iloc(21)=179,  jloc(21)=14,   kloc(21)=22,

    iloc(22)=2,    jloc(22)=19,   kloc(22)=22,
    iloc(23)=26,   jloc(23)=19,   kloc(23)=22,
    iloc(24)=41,   jloc(24)=19,   kloc(24)=22,
    iloc(25)=130,  jloc(25)=19,   kloc(25)=22,
    iloc(26)=179,  jloc(26)=19,   kloc(26)=22,

remark='define location for velocity probe',

remark='at location (4.9,0.9,0.3), (4.5, 0.9, 0.7), (4.9, 0.9, 0.9)
    iloc(27)=65,   jloc(27)=6,    kloc(27)=3,
    iloc(28)=63,   jloc(28)=6,    kloc(28)=5,
    iloc(29)=56,   jloc(29)=6,    kloc(29)=6,
 $end
 $parts
 $end
```